Authors' Reponses to Reviewer Comments

Congbo Song*

E-mail: songcongbo@163.com

MS No.: acp-2018-387

Title: Vehicular volatile organic compounds (VOCs)-NO$_x$-CO emissions in a tunnel study in northern China: emission factors, profiles, and source apportionment

Referee #1

General comments:

The manuscript by Song C. et al is a study for primary emission factors (EFs) of vehicular volatile organic compounds (VOCs)-NOx-CO, and source profiles of vehicular VOCs through a well-designed tunnel test in the northern China. The fleet-average EFs and source profiles are limited in the northern China because of few tunnel studies. In this study, the EFs of VOCs from tailpipe and evaporative emissions resolved by PMF were obtained, which should be the key research highlight. The methods used in this study and corresponding conclusions are much helpful for tunnel tests and also for following source apportionment, evaluation of EFs, emission inventory and control policy assessment researches. The paper is well written and structured and is full of high quality data. I suggest that the manuscript needs minor revision before published.

General response:

Thanks a lot for your positive comments on this manuscript. We have improved this manuscript by answering the reviewers' comments and suggestions.

Specific comments:

Q1:

In the present manuscript, the paper presented ozone formation potential (OFP) from fleet-average vehicle emissions. It could be better to further quantify the ozone or SOA formation potential from tailpipe and evaporative VOCs. The break-down knowledge for different sources (tailpipe and evaporative VOC emissions) will provide insights into useful emission control strategies.

A1:

In our previous manuscript, we estimated the average emission factors for 30 species from tailpipe and evaporative VOCs in Table S5. In the revised manuscript ,we made some changes to reduce the 30 species to 20 species. To minimize the uncertainties caused by the NMVOC species with low ΔNMVOCs values, the top 30 NMVOC species from vehicular emissions were considered in source apportionment by PMF. Additionally, the species with a number of samples of non-negative ΔNMVOCs (i.e., $C_{Outlet} - C_{Inlet}$>0) less than 75% were excluded from the PMF model. Finally, the 20 NMVOC species (Table 1, see below) were introduced into the PMF model.

As listed in Table 1, the EFs of the top 20 VOC compounds in vehicular evaporative and tailpipe emissions were estimated via relative contributions (Fig.1a) and fleet-average EFs. The EFs for vehicular evaporative and tailpipe emissions were estimated to be 24.9±7.5 and 15.7±3.3 mg km^{-1} veh^{-1}, respectively. In addition, the EFs and OFP from vehicular evaporative and tailpipe emissions were 60.3±4.1 and 74.9±4.5 mg km^{-1} veh^{-1}, respectively. During the measurement campaign, evaporative emissions accounted for over half (62.7±37.3%) of the total vehicular NMVOC emissions, and nearly half (44.6%) of the total vehicular OFP.

Thank you for your kind advice. The relevent contens have been added to the revised manuscript.

Table 1: The slope and R^2 from the linear regression between the measured and modeled VOCs concentrations for 2-factor solution, and the estimated EFs (mg km^{-1} veh^{-1}) of VOCs from evaportative and tailpipe emissions.

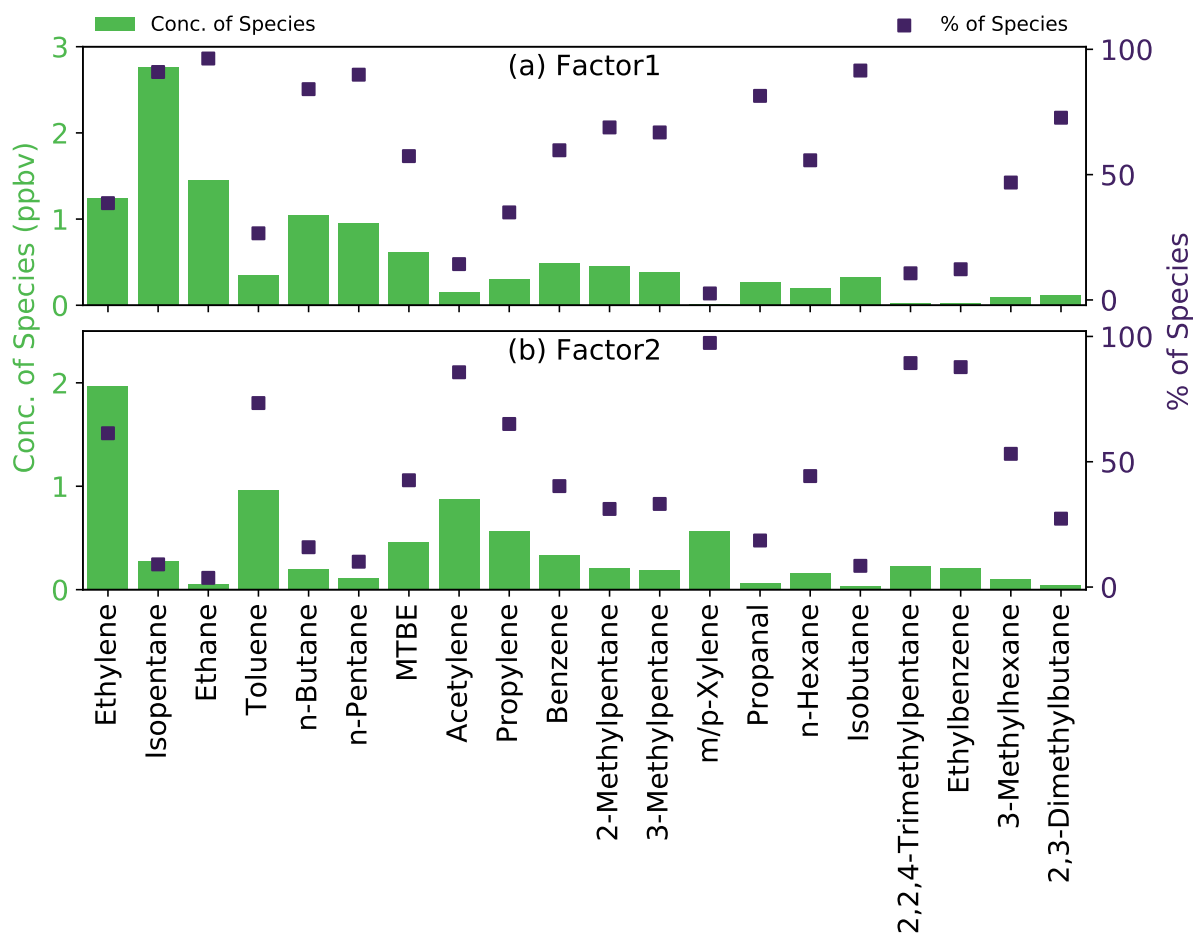| Compound	Slope	R^2	EFs (mg km^{-1} veh^{-1})	
			Evaporative	Tailpipe
Ethylene	1.02	0.83	0.99±0.18	1.57±0.28
Isopentane	0.98	0.83	6.19±2.14	0.62±0.2
Ethane	0.84	0.76	1.85±0.82	0.07±0.03
Toluene	0.91	0.72	0.88±0.3	2.42±0.79
n-Butane	0.99	0.87	1.71±0.75	0.3±0.16
n-Pentane	0.99	0.95	1.93±0.9	0.22±0.1
MTBE	0.79	0.86	1.43±0.7	1.06±0.5
Acetylene	0.76	0.45	0.1±0.03	0.59±0.16
Propylene	0.92	0.70	0.36±0.08	0.67±0.14
Benzene	0.99	0.87	1.16±0.31	0.78±0.2
2-Methylpentane	0.97	0.95	1.1±0.41	0.5±0.18
3-Methylpentane	0.90	0.94	0.93±0.37	0.46±0.17
m/p-Xylene	0.79	0.67	0.04±0.01	1.39±0.4
Propanal	0.50	0.44	0.52±0.29	0.12±0.06
n-Hexane	0.82	0.93	0.48±0.15	0.38±0.12
Isobutane	0.89	0.65	0.51±0.25	0.05±0.02
2,2,4-Trimethylpentane	1.00	0.92	0.07±0.01	0.6±0.09
Ethylbenzene	0.70	0.58	0.08±0.03	0.58±0.22
3-Methylhexane	0.92	0.97	0.26±0.07	0.29±0.08
2,3-Dimethylbutane	0.91	0.94	0.29±0.11	0.11±0.04
NMVOCs	0.98	0.98	24.89±7.52	15.67±3.32

Figure 1: The source profiles (% of species, represented by scatters) and contributions (Conc. of Species, represented by bars) of 2-factor (a: Factor1, b: Factor2) solution by the PMF model. Factor1 and Factor2 was identified as evaporative and tailpipe emissions, respectively.

Q2:

The resolved source profiles of tailpipe and evaporative VOCs by PMF should be compared with other published studies.

A2:

Thank you for your kind suggestion. In the present study, we aimed at providing new methods of source apportionment of on-road vehicular VOC emissions. It is of great important to quantify the relative contribution of tailpipe and evaporative emissions to on-road vehicular VOC emissions. There were some uncertainties underlying the resolved source profiles by PMF model as there were limited samples. In addition, We discussed the source identification of the resolved factors in details in the manuscript from the perspective of both the tracers and the temperature dependence. We belive that the resolved factors (Figure 1) could be identified as tailpipe and evaporative emissions.

Q3:

Accurate measurement of the fluxes of inlet and outlet is essential to the calculation of EFs. It would be useful to have a brief description of the methods used to measure the fluxes.

A3:

Thank you for your suggestion. In this study, the actual volumetric flow rates induced by the vehicular fleet and the prevailing winds in the tunnel were continuously measured using ultrasonic gas flowmeters (Flowsick-200 SICK MAIHAK, Germany) with a time resolution of 1 min, which have also been used in previous tunnel tests[1–3].

The FLOWSIC 200 operates by measuring the transit delay of an ultrasonic pulse. Sender/receive unites are mounted on both sides of the tunnel at a certain angle to the flow direction (Figure 2).

The measuring path L is equal to the active measuring distance, that is, the area through which the air flows. Given the measuring path L, sound velocity c, and the angle of inclination a between the sound and flow direction, the sound transit time when the signal is transmitted in the direction of the flow (forward direction) can be expressed as:
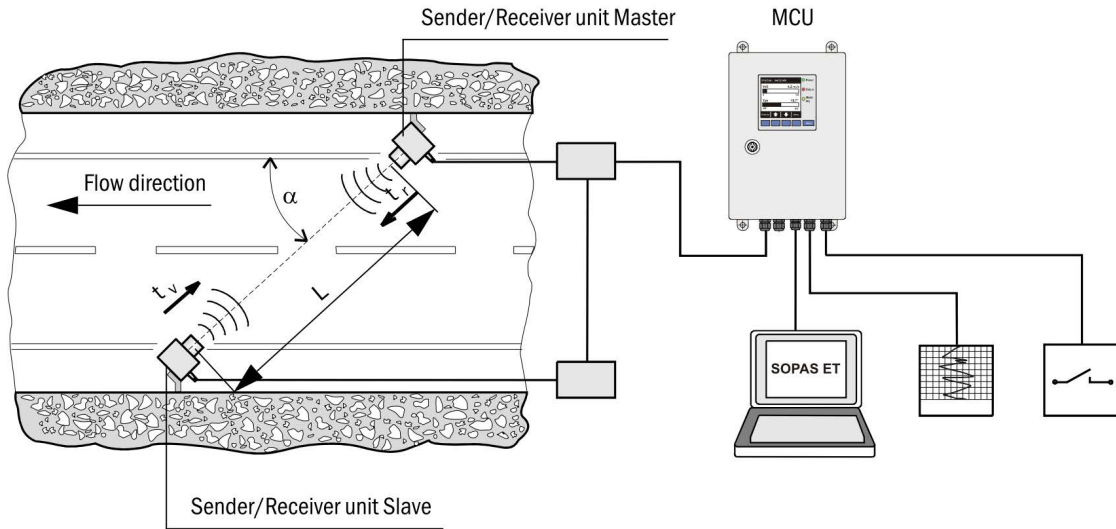
$$t_v = \frac{L}{c + v \cdot cos\alpha} \qquad (1)$$

The sound transmit against the direction of flow:

$$t_r = \frac{L}{c - v \cdot cos\alpha} \qquad (2)$$

Conversation to v:

$$v = \frac{L}{2 \cdot cos\alpha} \cdot (\frac{1}{t_v} - \frac{1}{t_r}) \qquad (3)$$

FLOWSIC200 operating principle

$$v = \frac{L}{2 \cdot \cos \alpha} \cdot \left(\frac{1}{t_v} - \frac{1}{t_r} \right)$$

v   = Flow velocity in m/s
L   = Measuring distance (path length) in m
α = Installation angle in °
t_v = Signal transit time in the direction of the flow
t_r = Signal transit time in the direction opposite the flow

Figure 2: FLOWSIC 200 operating principle.

Q4:

Is it possible to resolve tailpipe and evaporative VOCs by the method of chemical mass balance (CMB)?

A4:

Thank you for your suggestion. Vehicular emissions in the tunnel consisted of tailpipe and evaporative emissions. Profiles of tailpipe and evaporative emissions are necessary for CMB analysis to apportion these two factors. Vehicular evaporative emissions can be generally grouped into hot soak, diurnal, permeation, refueling process, and running loss [4,5]. However, source profiles and EFs of VOC from hot soak, diurnal, permeation and refueling process have been well characterized in laboratories, but VOC emissions from running loss are less understood because no facility in China could accommodate the test procedures or track-based tank temperature profile generation [5]. Thus, the source profile of evaporative emissions could be hardly obtained since the limited information for running loss. Thus, the CMB method is not ideally suitable for source aportionment of on-road vehicular VOC emissions in this case.

Only if we could quantify running losses in the laboratory test, we could conduct CMB analysis for source aportionment of on-road vehicular VOC emissions. Moreover, our study provide a detailed experiments and mathods to quantify the relation contribution of tailpipe and evaporative emissions to on-road vehicular VOC emissions.

Q5:

I suggest to conduct the similar study in other seasons with different ranges of ambient temperature.

A5:

Thank you for your suggestion. Vehicular emissions are greatly influence by ambient temperature, mainly consisting of cold-start and evaporative emissions. In this study, we quantified the temperature-dependent evaporative emissions (Figure 3). It is very meaningful to conduct the similar study in other seasons with different ranges of ambient temperature.

However, it is very hard to conduct such campagin considering the safety and permission. We will try to work on it in the future.
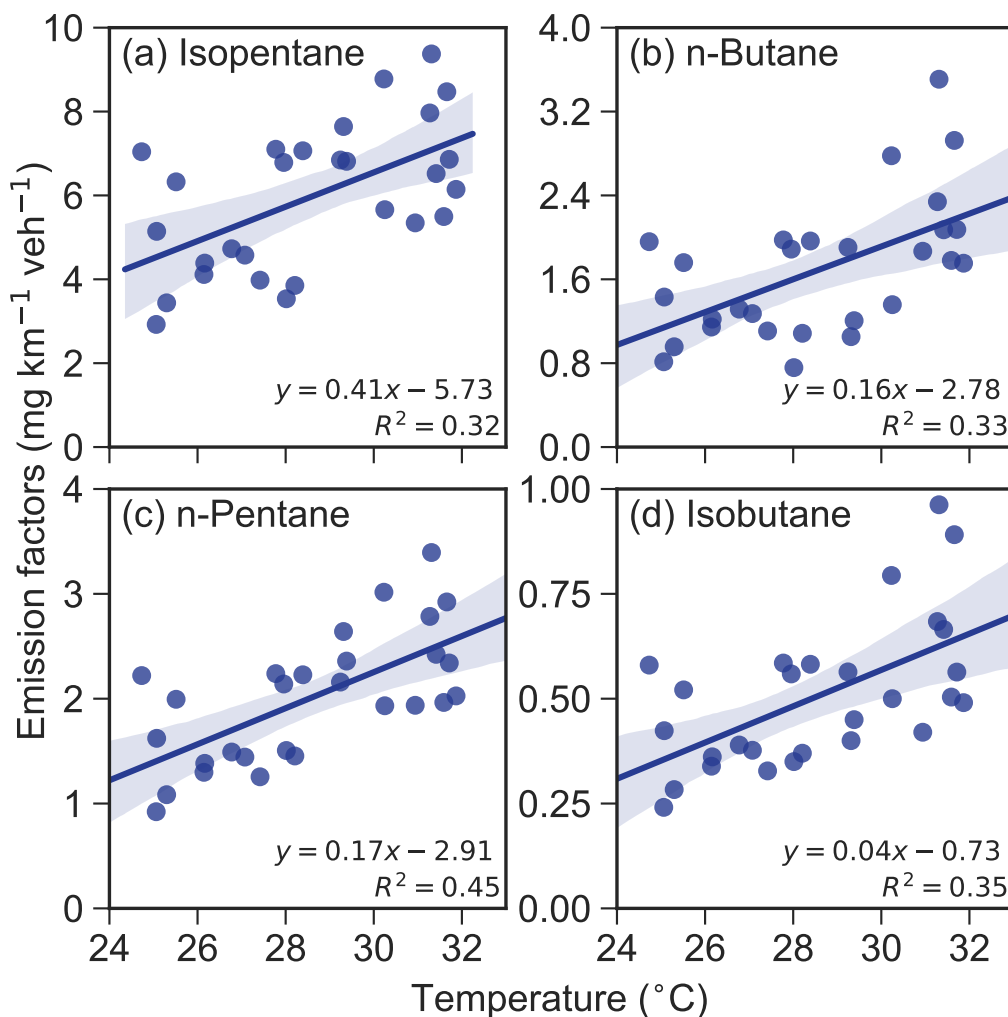

Figure 3: The linear regressions (filled with 95% regression confidence intervals) between emission factors of (a) Isopentane, (b) n-Butane, (c) n-Pentane, and (d) Isobutane against ambient temperature data.

References

(1) Song, C.; Ma, C.; Zhang, Y.; Wang, T.; Wu, L.; Wang, P.; Liu, Y.; Li, Q.; Zhang, J.; Dai, Q.; Zou, C.; Sun, L.; Mao, H. Heavy-duty diesel vehicles dominate vehicle emissions

in a tunnel study in northern China. *Science of The Total Environment* **2018**, *637-638*, 431 – 442.

(2) Zhang, Q.; Wu, L.; Fang, X.; Liu, M.; Zhang, J.; Shao, M.; Lu, S.; Mao, H. Emission factors of volatile organic compounds (VOCs) based on the detailed vehicle classification in a tunnel study. *Science of The Total Environment* **2018**, *624*, 878 – 886.

(3) Imhof, D.; Weingartner, E.; Prévôt, A. S. H.; Ordóñez, C.; Kurtenbach, R.; Wiesen, P.; Rodler, J.; Sturm, P.; McCrae, I.; Ekström, M.; Baltensperger, U. Aerosol and NO_x emission factors and submicron particle number size distributions in two road tunnels with different traffic regimes. *Atmospheric Chemistry and Physics* **2006**, *6*, 2215–2230.

(4) Yue, T.; Yue, X.; Chai, F.; Hu, J.; Lai, Y.; He, L.; Zhu, R. Characteristics of volatile organic compounds (VOCs) from the evaporative emissions of modern passenger cars. *Atmospheric Environment* **2017**, *151*, 62 – 69.

(5) Liu, H.; Man, H.; Tschantz, M.; Wu, Y.; He, K.; Hao, J. VOC from Vehicular Evaporation Emissions: Status and Control Strategy. *Environmental Science & Technology* **2015**, *49*, 14424–14431.

Vehicular volatile organic compounds (VOCs)-NO$_x$-CO emissions in a tunnel study in northern China: emission factors, profiles, and source apportionment

Congbo Song[1], Yan Liu[1], Shida Sun[1], Luna Sun[1], Yanjie Zhang[1], Chao Ma[1], Jianfei Peng[2], Qian Li[1], Jinsheng Zhang[1], Qili Dai[1], Baoshuang Liu[1], Peng Wang[2], Yi Zhang[1], Ting Wang[1], Lin Wu[1], Min Hu[3], and Hongjun Mao[1]

[1]Center for Urban Transport Emission Research & State Environmental Protection Key Laboratory of Urban Ambient Air Particulate Matter Pollution Prevention and Control, College of Environmental Science and Engineering, Nankai University, Tianjin, 300071, China

[2]Zachry Department of Civil Engineering, Texas A and M University, College Station, TX, 77845, USA

[3]Laboratory of Environmental Simulation and Pollution Control, College of Environmental Sciences and Engineering, Peking University, Beijing, 100871, China

Correspondence: Hongjun Mao (hongjunm@nankai.edu.cn)

Abstract. Vehicular emission is a key contributor to ambient volatile organic compounds (VOCs) and NO$_x$ in Chinese megacities. However, the information of real-world emission factors (EFs) for a typical urban fleet is still limited, hindering the development of a more reliable emission inventory in China. Based on a more-than-two-week (August 8-24, 2017) tunnel test in urban Tianjin in northern China, and on the use of a statistical regression model, the Positive Matrix Factorization (PMF) receptor model, and the Calculate Emissions from Road Transport (COPERT) IV model, characteristics of vehicular VOCs-NO$_x$-CO emissions were analyzed systematically. The fleet-average EFs (pollutant: downslope, upslope, and overall in mg km^{-1} veh^{-1}) were estimated respectively as follows: (NO: 61.92$\pm$72.46, 158.58$\pm$73.48, 97.52$\pm$69.84), (NO$_2$: 16.52$\pm$11.49, 23.98$\pm$20.14, 15.86$\pm$9.38), (NO$_x$: 79.45$\pm$78.43, 181.22$\pm$88.29, 116.56$\pm$77.61), and (CO: 269.96$\pm$342.38, 577.76$\pm$382.22, 344.67$\pm$250.01). The EFs of NO-NO$_2$-NO$_x$ and CO from heavy-duty vehicles (or diesel vehicles) were differentiated from light-duty vehicles (or gasoline vehicles). The ratios (v/v) of NO$_2$ to NO$_x$ in the primary vehicular exhaust were approximately 0.18$\pm$0.09, 0.10$\pm$0.22 and 0.10$\pm$0.05 for downslope, upslope, and the entire tunnel, respectively. The fleet-average EF of the 99-target non-methane VOCs (NMVOCs) was 40.56$\pm$12.18 mg km^{-1} veh^{-1}, lower than the previous studies in China. The BTEX (benzene, toluene, ethylbenzene, p-xylene, m-xylene and o-xylene) levels decreased by approximately 79% when emission standards increased from China I to China V. The ~~source profiles of NMVOCs from the tailpipe and evaporative emissions were~~ vehicular T/B emission ratio (ER, v/v) was 1.42$\pm$0.33. Isopentane could be employed as a suitable indicator of vehicular emission. The characteristic ratios (v/v) of C6-C8 aromatics to isopentane from vehicular emissions were 0.29$\pm$0.07 (benzene), 0.42$\pm$0.19 (toluene), 0.17$\pm$0.08 (m,p-xylene), 0.06$\pm$0.03 (o-xylene), 0.01$\pm$0.00 (styrene), and 0.08$\pm$0.06 (ethylbenzene), respectively. Evaporative (mostly running loss) and tailpipe VOC emissions in tunnel tests could be resolved by the PMF model. The evaporative emissions accounted for nearly one-half of the total vehicular VOC emissions and ozone formation poential, indicating that evaporative and tailpipe emissions contributed equally to ~~VOC emissions~~NMVOC

emission inventories, air quality, and energy. The relative contributions of evaporative NMVOC emissions to total vehicular NMVOC emissions are temperature-dependent with the average increasing ratio of ~~7.55~~4% °C^{-1}. The primary ~~emission ratio (ER ,~~ ER (m/m) of VOCs/NO$_x$ was approximately 2.04, suggesting that vehicular NO$_x$ and VOCs can be co-emitted with a proper ER. According to the vehicular ERs of VOCs/NO$_x$ in Tianjin (2000-2016) and China (2010-2030), as even more stringent emission standards are implemented in the future, the O$_3$ chemical regimes were likely to be VOCs-limited (i.e., 8:1 threshold) for cities or regions where VOCs and NO$_x$ emissions are dominated by vehicular exhaust. Our study enriched the database on the fleet-average emission factors of on-road vehicles for emission inventory, air quality modeling, and health effects studies, provided ~~implications for following O$_3$ control in China from the view of primary emission~~diagnositc ratios (v/v) of primarily vehicular emissions for apportioning vehicular and non-vehicular contributions to reactive species and determination of the photochemical age of air masses, and highlighted the importance of further control of evaporative emissions.

1 Introduction

Volatile organic compounds (VOCs) and NO$_x$, largely emitted from fossil-fuel-powered vehicles in urban areas, are always associated with severe haze, tropospheric ozone (O$_3$) episodes and human health risks (Lelieveld and Pöschl, 2017; Li et al., 2017; Song et al., 2017b; Peng et al., 2017; Kelly and Zhu, 2016; Liu et al., 2015b; Guo et al., 2014; Parrish and Zhu, 2009). VOCs are precursors of secondary organic aerosol (SOA) and tropospheric O$_3$ (Huang et al., 2015; Atkinson and Arey, 2003; Carter, 1994). NO$_x$ controls have been reported to be more beneficial than SO$_2$ controls for improvement of PM$_{2.5}$ air quality in northern China (Song et al., 2017b; Cheng et al., 2016). Vehicular activity is the most significant contributor to ambient VOCs in Chinese megacities, such as Beijing (Wang et al., 2016), Tianjin (Liu et al., 2016; Han et al., 2015), Shanghai (Cai et al., 2010), and Guangzhou (Wu et al., 2016). Vehicle emissions have also been recognized as a major source of NO$_x$ in northern China (Jing et al., 2016; He et al., 2016; Tan et al., 2016). Establishing reliable emission inventories for VOCs, NO$_x$ and CO are crucial for the photochemical study and simulating the complex atmospheric environment changes (Zhang et al., 2018a; Wang et al., 2017). Although emission factors (EFs) of VOCs, NO$_x$ and CO from individual vehicle have been widely tested by the portable emission measurement system (PEMS) (Zhang et al., 2016b), information on real-world EFs for a typical urban fleet is still limited (Song et al., 2018), hindering the development of a more reliable emission inventory in China.

It is known that there are two types of VOC emissions from vehicles: tailpipe emissions and evaporative emissions. Tailpipe emissions have been well-controlled across the global, but vehicular evaporative emissions have been largely neglected in China. With the control of tailpipe exhaust emissions, the contribution of evaporative emissions to vehicular VOC emissions is rapidly increasing. Vehicular evaporative emissions can be generally grouped into hot soak, diurnal, permeation, refueling process, and running loss (Yue et al., 2017; Liu et al., 2015a). Source profiles and EFs of VOC from hot soak, diurnal, permeation and refueling process have been well characterized in laboratories, but VOC emissions from running loss are less understood because no facility in China could accommodate the test procedures or track-based tank temperature profile generation (Liu et al., 2015a). Tunnel test might be the most idealized measure to estimate primary vehicular VOC emissions including both

tailpipe and evaporative emissions (mostly running loss) without oxidation degradation by ultraviolet (UV) light (Kowal et al., 2017). Source apportionment methods could be used to apportion tailpipe and evaporative VOC emissions (Gertler et al., 1996). Currently, the relative contributions of tailpipe and evaporative emissions to vehicular VOC emissions in China remain poorly quantified, though evaporative emissions are a major source of VOC emissions in China (Liu et al., 2015a).

5   In addition, few studies have been performed to determine the emission ratio (ER) of VOCs to NO_x (Ehlers et al., 2016), which plays a critical role in identifying the O_3 chemical regimes for reducing atmospheric secondary pollution (Edwards et al., 2014; Liu et al., 2013; Schnell et al., 2009). Although all emission control strategies have benefits in the reduction of O_3 precursors, inappropriate reduction ratios of VOCs to NO_x can lead to an increase in surface O_3 (Liu et al., 2013). The well accepted theory is that a transition from a VOCs-limited to NO_x-limited regime appeared at a VOCs/NO_x ratio of

10   approximately, e.g., 8:1, for VOCs expressed as the concentration of carbon atoms (Seinfeld, 1989). Thus far, the vehicular emission ratio of VOCs/NO_x remain under study, though vehicular emission is the key contributor to both ambient VOCs and NO_x in Chinese megacities. The NO_x emitted from on-road vehicles is released into the atmosphere as a mixture of NO and NO_2 (Song et al., 2018). NO_2, instead of NO_x, is among the criteria pollutants according to the World Health Organization (WHO) Air Quality Guidelines because of associated adverse health effects. Understanding the ratio of NO_2 to NO_x in primary

15   vehicular exhaust (f_{NO_2}) is necessary for photochemical production of O_3 and vehicle emission control strategies (Ehlers et al., 2016; Jenkin, 2014; Clapp and Jenkin, 2001).

    Beginning in the 1990s, China has implemented vehicular emission control programs, including controls for new vehicles and in-use vehicles, improvements in fuel quality (e.g., the promotion of unleaded gasoline and low-sulfur fuels), and promotion of alternative fuels and incentives for electric vehicles (Wu et al., 2017). Emission standards have been upgraded from China

20   I (equals to Euro I) in 2001, to China V in 2015. China is experiencing a rapid improvement in vehicle emission control technologies that have impacted vehicular emissions. However, information on real-world EFs for a typical urban fleet remains limited, particularly for VOCs including tailpipe and evaporative emissions. The fleet-average EFs measured from a inner urban tunnel are EFs of typical driving cycles in urban areas. The overall objectives of this study were to: (1) update real-world local EFs of VOCs, NO-NO_2-NO_x, and CO from detailed vehicular types in Tianjin in northern China; (2) investigate the

25   primary NO_2/NO_x ratio and VOCs/NOx ratio for on-road vehicular emissions; (3) explore the source profiles of tailpipe and evaporative emissions and their relative contributions to vehicular VOC emissions; and (4) diagnose the trends of the vehicular EFs of VOCs-NO_x-CO in China. The results from this study enriched the database on the fleet-average emission factors of on-road vehicles for source apportionment, emission inventory, air quality modeling, and health effects studies, and provided new insights into tailpipe and evaporative VOC emissions.

2 Materials and methods

2.1 Tunnel description

The measurement campaign was conducted from August 8th to August 24th, 2017, in the Wujinglu (WJL) tunnel ($117°12'15''$, $39°8'31''$), an urban tunnel in the city center of Tianjin in northern China. In the WJL tunnel (as shown in Fig.1), 14866 ± 900 (mean±standard deviation) vehicles passed through per day during the measurement campaign. As there is a 40 km h^{-1} speed limit in the tunnel, the average traffic speeds during the study period were 35.6 ± 1.7 km h^{-1} at the entrance of the tunnel, and 38.7 ± 2.1 km h^{-1} at the tunnel exit. The fleet in the WJL tunnel was mainly comprised of light-duty passenger vehicles (LDPVs), which accounted for $96.33\pm0.69\%$ of the total vehicles. Gasoline vehicles (GVs) was the majority ($94.24\pm0.32\%$) in the fleet. Measurements were continuously conducted at inlet (1#, 45 m from the tunnel entrance), middle (2#, 605 m from the tunnel entrance), and outlet (3#, 975 m from the tunnel entrance) sites on the same side in the north bore. The validated lengths for the downslope (1#-2#, gradient of approximately -4%), upslope (2#-3#, gradient of approximately 4%), and overall (1#-3#) of the tunnel are 560, 370, and 930 m, respectively. The cross-sectional area of the tunnel is approximately 54 m^2. There was no fresh air supply throughout the bores; therefore, dilution of air pollutants was eliminated. Longitudinal jetting ventilation fans along the ceiling throughout the tunnel were inactive during the sampling periods. Ventilation was thus only induced by the flow of traffic through the tunnel and prevailing winds. As the traffic light control is at least 250 m from the entrance of the tunnel, cold start vehicular emissions were negligible.

2.2 Measurements and analytic methods

Meteorological data including temperature (T), relative humidity (RH), wind speed (WS), wind direction (WD), and atmospheric pressure (P) were measured using VAISALA WXT520 (Helsinki, Finland) automatic weather stations with a time resolution of 1 min. The actual volumetric flow rates induced by the vehicular fleet and the prevailing winds in the tunnel were continuously measured using ultrasonic gas flowmeters (Flowsick-200 SICK MAIHAK, Germany) with a time resolution of 1 min, which have also been used in previous tunnel tests (Song et al., 2018; Zhang et al., 2018b; Imhof et al., 2006).

Traffic count and vehicular speed were continuously monitored using roadside laser loop detectors (AxleLight RLU11) that were installed at both the inlet (1#) and middle (2#) of the WJL tunnel. The vehicles could be grouped into 14 categories based on wheelbases and axle-number. A high-definition vehicular license plate recognition system was installed at a pedestrian overpass approximately 115 m from the exit of the tunnel. Additionally, video footage was also recorded for data validation and review. The license plates of vehicles passing through the tunnel during the measurement campaign were matched with the registered vehicle database (until August 2017) of Tianjin to obtain vehicular types, in-use fuel types, emission standards, and other information regarding the vehicles. Vehicular classification results were obtained from the license plates in this study, instead of those from the loop detectors. The fleet was classified into gasoline vehicles (GVs), diesel vehicles (DVs), and alternative-fuel vehicles based on the in-use fuel types. On-road vehicles were divided into light-duty vehicles (LDV), and heavy-duty vehicles (HDV). The fleet comprised China I to China V vehicular emission standards.

The NO-NO$_2$-NO$_x$, O$_3$, and CO were measured by micro-monitoring station (Environnement S.A, France), which integrated AC32M module for NO-NO$_2$-NO$_x$ analyzer, O342 module for O$_3$ analyzer, and CO12 module for CO analyzer (Song et al., 2018). The AC32M measurement module was used to continuously measure NO-NO$_2$-NO$_x$, which operates on the principle that NO will emit light (chemiluminescence) in the presence of highly oxidizing O$_3$ molecules. The O342 measurement module (specifically recording low concentrations) uses the principle of O$_3$ detection by absorption in ultraviolet light. The continuous CO12 measurement module uses the principle of detection by absorption in infrared light. The minimum detectable limits for the NO-NO$_2$-NO$_x$, O$_3$, and CO analyzers are 0.4ppb, 0.4ppb, and 0.05 ppm, respectively. We regularly maintained, calibrated, and cleaned the instruments to ensure that the measurements were reliable. Datasets for NO-NO$_2$-NO$_x$, O$_3$ and CO were available as 1 min values, which were then aggregated to 1 h mean values. Additionally, ambient concentrations of air pollutants (PM$_{2.5}$, NO-NO$_2$-NO$_x$, O$_3$ and CO) during the measurement periods were collected from national air quality monitoring sites (NAQMS) (Song et al., 2017b).

The non-methane VOCs (NMVOCs) samples were collected at 3-h intervals both in the inlet (1#) and middle (2#) of the tunnel in 3.2-L pre-evacuated stainless-steel canisters (Entech Instruments, Inc., Simi Valley, CA, USA) at a constant flow rate of 17.8 mL min^{-1} on August 10-11 and August 19-20, 2017 (two weekdays and two weekend days). The NMVOCs samples were collected at 3-h intervals (00:00-03:00, 03:00-06:00, 06:00-09:00, 09:00-12:00, 12:00-15:00, 15:00-18:00, 18:00-21:00, and 21:00-00:00 LT) on each sampling day. The samples in the canisters were drawn into the pre-concentrator from one of the two-channel samples. A total of 99 target NMVOC species (29 alkanes, 12 alkenes, 16 aromatics, 28 Halocarbons, and 14 OVOCs (oxygenated VOCs)) were analyzed using a high-resolution gas chromatography-flame ionization detector (GC-FID) and gas chromatography-mass selective detector (GC-MS). Details regarding the laboratory analysis of the NMVOCs can be found in our previous study (Zhang et al., 2018b).

2.3   Emission factor calculation

The average EFs for vehicles traveling through the tunnel were estimated using the following formula which has been widely used in previous studies (Song et al., 2018; Fang et al., 2018; Zhang et al., 2018b; Gertler et al., 1996; Pierson et al., 1996; Pierson and Brachaczek, 1983).

$$EF_{fleet} = \frac{(C_{Outlet} - C_{Inlet}) \times M \times A \times v \times T}{V_m \times N \times L} \tag{1}$$

where, EF (mg km^{-1} veh^{-1}) is the fleet-average emission factor. C_{Outlet} and C_{Inlet} (ppm) are the air pollutants concentrations at the outlet and inlet of the tunnel, respectively. M (g mol^{-1}) is the relative molecular mass of the air pollutant. A (m^2) is the tunnel cross section area in m^2 (54 m^2). v (m s^{-1}) is the air velocity parallel to the tunnel measured by the ultrasonic gas flowmeters. V_m is the standard molar volume (22.4 L mol^{-1} in this study). N (veh) is the traffic count traveling through the tunnel during the time interval (T = 3600 s). L (m) is the validated length between the two sampling sites (downslope: 560 m, upslope: 370 m, and overall: 930 m).

NO at the inlet of the tunnel can be converted to NO_2 in the presence of O_3 transported from outside of the tunnel mainly by the following reaction:

$$NO + O_3 \rightarrow NO_2 + O_2 \tag{R1}$$

Thus, there were three NO_2 sources measured at the outlet of the tunnel: ambient NO_2 carried into the tunnel due to the piston effect, the transformation of NO, and the primary vehicular NO_2. The ratios of the EFs of NO_2 to EFs of NO_x from on-road vehicles were defined as follows:

$$Ratio1 : ER_{NO_2/NO_x} = \frac{[NO_2]_{Outlet} - [NO_2]_{Inlet}}{[NO_x]_{Outlet} - [NO_x]_{Inlet}} \tag{2}$$

$$Ratio2 : ER_{NO_2/NO_x} = \frac{([NO_2]_{Outlet} - [NO_2]_{Inlet}) - ([O_3]_{Inlet} - [O_3]_{Outlet})}{[NO_x]_{Outlet} - [NO_x]_{Inlet}} \tag{3}$$

where Ratio 1 is the ratio of the primary emitted and transformed NO_2 to primary emitted NO_x by volume. Ratio 2 is the ratio of the primary emitted NO_2 excluding the O_3 titration ~~reaction (~~ (Reaction R1) to primary emitted NO_x by volume. Thus, the $C_{Outlet} - C_{Inlet}$ in equation (1) were $([NO]_{Outlet} - [NO]_{Inlet}) + ([O_3]_{Inlet} - [O_3]_{Outlet})$ for NO, and $([NO_2]_{Outlet} - [NO_2]_{Inlet}) - ([O_3]_{Inlet} - [O_3]_{Outlet})$ for NO_2 when estimating the primary EFs of the NO and NO_2 for on-road vehicles (Song et al., 2018).

A regression method was used to differentiate between the EFs of HDV and LDV, and DVs and GVs. The regression model (Song et al., 2018; Colberg et al., 2005; Gertler et al., 1996; Pierson et al., 1996) is as follow:

$$EF = \alpha + \beta \times pCV + \epsilon \tag{4}$$

where EF is the fleet-average emission factor, α is the EF of the LDV (or GVs), $\alpha + \beta$ is the EF of the HDV (or DVs), pCV is the proportion of the specific vehicle categories (HDV or DVs), and ϵ is the random error.

2.4 Ozone formation potential

NMVOCs play a significant role in the formation of troposphere O_3 (Edwards et al., 2014; Seinfeld, 1989). Ozone formation potential (OFP) is widely used to assess VOC species involved in O_3 formation. The maximum incremental reactivity (MIR) factors from Carter (1994) were used to calculate the OFP from vehicle emissions. The MIR factors are in units of grams of O_3 per gram of NMVOCs; therefore, the EF of potential O_3 for individual NMVOC could be estimated by the MIR coefficient times the EF for each NMVOC species (Zhang et al., 2018b; Cui et al., 2018; Ho et al., 2009).

2.5 PMF receptor model description

Positive matrix factorization (PMF) is an advanced receptor model that decomposes a matrix of sample data (X) into two matrix, source contribution matrix (G) and source matrix (F), based on observations at the sampling site. The PMF model can

be expressed as follows (Paatero and Tapper; Paatero, 1997):

$$X_{ij} = \sum_{k=1}^{p} g_{ik} f_{kj} + e_{ij} \tag{5}$$

where, X_{ij} is the jth compound concentration of the ith sample, g_{ik} is the contribution of the kth source to the ith sample, f_{kj} is the source profile of jth compound in the kth source, e_{ij} is the residual matrix for the jth compound in the ith sample, and

5   p is the total number of independent sources.

The elements (g_{ik} and f_{kj}) are constrained to non-negative values. The task of PMF is to calculate the minimum value Q, as follows:

$$Q(E) = \sum_{i=1}^{n} \sum_{k=1}^{m} (\frac{e_{ij}}{\sigma_{ij}})^2 \tag{6}$$

where, σ_{ij} is the uncertainty in the jth compound for the ith sample. In this study, EPA PMF 5.0 was used for distinguishing

10 tailpipe and evaporative sources in vehicular NMVOC emissions. More detailed PMF operations were reported in previous studies (Liu et al., 2018; Zheng et al., 2018; Liu et al., 2016).

2.6   COPERT IV model

The inter-annual trends of vehicular emission were estimated by the Calculate Emissions from Road Transport (COPERT) IV model. Because Chinese vehicular emission standards are similar to Europe's, the COPERT model, used to estimate emission

15 inventories in European countries, could also be used to calculate vehicle emissions in China (Sun et al., 2016; Jing et al., 2016). The COPERT IV model is an "average speed" model, and the assessment of vehicle emission factors relies on speed-dependent equations. The COPERT IV model has been widely used to establish vehicular emission inventories in China (Sun et al., 2016; Jing et al., 2016).

3   Results and discussion

20 ### 3.1   Measurements data overviews

Variations in concentrations of the air pollutants (NO-NO_2-NO_x, O_3, and CO), flow velocity (measured by the Flowmeter), and traffic flow (measured by the loop detector) during the measurement campaign are shown in Fig.A1-A2. Diurnal cycles in the concentrations of air pollutants, flow velocity, and traffic flow were found at both the inlet (1#), middle (2#) and outlet (3#) of the tunnel, implying that the air pollutants at near-traffic sites are generally affected by traffic activities. The WS measured

25 in the inlet of the tunnel were mainly influenced by the prevailing wind in the ambient air, with the Pearson's correlation coefficient (Pearson's r) of 0.23 ($p<0.001$). The velocity flow measured in the middle (2#) of the tunnel using the flowmeters (Fig.A2a) were more representative of the actual volumetric flow rate, which showed a good correlation with traffic flow with explained variance of 79.2% (Fig.A2c). Thus, the velocity flow data measured using the flowmeters were used to estimate the fleet-average EFs using equation (1).

Average meteorological factors and the concentrations of air pollutants during the measurement campaign are summarized in Table A1. To some degree, the air pollutant concentrations measured at the inlet of the tunnel can be regarded as roadside air pollution characteristics. The average NO, NO_2, NO_x, O_3 and CO concentrations at the inlet (roadside) were 6.15 ± 7.60, 5.01 ± 2.56, 5.49 ± 2.87, 0.36 ± 0.20, and 2.31 ± 0.66 times greater than those in the ambient air, respectively. The average NO, NO_2, NO_x, O_3 and CO concentrations at the middle of the tunnel were 39.81 ± 30.81, 8.02 ± 5.12, 12.00 ± 7.63, 0.02 ± 0.04, and 2.62 ± 0.77 times greater than those in the ambient air, respectively. The average NO, NO_2, NO_x, O_3 and CO concentrations at the outlet of the tunnel were 114.84 ± 71.79, 9.01 ± 6.32, 23.95 ± 17.12, 0.002 ± 0.01, and 2.98 ± 1.04 times greater than those in the ambient air, respectively. Relatively higher air pollutant concentrations throughout the tunnel (inlet, middle and outlet) were observed as compared with those in the ambient air, except for O_3 because of titration reaction. The average NMVOC concentrations at the inlet and middle of the tunnel were 73.46 ± 26.70 ppb and 104.31 ± 23.06 ppb, approximately 1.50 and 2.13 times greater than the average concentration of the ambient air NMVOCs in Tianjin in August (Liu et al., 2016), respectively, suggesting that traffic activity is a key contributor to near-road VOCs. Adverse health effects have been reported to be associated with the traffic-related air pollution exposure (Sinharay et al., 2017; Cepeda et al., 2017; Chen et al., 2017; Gauderman et al., 2015; Hoek et al., 2002). Our results suggested that the air pollution levels at roadside and tunnel micro-environments were far higher than those measured in the ambient air (NAQMS), indicating high traffic-related health risks because of the high population density living near major roads. The traditional assessment of the health burden associated with exposure to air pollution might be underestimated due to the low spatial resolution of exposure assignment (Song et al., 2017a), and should be carefully adjusted to account for the high traffic-related exposure risks.

The highest NO_2/NO_x (v/v) were observed in the ambient air (0.85 ± 0.08), followed by the inlet (0.79 ± 0.11), middle (0.58 ± 0.15) and outlet (0.34 ± 0.11). The NO_2/NO_x decreased as the measurement site moved closer to vehicular emission sources. During the study period, NO_2 constituted the dominant fraction of NO_x at all three sites, although NO was the dominant proportion of NO_x from the vehicular emissions (Wild et al., 2017; Simmons and Seakins, 2012; Soltic and Weilenmann, 2003). Our results differed from previous studies, which reported that NO constituted the dominant fraction of NO_x in the United Kingdom (UK) (Carslaw, 2005) and Korea (Pandey et al., 2008). However, the NO_2/NO_x ratio was reported to be 0.60 in Beijing (Wang et al., 2015b) and 0.61 in Langfang (Song et al., 2016), two neighboring cities of Tianjin. The high fractions of NO_2 in NO_x at the three sites were likely because of the strongly oxidizing atmosphere in the Beijing-Tianjin-Hebei region. The O_x (NO_2+O_3) levels were highest at the outlet (99.53 ± 30.42 ppb), followed by the middle (90.03 ± 28.42 ppb), inlet (77.17 ± 17.21 ppb), and ambient air (60.17 ± 22.38). The different pollution characteristics of the photochemical oxidants in the ambient, inlet, middle and outlet of the tunnel might be attributed to the oxidant partition induced by the NO_x variability (Jenkin, 2014; Clapp and Jenkin, 2001). Estimation of the primary on-road vehicular NO_2/NO_x emission ratios could help to understand the oxidation of NO to NO_2 in the traffic micro-environment. VOCs/NO_x ratios have been widely used to determine the O_3 chemical regimes (Seinfeld, 1989; Zou et al., 2015). Seinfeld (1989) reported that O_3 formation transited from VOCs-limited to NO_x-limited when the VOCs/NO_x ratio was greater than 8:1 for the VOCs expressed as the concentration of carbon atoms (ppbC). The inlet (3.43 ± 1.50 ppbC/ppbv) and outlet (2.74 ± 0.90 ppbC/ppbv) of the tunnel were VOCs-limited regions during the measurement campaign according to the VOCs/NO_x ratios (i.e., the 8:1 threshold) (Seinfeld, 1989).

3.2 Emission factors of NO-NO$_2$-NO$_x$ and CO

As shown in Fig.2, we estimated fleet-average EFs under road conditions of downslope (1#-2#), upslope (2#-3#), and over-all (1#-3#). The fleet-average EFs in this study (pollutant: downslope EF, upslope EF, and overall EF in mg km^{-1} veh^{-1}) were estimated, respectively, as follows: (NO: 61.92±72.46, 158.58±73.48, 97.52±69.84), (NO$_2$: 16.52±11.49, 23.98±20.14, 15.86±9.38), (NO$_x$: 79.45±78.43, 181.22±88.29, 116.56±77.61), and (CO: 269.96±342.38, 577.76±382.22, 344.67±250.01). The fleet-average upslope EFs of NO, NO$_2$, NO$_x$, and CO were approximately 2.6, 1.4, 2.3, 2.1 times greater than those of the downslope, suggesting the EFs of NO-NO$_2$-NO$_x$ and CO are greatly affected by road gradients. These results were comparable with Chang et al. (2008)'s study which noted that upslope (gradient of around 1.3%) pollutant EFs for PM$_{2.5}$, PM$_{10}$, CO, NO$_x$, SO$_2$ are twice as large as those of the downslope. The EFs of NO-NO$_2$-NO$_x$ and CO in this study were compared to those from other tunnel studies in China (Table 1). The downslope (upslope) EFs (mg km^{-1} veh^{-1}) of NO$_x$ and CO improved from 145±67 (331±166) and 910±470 (1470±630) in 2006 (Chang et al., 2008) to 79±78 (181±88) and 270±342 (578±382) in 2017. In addition, our results were the lowest compared with other tunnel studies in China mainly because of the low propor-tion of heavy-duty diesel vehicles (0.35±0.35%) in the fleet and the strict enforcement of vehicular emission control strategies (China IV: 40.20±0.85%, China V: 47.76±1.29%).

As shown in Fig.2, the average EFs of NO, NO$_2$, NO$_x$, and CO showed similar diurnal variations, with the highest values before dawn (00:00-05:00 LT). As tested by Zhang et al. (2015) in Guangzhou in 2014, the EF of PM$_{2.5}$ also varied diurnally, with the highest values between 22:00-02:00 LT. The average EFs of NO, NO$_2$, NO$_x$, and CO before dawn (00:00-05:00 LT) were 2.8, 1.8, 2.1, and 2.5 times, respectively, greater than those during other hours (06:00-23:00 LT) of the day, suggesting that the average EFs of the nighttime fleet were higher than those of the daytime fleet. This could be attributed to the increased proportions of HDV and DVs in the fleet at night (Fig.A3a-b). In the WJL tunnel, the fractions of HDV and DVs in the fleet before dawn (00:00-05:00 LT) were 1.5 and 1.9 times those at 06:00-23:00 LT, respectively. This finding was also consistent with Shen et al. (2014)'s study in Beijing, which demonstrated that DVs contributed more to emissions at night than during the day. The proportion of HDV was strongly correlated (R^2=0.70) with that of DVs because DVs accounted for approximately 87.7% of the total HDV traversing the WJL tunnel.

The diurnal variations in the proportions of HDV (or DVs) in the fleet allowed us to conduct linear regressions (equation (4)). According to the regression results (Fig.3 and Table A2), positive correlations between the average EFs and the proportion of HDV (or DVs) were observed for NO-NO$_2$-NO$_x$, and CO, which further demonstrated the significant contribution of HDV (or DVs) to the before-dawn fleet in Tianjin.

The average EFs for the fleet, GVs/DVs, and LDV/HDV are summarized in Table A2. In general, the average upslope EFs of NO, NO$_2$, and NO$_x$ for HDV were 28, 34, 27 times greater than those for LDV. The average downslope EFs of NO, NO$_x$, and CO for HDV were approximately 37, 23, 55 times greater than those for LDV. Additionally, the average upslope EFs of NO, NO$_2$, and NO$_x$ for DVs were approximately 29, 25, 27 times greater than those for GVs. The average downslope EFs of NO, NO$_x$, and CO for DVs were approximately 39, 26, 33 times greater than those for GVs. Our results are comparable to those from Dallmann et al. (2013)'s study, which reported that the EFs of organic aerosol and black carbon from heavy-duty diesel trucks

were 10 and 50 times higher than those of LDV in the United States in 2010, respectively. However, because of the insignificant variation in the compositions of the vehicular emission standards (from China I to China V) during the measurement campaign (Fig.A3c), an attempt to differentiate EFs under different emission standards by multiple linear regression (Zhang et al., 2018b; Hwa et al., 2002) failed. Although the EFs estimated by the tunnel tests were considered as EFs in a real-world setting, there were still several limitations, such as the limited speeds and accelerations, and that most of the vehicles were operating under hot-stabilized conditions (Gertler, 2005). During the study campaign, the average proportion of HDV (DVs) traversing the WJL tunnel was 1.56±1.26% (1.97±0.32%). Although the low proportion of HDV (DVs) limited the accuracy of the estimated EFs of HDV (DVs) using the linear regression model, the fleet-average EFs in the urban tunnel were more representative of urban areas because of the similar fleet composition between the urban tunnel and the urban areas.

3.3 Primary vehicular f_{NO_2}

The fractions of NO_2 in NO_x (f_{NO_2}, v/v) from vehicular emissions were determined in this tunnel study. As shown in Fig.4, the ratio of the primary emitted and transformed NO_2 to the primary emitted NO_x (Ratio 1) were approximately 0.40±0.21 for downslope (Fig.4a), 0.11±0.23 for upslope (Fig.4e), and 0.19±0.09 for overall (Fig.4f). Excluding the O_3 titration effects (Ratio 2), the fleet-average f_{NO_2} by volume were approximately 0.18±0.09 for downslope (Fig.4b), 0.10±0.22 for upslope (Fig.4f), and 0.10±0.05 for overall (Fig.4j). Student's test (t-test) indicated that there was a significant ($p<0.05$) decrease for downslope and overall f_{NO_2} from Ratio 1 to Ratio 2 because of the relatively high O_3 concentrations at the inlet of the tunnel (Fig.A1d). However, no significant difference ($p>0.05$) was found between upslope f_{NO_2} in Ratio 1 and Ratio 2 because of the inherent low O_3 concentrations from the middle (2#) to the outlet (3#) of the tunnel (Fig.A1d). Considering the primary vehicular f_{NO_2} (Ratio 2), the transformed NO_2 excluding Reaction (R1) contributed 22%, 1%, and 9% to Ratio 2 under the downslope, upslope, and overall condition, respectively. Yao et al. (2005)'s tunnel study also estimated the transformed NO_2 excluding O_3 titration effects contributed 13% to Ratio 2. The upslope primary f_{NO_2} is 44.4% less than those for downslope, indicating a larger fraction of vehicular NO was emitted during the upslope than during the downslope.

Simmons and Seakins (2012) conducted tunnel measurements in a United Kingdom road tunnel and concluded that the f_{NO_2} showed a pronounced diurnal cycle with an average value of 0.17 (95% confidence intervals: 0.14, 0.18) by volume from 7:00 to 19:00 LT. Our analysis suggested that the downslope f_{NO_2} (Ratio 1 and 2) showed a sharp increase from early morning (06:00 LT) to noon (12:00 LT) and a decrease before dawn (00:00-05:00 LT). The diurnal variation in the downslope f_{NO_2} was opposite that of the proportion of HDV (Fig.4c) and DVs (Fig.4d), with the proportion being higher before dawn (00:00-05:00 LT) and lower during the day. The increase in downslope f_{NO_2} could be attributable to a decrease in the proportion of HDV (or DVs) in the total fleet because of the negative correlations between the f_{NO_2} and the proportion of HDVs (or DVs), which is consistent with Simmons and Seakins (2012)'s study. However, no obviously diurnal cycles in upslope and overall f_{NO_2} (Ratio 1 and 2) were observed in this study, particularly for the upslope f_{NO_2}. Additionally, the correlations between upslope (or overall) f_{NO_2} and proportions of HDV (or DVs) were statistically insignificant ($p>0.05$). The results suggested that there were no significant differences in upslope f_{NO_2} among different vehicular types (or fuel types).

The primary vehicular f_{NO_2} can vary considerably depending on such parameters as the vehicular type, fuel type, inspection and maintenance system (I/M), vehicle operation conditions (e.g., cold start, idling, low-speed), and after-treatment devices (e.g., selective catalytic reduction systems, diesel particulate filter, diesel oxidation catalyst) (O'Driscoll et al., 2016; Williams and Carslaw, 2011; Shon et al., 2011; Alvarez et al., 2008; Soltic and Weilenmann, 2003). O'Driscoll et al. (2016) reported
5 that the average f_{NO_2} was 0.44±0.20, and the selective catalytic reduction (SCR) systems had a higher f_{NO_2} (0.55±0.12) for Euro VI diesel passenger cars based on the PEMS. The future f_{NO_2} was projected to increase with the introduction of diesel-oxidation-catalysts (DOC), other after-treatment devices for DVs, and the improvement of fuel quality to meet the successively stringent emission standards in China.

3.4 Emission factors of NMVOCs

10 The average EFs for the 99-target NMVOC species measured in the tunnel in Tianjin are shown in Table A4 (zero emission factors for some NMVOCs results from C_{Outlet} less than or equal to C_{Inlet}). The EFs for NMVOCs reported from a tunnel study in Hong Kong in 2003 (Ho et al., 2009), Guangzhou in 2014 (Zhang et al., 2018c), Nanjing in 2015 (Zhang et al., 2018b), and Hong Kong in 2015 (Cui et al., 2018) are also listed in Table A4. The fleet-average EFs (mg km^{-1} veh^{-1}) for the NMVOCs in the tunnel were 40.56±12.18, which was lower than those of previous studies in Hong Kong in 2003 (568 mg km^{-1} veh^{-1})
15 (Ho et al., 2009), Guangzhou in 2014 (1.10×10^3 mg km^{-1} veh^{-1}) (Zhang et al., 2018c), Nanjing in 2015 (373.88 mg km^{-1} veh^{-1}) (Zhang et al., 2018b), and Hong Kong in 2015 (58.8±50.7 mg km^{-1} veh^{-1}) (Cui et al., 2018). This might be attributed to the improvement of fuel quality and emission standards in China. By group, alkanes, alkenes, aromatics, halocarbons, and OVOCs had average EFs of 19.59±6.84, 5.52±1.31, 9.02±2.25, 0.20±0.14, and 5.29±2.22 mg km^{-1} veh^{-1}, respectively (Fig.5a).
20 The five most abundant VOC species (Fig.6) in the vehicular emissions were, in decreasing order, isopentane (6.80 mg km^{-1} veh^{-1}), toluene (3.29 mg km^{-1} veh^{-1}), ethylene (2.56 mg km^{-1} veh^{-1}), methyl tert-butyl ether (MTBE: 2.48 mg km^{-1} veh^{-1}), and n-pentane (2.14 mg km^{-1} veh^{-1}) (Table A4), accounting for 37.90±5.37% of the total NMVOCs emissions. The abundance (v/v) of isopentane (12.89±5.98%), toluene (8.01±2.51%) and n-pentane (4.88±1.41%) were high in the emission of the tunnel fleet (Fig.6), which is consistent with Tsai et al. (2006)'s study. These three species are primary indicators of
25 gasoline evaporation (Liu et al., 2008; Yue et al., 2017; Hwa et al., 2002; Tsai et al., 2006), implying that the control of vehicular evaporative emission becomes increasingly important with the improvement in fuel quality and emission standards in China (Liu et al., 2015a). It should be noted that MTBE, a gasoline oxygenation additive used to increase the octane number and reduce vehicular emissions of carbon monoxide, accounted for 5.73±1.53% of the vehicular NMVOCs emissions. MTBE is a maker specific to gasoline-related sources and it can be present in both gasoline vapors and gasoline-powered vehicle
30 exhausts due to incomplete combustion (Zhang et al., 2013; Poulopoulos and Philippopoulos, 2000).

Our previous tunnel study in Nanjing in 2015 (Zhang et al., 2018b) reported that the five most abundant VOC species in vehicle emissions were, in decreasing order, ethane (52.47±6.72 mg km^{-1} veh^{-1}), isopentane (17.82±11.97 mg km^{-1} veh^{-1}), propane (11.80±3.48 mg km^{-1} veh^{-1}), ethylene (10.17±1.05 mg km^{-1} veh^{-1}), and toluene (9.36±5.27 mg km^{-1} veh^{-1}). The relatively high EFs of ethane and propane measured in Nanjing in 2015 are associated with the large fractions of liquefied

natural gas (LNG) fueled vehicles (13%) in the fleet. The most abundant VOC species in vehicular emissions measured in a tunnel in Hong Kong in 2003 (Ho et al., 2009) was ethylene (12.6±4.3 mg km^{-1} veh^{-1}), followed by toluene (12.1±3.9 mg km^{-1} veh^{-1}), n-butane (8.7±3.1 mg km^{-1} veh^{-1}), propane (5.7±2.5 mg km^{-1} veh^{-1}), and isopentane (5.6±2.1 mg km^{-1} veh^{-1}). Generally, isopentane, toluene, and ethylene are the three species frequently observed as the most abundant VOC
5   species in vehicular emissions.

NMVOCs are precursors of O$_3$ formation. The EFs of the O$_3$ formation potential for each VOCs were estimated by the MIR coefficient times the EF for each NMVOC species. The total O$_3$ formation potential was approximately 135.14±36.78 mg km^{-1} veh^{-1}, which is lower than those reported from previous studies in Hong Kong in 2003 (568 mg km^{-1} veh^{-1}) (Ho et al., 2009), Guangzhou in 2014 (1.10×10^3 mg km^{-1} veh^{-1}) (Zhang et al., 2018c), and Nanjing in 2015 (373.88 mg
10   km^{-1} veh^{-1}) (Zhang et al., 2018b). The lower OFP observed in this study is likely attributed to the progression of vehicular technology combined with emission standards (China IV: 40.20±0.85%, China V: 47.76±1.29%). As shown in Fig.5b, the OFPs of alkanes, alkenes, aromatics, halocarbons, and OVOCs were 23.59±9.05, 49.25±11.78, 42.22±14.36, 0.04±0.03, and 15.92±7.77 mg km^{-1} veh^{-1}, respectively. The alkenes (aromatics) accounted for 13.90±2.80% (22.8±4.9%) of total vehicular NMVOCs emissions observed in the tunnel but were nevertheless responsible for 37.60±6.41% (32.2±5.77%) of
15   the total vehicular OFP.

The top five VOC species as the largest contributors to O$_3$ production for individual vehicles were ethylene (22.75±4.24 mg km^{-1} veh^{-1}), toluene (12.94±4.36 mg km^{-1} veh^{-1}), m/p-xylene (12.89±5.47 mg km^{-1} veh^{-1}), propylene (10.99±4.00 mg km^{-1} veh^{-1}), and isopentane (7.93±4.47 mg km^{-1} veh^{-1}) (Fig.6). These findings were consistent with our previous tunnel study in Nanjing in 2015 (Zhang et al., 2018b). Ethylene emissions contributed 17.46±3.84% to the measured VOCs reactivity
20   for vehicular emissions, which was nearly 20.12% in Nanjing in 2015 (Zhang et al., 2018b) and 23% in Hong Kong in 2003 (Ho et al., 2009).

3.5   Source identification of NMVOCs

The fleet-average source profiles of NMVOCs were estimated in section 3.4 by the emission factor method (equation (1)). The VOCs from vehicular emissions were mainly comprised of tailpipe and evaporative emissions. Thus, the fleet-average
25   source profiles were mixed by two factors, tailpipe emissions and evaporative emissions. In the present work, we attempted to distinguish source profiles of NMVOCs from tailpipe and evaporative emissions by PMF methods.

For each NMVOC species, the corresponding inlet concentrations were subtracted (ΔNMVOCs: $C_{Outlet} - C_{Inlet}$) to isolate the emission signals from vehicles traveling through the tunnel. To minimize the uncertainties caused by the NMVOC species with low ΔNMVOCs values, the top 30 NMVOC species (Fig.6) from vehicular emissions were ~~used~~ considered
30   in source apportionment by PMF. Additionally, the species with a number of samples of non-negative ΔNMVOCs (i.e., $C_{Outlet} - C_{Inlet} > 0$) less than 75% were excluded from the PMF model. Finally, the 20 NMVOC species (Fig. 7) were introduced into the PMF model. The highly reactive NMVOCs species were not excluded in the source apportionment because of the low chemical reactions in the tunnel where there is weaker solar radiation, which is different from traditional source apportionment of ambient VOCs (Zheng et al., 2018; Liu et al., 2016).

Two factors (Factor1 and Factor2) were resolved by the PMF analysis~~and their contribution to each species (Fig. 7a) and source profiles (Fig.7b-c) are shown. Approximately 97.07~~. Approximately 98% of the measured NMVOCs from vehicular emissions were explained using the PMF (Fig.A4a). Moreover, for the top ~~30~~ 20 individual NMVOCs species, the PMF model also reproduced the predicted values well, with the ~~average~~ R^2 ~~being 0.71±0.24~~ ranging from 0.44 to 0.97 (Table.~~A3~~A5).
Therefore, we considered that the ΔNMVOCs concentrations in the tunnel could be resolved by the two factors using the PMF model.

The fleet-average EFs of isopentane, ~~toluene~~n-butane, n-pentane, and ~~n-butane~~ isobutane generally showed good correlations with ambient temperature data (Fig.8), suggesting that these four compounds could be recognized as primary indicators of evaporation emissions (Yue et al., 2017; Liu et al., 2008; Tsai et al., 2006; Hwa et al., 2002). High loadings of isopentane (~~65.53~~90.9%), ~~toluene (54.87~~n-butane (84.1%), n-pentane (~~70.29~~89.9%), and ~~n-butane (73.18~~isobutane (91.5%) were found in Factor1. The source apportionment of the NMVOC samples at 3-h intervals provide a unique opportunity to discuss the diurnal variations in factor contributions (Fig.A4b). Factor1 had a higher contribution to vehicular VOC emissions during the daytime, and a lower contribution during the nighttime. In addition, diurnal variations in Factor1 contribution (%) linearly correlated with diurnal variations in temperatures (~~$y = 0.0755x(°C) − 1.8173, R^2 = 0.722$~~$y = 0.04x(°C) − 0.61, R^2 = 0.722$).
Therefore, Factor1 was identified as evaporative emissions, and Factor2 was identified as tailpipe emissions.

As listed in Table.A5, the EFs of the top ~~30~~ 20 VOC compounds in vehicular evaporative and tailpipe emissions were estimated via relative contributions (Fig.7a) and fleet-average EFs (Fig.A4). The EFs for vehicular evaporative and tailpipe emissions were estimated to be 24.9±7.5 and 15.7±3.3 mg km^{-1} veh^{-1}, respectively. In addition, the EFs of OFP from vehicular evaporative and tailpipe emissions were 60.3±4.1 and 74.9±4.5 mg km^{-1} veh^{-1}, respectively.

During the measurement campaign, evaporative emissions accounted for ~~nearly half (49.33~~over half (62.7±~~22.90%)~~37.3%) of the total vehicular NMVOC emissions, and nearly half (44.6%) of the total vehicular OFP. However, the tailpipe emissions of NMVOCs might be underestimated due to the downslope (1#-2#) road conditions. A previous tunnel study noted that the upslope EF of NMVOCs is only 1.3 times that of the downslope (Chang et al., 2008). Thus, the upslope evaporative emissions were estimated to account for ~~approximately 42.82%~~over one-half (56.4%) of the total vehicular upslope NMVOC emissions, supposing that there was no significant difference between evaporative emissions under downslope and upslope conditions, and the upslope EF of NMVOCs is 1.3 times that of the downslope.

It should be noted that the evaporative NMVOC emissions estimated from tunnel tests are mostly running loss emissions, other evaporative emissions (i.e., diurnal, hot soak, permeation, and refueling process) were generally not included, which are also major components of vehicular VOCs emissions. Thus, the evaporative and tailpipe emissions contribute equally to NMVOC emission inventories, air quality, and energy. ~~Nevertheless~~However, the relative contributions of evaporative NMVOC emissions to total vehicular NMVOC emissions ~~are found to be~~ were temperature-dependent with increasing ratio of ~~7.5~~54% °C^{-1} in this study (average ambient temperature: ~~27.13~~27.1±~~2.3~~2.3 °C), suggesting the contribution of evaporative NMVOC emissions estimated during the study period might be overestimated in terms of the whole year (with annual temperature of 12∼15 °C in Tianjin).

3.6 BTEX and diagnostic ratios

The aromatic group of NMVOCs, in particular benzene, toluene, ethylbenzene, p-xylene, m-xylene and o-xylene, which are toxic VOCs known as the BTEX group and have been the subject of intensive studies (Zhang et al., 2018b, 2016a). Emissions from combustion of gasoline and diesel fuels are the largest contributions to ambient BTEX concentrations (Bolden et al., 2015). According to our tunnel ~~tests~~ test in Tianjin, the EFs (mg km^{-1} veh^{-1}) were 1.97±0.52 for benzene, 0.66±0.26 for ethylbenzene, 3.29±1.10 for toluene, 0.48±0.19 for o-xylene, and 1.42±0.42 for m/p-xylene. The emission level of BTEX in this study was compared to that of reported tunnel studies in Taiwan in 2000 (Hwa et al., 2002), Hong Kong in 2003 (Ho et al., 2009), Guangzhou in 2004 (Zhang et al., 2018c), Taiwan in 2005 (Hung-Lung et al., 2007), Guangzhou in 2014 (Zhang et al., 2018c), Nanjing in 2015 (Zhang et al., 2018b), and Hong Kong in 2015 (Cui et al., 2018). As shown in Fig.9, the BTEX levels tested in recent four years (Guangzhou in 2014, Nanjing in 2015, Hong Kong in 2015, and Tianjin in 2017) decreased when compared to those tested during the last decades (Taiwan in 2000, Hong Kong in 2003, Guangzhou in 2004, and Taiwan in 2005). Cui et al. (2018) and Zhang et al. (2018c) noted that the EFs of VOCs from on-road vehicles decreased by 44.7% in Hong Kong from 2003 to 2015, and 9% in Guangzhou from 2004 to 2014, respectively. We conducted the linear regression between BTEX levels and the test year from previous studies and this study, and found the average BTEX levels in China have dramatically decreased during the last decade.

Since the 1990s, China has started vehicular emission control programs, including controls for new vehicles and in-use vehicles, improvements in fuel quality (e.g., the promotion of unleaded gasoline and low-sulfur fuels), promotion of alternative fuels and incentives for electric vehicles (Wu et al., 2017). Emission standards have been upgraded from China I (equals to Euro I) in 2001 to China V in 2015. By estimation from the regressions, the EFs (mg km^{-1} veh^{-1}) in 2000 (before China I) were 12 (95% confidence interval (CI): 5.04, 19.14) for benzene, 5.87 (95%CI: 1.82, 9.92) for ethylbenzene, 29.4 (95%CI: 18.68, 39.97) for toluene, 7.3 (95%CI: 3.53, 11.06) for o-xylene, and 12.41 (95%CI: 0.86, 23.96) for m/p-xylene. The EFs (mg km^{-1} veh^{-1}) in 2017 (after China V) were 1.89 (95%CI: 0, 8.31) for benzene, 2.33 (95%CI: 0, 6.02) for ethylbenzene, 5.24 (95%CI: 0, 14.93) for toluene, 0.92 (95%CI: 0, 4.35) for o-xylene, and 3.54 (95%CI: 0, 14.04) for m/p-xylene. The EFs from on-road vehicles decreased by 84% for benzene, 60% for ethylbenzene, 82% for toluene, 87% for o-xylene, and 71% for m/p-xylene. Generally, the BTEX levels decreased by approximately 79% when emission standards increased from China I to China V. Our result demonstrate that an improvement in fuel quality can significantly reduce vehicular BTEX emissions and bring great health benefits for human beings.

Table 2 presents ratios (v/v) of paired VOCs that have been widely used to indicate relative contributions from different emission sources (Zhang et al., 2013). Among the different NMVOCs measured in the tunnel, toluene and benzene are of particular interest. The ratio of these two NMVOCs is often used either to discriminate traffic emission sources from other anthropogenic sources (Ait-Helal et al., 2015; Steinbacher et al., 2005; Hedberg et al., 2002) or as a chemical clock for the determination of the photochemical age of air masses ~~(Nelson and Quigley, 1983)~~(Du et al., 2018; Nelson and Quigley, 1983). The average toluene-to-benzene ratio (T/B) were 0.78±0.17 for the inlet, and 1.00±0.14 for the middle of the tunnel. Additionally, the vehicular T/B emission ratio was 1.42±0.33. The T/B ratios generally ranged from 2.0-5.8 in refueling vapors (Zhang et al.,

2013), 1.6-5.6 in headspace vapors (Zhang et al., 2013; Liu et al., 2008; Na et al., 2004; Harley et al., 2000), and 1.42-4.19 in tunnel studies (Table 2). Gelencsér et al. (1997) noted that T/B increased as the measurement site moved closer to the vehicular emission sources. In our case, the average T/B measured at the middle was larger than that measured at the inlet of the tunnel, further validating T/B concentration ratio as a tool for characterizing the contributions of vehicular emission sources. ~~The T/B~~
5   ~~ratio for evaporative and tailpipe emissions was 1.56 and 1.23 (v/v), respectively. A higher ratio of the toluene and benzene from~~ ~~evaporation was observed because of the high tolueneconcentration in gasoline in Asia (Liu et al., 2015a; Zhang et al., 2013)~~

    Determining one suitable species to be used as the indicator of vehicular emissions is of great importance. The basic criterion for being a vehicular indicator is that its atmospheric presence is solely and exclusively from vehicular sources. According to the source profile (Fig.6), ethylene and isopentane were the two most abundant species in vehicular NMVOC emissions.
10   However, ethylene is not a reliable tracer for vehicular emission since ethylene is generally emitted from petrochemical industry (Zheng et al., 2018; Liu et al., 2016). Isopentane could be employed as a suitable indicator of vehicular emission. Understanding the vehicular emission ratios of VOC species to isopentane could help apportion the vehicular and non-vehicular contributions to reactive species (Wang et al., 2015a). In our case in WJL tunnel in Tianjin, the characteristic ratios of C6-C8 aromatics to isopentane from vehicular emissions were 0.29 ± 0.07 (benzene), 0.42 ± 0.19 (toluene), 0.17 ± 0.08 (m,p-xylene),
15   0.06 ± 0.03 (o-xylene), 0.01 ± 0.00 (styrene), and 0.08 ± 0.06 (ethylbenzene), respectively. Additionally, based on the tunnel experiments in Chinese major cities from 2014 to 2017 (Table 2), the characteristic ratios of C6-C8 aromatics to isopentane of vehicular emissions were 0.31 ± 0.14 (benzene), 0.78 ± 0.69 (toluene), 0.28 ± 0.15 (m,p-xylene), 0.09 ± 0.13 (o-xylene), 0.09 ± 0.13 (styrene), and 0.13 ± 0.11 (ethylbenzene), respectively.

    The ratios of i-butane/n-butanes (i-B/n-B) ranged from 0.28 (this study) to 0.94 (previous study in Nanjing). A high i-B/n-B
20   ratio was associated with a high proportion of LNG fueled vehicles (Russo et al., 2010). Our previous tunnel study in Nanjing reported that the proportion of LNG vehicles in Nanjing were 13% in the fleet. In this study, the alternative-fueled (including LNG) vehicles only accounted for $3.8\pm0.32\%$ in the fleet in Tianjin. The i-pentane/n-pentane (i-P/n-P) ratios ranged from 1.31 to 3.64 according to the tunnel tests. The MTBE/Benzene (MTBE/B) and MTBE/Toluene (MTBE/T) ratios ranged from 0.38-1.12 and 0.18-0.79, respectively. The MTBE/B and MTBE/T ratios measured in the tunnel tests were much lower than
25   that of 4.1-6.6 and 0.7-3.3, respectively, in refueling vapors reported by Zhang et al. (2013). Higher MTBE/B and MTBE/T ratios in gasoline vapors might be indicators to differentiate between gasoline evaporative and tailpipe emissions. The vehicular ~~exhausts tested~~ emission in tunnel tests had ratios of B, T, E, m,p-X, and o-X to 2,2-DimB ranged from 2.87-24.82, 12.00-56.12, 1.90-8.93, ~~0.54-5.40~~5.50-9.13, and 2.28-6.57, respectively, significantly higher than those of 0.4-1.5, 0.9-4.8, 0.03-1.0, 0.1-1.3, and 0.04-0.8, in gasoline and headspace vapors (Zhang et al., 2013; Na et al., 2004; Harley et al., 2000). Thus, MTBE/B
30   and BTBE/T ratios, and ratios of B, T, E, m,p-X, and o-X to 2,2-DimB, were likely able to differentiate vehicular sources from mixed emission sources.

3.7   The relationship between NMVOCs and NO$_x$

The average NMVOCs/NO$_x$ ratio was approximately 3.43 ± 1.50 ppbC/ppbv at the inlet and 2.74 ± 0.90 ppbC/ppbv at the middle of the tunnel, much lower than the 8:1 threshold. This indicates that the O$_3$ formation was likely to be VOCs-limited

at near-road sites. The diurnal variations in the NMVOCs/NO_x ratios for the middle of the tunnel showed a similar trend to those for the inlet, with a V-shape being minimum during the day (09:00-18:00 LT) and maximum at night (18:00-09:00 LT) (Fig.10a). However, the diurnal variation in the NMVOCs/NO_x ratios measured in the ambient air generally showed a signal peak tendency with a maximum appearing at 14:00-15:00 LT (Liu et al., 2016; Zou et al., 2015). This discrepancy might be associated with the photochemical reactions in the ambient air. In the absence of solar irradiation at the inlet and outlet of the tunnel, O_3-involved photochemical reactions were generally inhibited. Thus, the NMVOCs/NO_x ratios in the tunnel environment were more likely to be influenced by the vehicular emission ratios of NMVOCs to NO_X.

Fig. 10b shows the To investigate the vehicular emission ratios of NMVOCs to NO_X, linear relationships between ΔNMVOCs (i.e., $C_{Outlet} - C_{Inlet}$) and ΔNO_x , and were conducted (as shown in Fig.10b). Generally, ΔNO_x accounted for 80%, 80%, and 94% of the total variance in the NMVOCs expressed as a concentration by volume (ppbv), carbon atoms (ppbC), and mass (μ g m^{-3}), respectively. The good correlations between ΔNMVOCs and ΔNO_x indicated that there were relatively stable average constant ERs of the NMVOCs to NO_x for on-road vehicles. Based on the slope of the regression line, the ER of the NMVOCs to NO_x during the measurement campaign was approximately 0.84 (95%CI: 0.67, 1.01) for VOCs expressed as the concentration of carbon atoms (ppbC), much lower than the 8:1 threshold. Thus, O_3 chemical regimes were more likely to be VOCs-limited for cities or regions where VOCs and NO_x emissions are dominated by vehicular exhaust. Liu et al. (2016) and Han et al. (2015) noted that vehicular activities were the most significant contributor to the ambient VOCs in Tianjin. In addition, Wu et al. (2016) and Wang et al. (2016) also found that vehicular emission was the highest contributor to VOCs in Guangzhou and Beijing, respectively. O_3 chemical regimes were generally observed to be VOCs-limited in major Chinese cities (Xue et al., 2014), which might be attributable to the low ER of the NMVOCs to NO_x from on-road vehicles. Moreover, good correlation (R^2=0.94) between ΔNMVOCs and ΔNO_x by mass concentration were also observed in our study, indicating the on-road vehicular emission of NMVOCs was proportional to the NO_x, and the ER was approximately 2.04 (95%CI: 1.83, 2.26). It should be noted that the ER values should be carefully treated to evaluate the NMVOCs emissions from NO_x emissions, because of the differences between real-world vehicles, including vehicular technology, fleet composition, driving conditions, and other variables.

To understand the interannual trends of the vehicular emission ratios of VOCs/NO_x, a critical value in identifying O_3 chemical regime, we estimated vehicular emissions of NO_x, CO, and VOCs in Tianjin from 2000 to 2016 (Fig.11a-c). The COPERT IV model, an "average speed" model, was used in this study to estimate vehicular emissions in Tianjin because Chinese vehicular emission standards are similar to Europe's (Jing et al., 2016; He et al., 2016; Sun et al., 2016). Total emissions of NO_x from the Tianjin vehicle fleet increased by 15.17% from 2000 (60.19 Gg) to 2011 (69.32 Gg), and decreased by 20.46% from 2011 to 2016 (55.14 Gg). Heavy-duty trucks (HDT) were the largest contributors of vehicular NO_x emissions since 2012 (Song et al., 2018), and their contribution has increased from 35.47% in 2000 to 46.86% in 2016. The Total emissions of CO and VOCs from the Tianjin vehicular fleet decreased by 52.47% and 51.44%, respectively. The results suggested that the environmental benefits from the decreased vehicular EFs of CO and VOCs from 2000 to 2016 (Fig.9) were great enough to offset the increased vehicle-kilometers traveled (VKT) and larger fleets. Passenger cars (PC) were the primary source of vehicular CO and VOCs emissions and accounted for 44.11% and 46.14% in 2000 to 77.42% and 81.75% in 2016.

We estimated annual emission ratios of VOCs/NO$_x$ in Tianjin from 2000 to 2016 (Fig.11d), and in China from 2010 to 2030 (Fig.11e). The estimated total vehicular emission ratios of VOCs to NO$_x$ in China for NAP (Standards are assumed at the same level of 2013 during the future years (e.g., China IV for LDGVs and China III for HDDVs)), PC1 (increasingly stringent emission standards and improved fuel quality are implemented according to a probably timetable), and PC2 scenarios (for internal combustion engine vehicles, the implementation of future emission standards is consistent with that under the PC1 scenario) from 2010 to 2030 were based on Wu et al. (2017)'s study. The annual emission ratios of VOCs/NO$_x$ from the Tianjin vehicle fleet decreased from 1.16 in 2000 to 0.62 in 2016. We estimated the emission ratio of VOCs/NO$_x$ to be approximately 2.04 (95%CI: 1.83, 2.26) through the tunnel test (Fig.10b), which is almost 3.3 times greater than that estimated from the COPERT IV model. This discrepancy might be attributable to the differences in fleet compositions between the tested tunnels and cities, especially cities that HDT are often not allowed to access to (Song et al., 2018). In general, PC (3.01±0.17) and LDV (3.07±1.47) have higher emission ratios of VOCs/NO$_x$ than HDT (0.15±0.04) and BUS (0.17±0.07) from 2000 to 2016. The high proportion of HDT (1.11%) in the Tianjin vehicular fleet, 5 times greater than that in the tunnel fleet (0.16%), led to lower emission ratios of VOCs/NO$_x$ than those in the tunnel test. The vehicular emission ratios of VOCs/NO$_x$ in China from 2010 to 2016 have a good agreement (r=0.84, p<0.05) with those in Tianjin. The emission ratios of VOCs/NO$_x$ in PC1 and PC2 scenarios were projected to increase from 0.45 and 0.40 in 2017 to 0.80 and 0.71 in 2030, respectively. And the emission ratios of VOCs/NO$_x$ under current emission standards were to remain nearly unchanged (0.33) since 2020. As even more stringent emission standards are properly implemented in the future, the O$_3$ chemical regimes were more likely to remain VOCs-limited (i.e., 8:1 threshold) for cities or regions where VOCs and NO$_x$ emissions are dominated by vehicular exhaust.

4 Conclusions

Based on a more-than-two-week test of on-road vehicular VOCs-NO$_x$-CO emissions in the Wujinglu tunnel in urban Tianjin in northern China, and on the use of the statistical regression model, PMF receptor model, and COPERT IV model, this study allowed for characterizing the primary VOCs-NO$_x$-CO emissions from vehicular exhaust systematically. The fleet-average EFs of VOCs, NO-NO$_2$-NO$_x$, and CO under upslope, downslope and overall road conditions were measured through tunnel tests.

The ratios (v/v) of NO$_2$ to NO$_x$ in the primary vehicular exhaust were approximately 0.18±0.09, 0.10±0.22 and 0.10±0.05 for downslope, upslope, and the entire tunnel, respectively. The fleet-average EFs for the 99-target NMVOCs in the tunnel were 40.56±12.18 mg km^{-1} veh^{-1}, which was lower than the previous studies. This study found that the improvement of fuel quality (from China I to China V) can significantly reduce feet-average EFs of VOCs (especially for BTEX). The BTEX (benzene, toluene, ethylbenzene, p-xylene, m-xylene and o-xylene) levels decreased by approximately 79% when emission standards increased from China I to China V.

The vehicular T/B emission ratio (ER) was 1.42±0.33. Isopentane could be employed as a suitable indicator of vehicular emission. The characteristic ratios of C6-C8 aromatics to isopentane from vehicular emissions were 0.29±0.07 (benzene), 0.42±0.19 (toluene), 0.17±0.08 (m,p-xylene), 0.06±0.03 (o-xylene), 0.01±0.00 (styrene), and 0.08±0.06 (ethylbenzene), respectively. Evaporative (mostly running loss) and tailpipe VOC emissions in tunnel tests could be resolved by the PMF

model, and ~~the evaporative and tailpipe emissions contributed equally to NMVOC emission inventories, air quality, and energy.~~ ~~The~~ evaporative emissions accounted for over half (62.7±37.3%) of the total vehicular NMVOC emissions, and nearly half (44.6%) of the total vehicular OFP. Besides, the relative contributions of evaporative NMVOC emissions to total vehicular NMVOC emissions are found to be temperature-dependent with increasing ratio of ~~7.55~~4% $°C^{-1}$.

5   The vehicular ER of the NMVOCs to NO_x during the measurement campaign was approximately 0.84 (95%CI: 0.67, 1.01) for VOCs expressed as the concentration of carbon atoms (ppbC), much lower than the 8:1 threshold. Thus, O_3 chemical regimes were more likely to be VOCs-limited for cities or regions where VOCs and NO_x emissions are dominated by vehicular exhaust. Our study enriched the database on the fleet-average emission factors of on-road vehicles for emission inventory, air quality modeling, and health effects studies, provided implications for following O_3 control in China from the view of primary

10   emission, and highlighted the importance of further control of evaporative emissions.

References

Ait-Helal, W., Beeldens, A., Boonen, E., Borbon, A., Boréave, A., Cazaunau, M., Chen, H., Daële, V., Dupart, Y., Gaimoz, C., Gallus, M., George, C., Grand, N., Grosselin, B., Herrmann, H., Ifang, S., Kurtenbach, R., Maille, M., Marjanovic, I., Mellouki, A., Miet, K., Mothes, F., Poulain, L., Rabe, R., Zapf, P., Kleffmann, J., and Doussin, J.-F.: On-road measurements of NMVOCs and NOx: Determination of light-duty vehicles emission factors from tunnel studies in Brussels city center, Atmospheric Environment, 122, 799 – 807, https://doi.org/10.1016/j.atmosenv.2015.09.066, 2015.

Alvarez, R., Weilenmann, M., and Favez, J.-Y.: Evidence of increased mass fraction of NO2 within real-world NOx emissions of modern light vehicles — derived from a reliable online measuring method, Atmospheric Environment, 42, 4699 – 4707, https://doi.org/10.1016/j.atmosenv.2008.01.046, 2008.

Atkinson, R. and Arey, J.: Atmospheric Degradation of Volatile Organic Compounds, Chemical Reviews, 103, 4605–4638, https://doi.org/10.1021/cr0206420, 2003.

Bolden, A. L., Kwiatkowski, C. F., and Colborn, T.: New Look at BTEX: Are Ambient Levels a Problem?, Environmental Science & Technology, 49, 5261–5276, https://doi.org/10.1021/es505316f, 2015.

Cai, C., Geng, F., Tie, X., Yu, Q., and An, J.: Characteristics and source apportionment of VOCs measured in Shanghai, China, Atmospheric Environment, 44, 5005 – 5014, https://doi.org/10.1016/j.atmosenv.2010.07.059, 2010.

Carslaw, D. C.: Evidence of an increasing NO2/NOX emissions ratio from road traffic emissions, Atmospheric Environment, 39, 4793 – 4802, https://doi.org/10.1016/j.atmosenv.2005.06.023, 2005.

Carter, W. P.: Development of Ozone Reactivity Scales for Volatile Organic Compounds, Air & Waste, 44, 881–899, https://doi.org/10.1080/1073161X.1994.10467290, 1994.

Cepeda, M., Schoufour, J., Freak-Poli, R., Koolhaas, C. M., Dhana, K., Bramer, W. M., and Franco, O. H.: Levels of ambient air pollution according to mode of transport: a systematic review, The Lancet Public Health, 2, e23 – e34, https://doi.org/10.1016/S2468-2667(16)30021-4, 2017.

Chang, S.-C., Lin, T.-H., and Lee, C.-T.: On-road emission factors from light-duty vehicles measured in Hsuehshan Tunnel (12.9 km), the longest tunnel in Asia, Environmental Monitoring and Assessment, 153, 187, https://doi.org/10.1007/s10661-008-0348-9, 2008.

Chen, H., Kwong, J. C., Copes, R., Tu, K., Villeneuve, P. J., van Donkelaar, A., Hystad, P., Martin, R. V., Murray, B. J., Jessiman, B., Wilton, A. S., Kopp, A., and Burnett, R. T.: Living near major roads and the incidence of dementia, Parkinson's disease, and multiple sclerosis: a population-based cohort study, The Lancet, 389, 718 – 726, https://doi.org/10.1016/S0140-6736(16)32399-6, 2017.

Cheng, Y., Lee, S., Ho, K., and Louie, P.: On-road particulate matter (PM2.5) and gaseous emissions in the Shing Mun Tunnel, Hong Kong, Atmospheric Environment, 40, 4235 – 4245, https://doi.org/10.1016/j.atmosenv.2006.04.002, 2006.

Cheng, Y., Zheng, G., Wei, C., Mu, Q., Zheng, B., Wang, Z., Gao, M., Zhang, Q., He, K., Carmichael, G., Pöschl, U., and Su, H.: Reactive nitrogen chemistry in aerosol water as a source of sulfate during haze events in China, Science Advances, 2, https://doi.org/10.1126/sciadv.1601530, 2016.

Clapp, L. J. and Jenkin, M. E.: Analysis of the relationship between ambient levels of O3, NO2 and NO as a function of NOx in the UK, Atmospheric Environment, 35, 6391 – 6405, https://doi.org/10.1016/S1352-2310(01)00378-8, 2001.

Colberg, C. A., Tona, B., Catone, G., Sangiorgio, C., Stahel, W. A., Sturm, P., and Staehelin, J.: Statistical analysis of the vehicle pollutant emissions derived from several European road tunnel studies, Atmospheric Environment, 39, 2499 – 2511, https://doi.org/10.1016/j.atmosenv.2004.07.037, 12th International Symposium, Transport and Air Pollution, 2005.

Cui, L., Wang, X. L., Ho, K. F., Gao, Y., Liu, C., Ho, S. S. H., Li, H. W., Lee, S. C., Wang, X. M., Jiang, B. Q., Huang, Y., Chow, J. C., Watson, J. G., and Chen, L.-W.: Decrease of VOC emissions from vehicular emissions in Hong Kong from 2003 to 2015: Results from a tunnel study, Atmospheric Environment, 177, 64 – 74, https://doi.org/10.1016/j.atmosenv.2018.01.020, 2018.

Dallmann, T. R., Kirchstetter, T. W., DeMartini, S. J., and Harley, R. A.: Quantifying On-Road Emissions from Gasoline-Powered Motor Vehicles: Accounting for the Presence of Medium- and Heavy-Duty Diesel Trucks, Environmental Science & Technology, 47, 13 873–13 881, https://doi.org/10.1021/es402875u, 2013.

Deng, Y., Chen, C., Li, Q., Hu, Q., Yuan, H., Li, J., and Li, Y.: Measurements of real-world vehicle CO and NOx fleet average emissions in urban tunnels of two cities in China, Atmospheric Environment, 122, 417 – 426, https://doi.org/10.1016/j.atmosenv.2015.08.036, 2015.

Du, Z., Hu, M., Peng, J., Zhang, W., Zheng, J., Gu, F., Qin, Y., Yang, Y., Li, M., Wu, Y., Shao, M., and Shuai, S.: Comparison of primary aerosol emission and secondary aerosol formation from gasoline direct injection and port fuel injection vehicles, Atmospheric Chemistry and Physics, 18, 9011–9023, https://doi.org/10.5194/acp-18-9011-2018, https://www.atmos-chem-phys.net/18/9011/2018/, 2018.

Edwards, P., Brown, S., Roberts, J., Ahmadov, R., Banta, R., DeGouw, J., Dubé, W., Field, R., Flynn, J., Gilman, J., Graus, M., Helmig, D., Koss, A., Langford, A., Lefer, B., Lerner, B., Li, R., Li, S.-M., McKeen, S., Murphy, S., Parrish, D., Senff, C., Soltis, J., Stutz, J., Sweeney, C., Thompson, C., Trainer, M., Tsai, C., Veres, P., Washenfelder, R., Warneke, C., Wild, R., Young, C., Yuan, B., and Zamora, R.: High winter ozone pollution from carbonyl photolysis in an oil and gas basin, Nature, 514, 351–354, https://doi.org/10.1038/nature13767, 2014.

Ehlers, C., Klemp, D., Rohrer, F., Mihelcic, D., Wegener, R., Kiendler-Scharr, A., and Wahner, A.: Twenty years of ambient observations of nitrogen oxides and specified hydrocarbons in air masses dominated by traffic emissions in Germany, Faraday Discuss., 189, 407–437, https://doi.org/10.1039/C5FD00180C, 2016.

Fang, X., Wu, L., Zhang, Q., Zhang, J., Wang, A., Zhang, Y., Zhao, J., and Mao, H.: Characteristics, emissions and source identifications of particle polycyclic aromatic hydrocarbons from traffic emissions using tunnel measurement, Transportation Research Part D: Transport and Environment, https://doi.org/10.1016/j.trd.2018.02.021, 2018.

Gauderman, W. J., Urman, R., Avol, E., Berhane, K., McConnell, R., Rappaport, E., Chang, R., Lurmann, F., and Gilliland, F.: Association of Improved Air Quality with Lung Development in Children, New England Journal of Medicine, 372, 905–913, https://doi.org/10.1056/NEJMoa1414123, 2015.

Gelencsér, A., Siszler, K., and Hlavay, J.: TolueneBenzene Concentration Ratio as a Tool for Characterizing the Distance from Vehicular Emission Sources, Environmental Science & Technology, 31, 2869–2872, https://doi.org/10.1021/es970004c, 1997.

Gertler, A. W.: Diesel vs. gasoline emissions: Does PM from diesel or gasoline vehicles dominate in the US?, Atmospheric Environment, 39, 2349 – 2355, https://doi.org/10.1016/j.atmosenv.2004.05.065, 12th International Symposium, Transport and Air Pollution, 2005.

Gertler, A. W., Fujita, E. M., Pierson, W. R., and Wittorff, D. N.: Apportionment of NMHC tailpipe vs non-tailpipe emissions in the Fort McHenry and Tuscarora mountain tunnels, Atmospheric Environment, 30, 2297 – 2305, https://doi.org/10.1016/1352-2310(95)00090-9, 1996.

Guo, S., Hu, M., Zamora, M. L., Peng, J., Shang, D., Zheng, J., Du, Z., Wu, Z., Shao, M., Zeng, L., Molina, M. J., and Zhang, R.: Elucidating severe urban haze formation in China, Proceedings of the National Academy of Sciences, 111, 17 373–17 378, https://doi.org/10.1073/pnas.1419604111, 2014.

Han, M., Lu, X., Zhao, C., Ran, L., and Han, S.: Characterization and source apportionment of volatile organic compounds in urban and suburban Tianjin, China, Advances in Atmospheric Sciences, 32, 439–444, https://doi.org/10.1007/s00376-014-4077-4, 2015.

Harley, R. A., Coulter-Burke, S. C., and Yeung, T. S.: Relating Liquid Fuel and Headspace Vapor Composition for California Reformulated Gasoline Samples Containing Ethanol, Environmental Science & Technology, 34, 4088–4094, https://doi.org/10.1021/es0009875, 2000.

He, J., Wu, L., Mao, H., Liu, H., Jing, B., Yu, Y., Ren, P., Feng, C., and Liu, X.: Development of a vehicle emission inventory with high temporal-spatial resolution based on NRT traffic data and its impact on air pollution in Beijing - Part 2: Impact of vehicle emission on urban air quality, Atmospheric Chemistry and Physics, 16, 3171–3184, https://doi.org/10.5194/acp-16-3171-2016, 2016.

Hedberg, E., Kristensson, A., Ohlsson, M., Johansson, C., Åke Johansson, P., Swietlicki, E., Vesely, V., Wideqvist, U., and Westerholm, R.: Chemical and physical characterization of emissions from birch wood combustion in a wood stove, Atmospheric Environment, 36, 4823 – 4837, https://doi.org/10.1016/S1352-2310(02)00417-X, 2002.

Ho, K. F., Lee, S. C., Ho, W. K., Blake, D. R., Cheng, Y., Li, Y. S., Ho, S. S. H., Fung, K., Louie, P. K. K., and Park, D.: Vehicular emission of volatile organic compounds (VOCs) from a tunnel study in Hong Kong, Atmospheric Chemistry and Physics, 9, 7491–7504, https://doi.org/10.5194/acp-9-7491-2009, 2009.

Hoek, G., Brunekreef, B., Goldbohm, S., Fischer, P., and Van Den Brandt, P.: Association between mortality and indicators of traffic-related air pollution in the Netherlands: A cohort study, Lancet, 360, 1203–1209, https://doi.org/10.1016/S0140-6736(02)11280-3, 2002.

Huang, C., Wang, H. L., Li, L., Wang, Q., Lu, Q., de Gouw, J. A., Zhou, M., Jing, S. A., Lu, J., and Chen, C. H.: VOC species and emission inventory from vehicles and their SOA formation potentials estimation in Shanghai, China, Atmospheric Chemistry and Physics, 15, 11 081–11 096, https://doi.org/10.5194/acp-15-11081-2015, 2015.

Huang, C., Tao, S., Lou, S., Hu, Q., Wang, H., Wang, Q., Li, L., Wang, H., Liu, J., Quan, Y., and Zhou, L.: Evaluation of emission factors for light-duty gasoline vehicles based on chassis dynamometer and tunnel studies in Shanghai, China, Atmospheric Environment, 169, 193 – 203, https://doi.org/10.1016/j.atmosenv.2017.09.020, 2017.

Hung-Lung, C., Ching-Shyung, H., Shih-Yu, C., Ming-Ching, W., Sen-Yi, M., and Yao-Sheng, H.: Emission factors and characteristics of criteria pollutants and volatile organic compounds (VOCs) in a freeway tunnel study, Science of The Total Environment, 381, 200 – 211, https://doi.org/10.1016/j.scitotenv.2007.03.039, 2007.

Hwa, M.-Y., Hsieh, C.-C., Wu, T.-C., and Chang, L.-F. W.: Real-world vehicle emissions and VOCs profile in the Taipei tunnel located at Taiwan Taipei area, Atmospheric Environment, 36, 1993 – 2002, https://doi.org/10.1016/S1352-2310(02)00148-6, 2002.

Imhof, D., Weingartner, E., Prévôt, A. S. H., Ordóñez, C., Kurtenbach, R., Wiesen, P., Rodler, J., Sturm, P., McCrae, I., Ekström, M., and Baltensperger, U.: Aerosol and NO_x emission factors and submicron particle number size distributions in two road tunnels with different traffic regimes, Atmospheric Chemistry and Physics, 6, 2215–2230, https://doi.org/10.5194/acp-6-2215-2006, 2006.

Jenkin, M.: Investigation of the impact of short-timescale NOx variability on annual mean oxidant partitioning at UK sites, Atmospheric Environment, 90, 43 – 50, https://doi.org/10.1016/j.atmosenv.2014.03.033, 2014.

Jing, B., Wu, L., Mao, H., Gong, S., He, J., Zou, C., Song, G., Li, X., and Wu, Z.: Development of a vehicle emission inventory with high temporal–spatial resolution based on NRT traffic data and its impact on air pollution in Beijing – Part 1: Development and evaluation of vehicle emission inventory, Atmospheric Chemistry and Physics, 16, 3161–3170, https://doi.org/10.5194/acp-16-3161-2016, 2016.

Kelly, F. J. and Zhu, T.: Transport solutions for cleaner air, Science, 352, 934–936, https://doi.org/10.1126/science.aaf3420, 2016.

Kowal, S. F., Allen, S. R., and Kahan, T. F.: Wavelength-Resolved Photon Fluxes of Indoor Light Sources: Implications for HOx Production, Environmental Science & Technology, 51, 10 423–10 430, https://doi.org/10.1021/acs.est.7b02015, 2017.

Lelieveld, J. and Pöschl, U.: Chemists can help to solve the air-pollution health crisis, Nature, 551, 291, 2017.

Li, M., Liu, H., Geng, G., Hong, C., Liu, F., Song, Y., Tong, D., Zheng, B., Cui, H., Man, H., Zhang, Q., and He, K.: Anthropogenic emission inventories in China: a review, National Science Review, 4, 834–866, https://doi.org/10.1093/nsr/nwx150, http://dx.doi.org/10.1093/nsr/nwx150, 2017.

Liu, B., Liang, D., Yang, J., Dai, Q., Bi, X., Feng, Y., Yuan, J., Xiao, Z., Zhang, Y., and Xu, H.: Characterization and source apportionment of volatile organic compounds based on 1-year of observational data in Tianjin, China, Environmental Pollution, 218, 757 – 769, https://doi.org/10.1016/j.envpol.2016.07.072, 2016.

Liu, B., Cheng, Y., Zhou, M., Liang, D., Dai, Q., Wang, L., Jin, W., Zhang, L., Ren, Y., Zhou, J., Dai, C., Xu, J., Wang, J., Feng, Y., and Zhang, Y.: Effectiveness evaluation of temporary emission control action in 2016 in winter in Shijiazhuang, China, Atmospheric Chemistry and Physics, 18, 7019–7039, https://doi.org/10.5194/acp-18-7019-2018, 2018.

Liu, H., Wang, X. M., Pang, J. M., and He, K. B.: Feasibility and difficulties of China's new air quality standard compliance: PRD case of $PM_{2.5}$ and ozone from 2010 to 2025, Atmospheric Chemistry and Physics, 13, 12 013–12 027, https://doi.org/10.5194/acp-13-12013-2013, 2013.

Liu, H., Man, H., Tschantz, M., Wu, Y., He, K., and Hao, J.: VOC from Vehicular Evaporation Emissions: Status and Control Strategy, Environmental Science & Technology, 49, 14 424–14 431, https://doi.org/10.1021/acs.est.5b04064, 2015a.

Liu, T., Wang, X., Wang, B., Ding, X., Deng, W., Lü, S., and Zhang, Y.: Emission factor of ammonia (NH3) from on-road vehicles in China: tunnel tests in urban Guangzhou, Environmental Research Letters, 9, https://doi.org/10.1088/1748-9326/9/6/064027, 2014.

Liu, T., Wang, X., Deng, W., Hu, Q., Ding, X., Zhang, Y., He, Q., Zhang, Z., Lü, S., Bi, X., Chen, J., and Yu, J.: Secondary organic aerosol formation from photochemical aging of light-duty gasoline vehicle exhausts in a smog chamber, Atmospheric Chemistry and Physics, 15, 9049–9062, https://doi.org/10.5194/acp-15-9049-2015, 2015b.

Liu, Y., Shao, M., Fu, L., Lu, S., Zeng, L., and Tang, D.: Source profiles of volatile organic compounds (VOCs) measured in China: Part I, Atmospheric Environment, 42, 6247 – 6260, https://doi.org/10.1016/j.atmosenv.2008.01.070, pRIDE-PRD 2004 Campaign : Program of Regional Integrated Experiments on Air Quality over Pearl River Delta of China, 2008.

Na, K., Kim, Y. P., Moon, I., and Moon, K.-C.: Chemical composition of major VOC emission sources in the Seoul atmosphere, Chemosphere, 55, 585 – 594, https://doi.org/10.1016/j.chemosphere.2004.01.010, 2004.

Nelson, P. and Quigley, S.: The m,p-xylenes:ethylbenzene ratio. A technique for estimating hydrocarbon age in ambient atmospheres, Atmospheric Environment (1967), 17, 659 – 662, https://doi.org/10.1016/0004-6981(83)90141-5, 1983.

O'Driscoll, R., ApSimon, H. M., Oxley, T., Molden, N., Stettler, M. E., and Thiyagarajah, A.: A Portable Emissions Measurement System (PEMS) study of NOx and primary NO2 emissions from Euro 6 diesel passenger cars and comparison with COPERT emission factors, Atmospheric Environment, 145, 81 – 91, https://doi.org/10.1016/j.atmosenv.2016.09.021, 2016.

Paatero, P.: Least squares formulation of robust non-negative factor analysis, Chemometrics and Intelligent Laboratory Systems, 37, 23 – 35, https://doi.org/10.1016/S0169-7439(96)00044-5, 1997.

Paatero, P. and Tapper, U.: Positive matrix factorization: A non-negative factor model with optimal utilization of error estimates of data values, Environmetrics, 5, 111–126, https://doi.org/10.1002/env.3170050203.

Pandey, S. K., Kim, K.-H., Chung, S.-Y., Cho, S.-J., Kim, M.-Y., and Shon, Z.-H.: Long-term study of NOx behavior at urban roadside and background locations in Seoul, Korea, Atmospheric Environment, 42, 607 – 622, https://doi.org/10.1016/j.atmosenv.2007.10.015, 2008.

Parrish, D. D. and Zhu, T.: Clean Air for Megacities, Science, 326, 674–675, https://doi.org/10.1126/science.1176064, http://science.sciencemag.org/content/326/5953/674, 2009.

Peng, J., Hu, M., Du, Z., Wang, Y., Zheng, J., Zhang, W., Yang, Y., Qin, Y., Zheng, R., Xiao, Y., Wu, Y., Lu, S., Wu, Z., Guo, S., Mao, H., and Shuai, S.: Gasoline aromatics: a critical determinant of urban secondary organic aerosol formation, Atmospheric Chemistry and Physics, 17, 10 743–10 752, https://doi.org/10.5194/acp-17-10743-2017, 2017.

Pierson, W. R. and Brachaczek, W. W.: Emissions of ammonia and amines from vehicles on the road, Environmental Science & Technology, 17, 757–760, https://doi.org/10.1021/es00118a013, 1983.

Pierson, W. R., Gertler, A. W., Robinson, N. F., Sagebiel, J. C., Zielinska, B., Bishop, G. A., Stedman, D. H., Zweidinger, R. B., and Ray, W. D.: Real-world automotive emissions—Summary of studies in the Fort McHenry and Tuscarora mountain tunnels, Atmospheric Environment, 30, 2233 – 2256, https://doi.org/10.1016/1352-2310(95)00276-6, 1996.

Poulopoulos, S. and Philippopoulos, C.: Influence of MTBE addition into gasoline on automotive exhaust emissions, Atmospheric Environment, 34, 4781 – 4786, https://doi.org/10.1016/S1352-2310(00)00257-0, 2000.

Russo, R. S., Zhou, Y., White, M. L., Mao, H., Talbot, R., and Sive, B. C.: Multi-year (2004-2008) record of nonmethane hydrocarbons and halocarbons in New England: seasonal variations and regional sources, Atmospheric Chemistry and Physics, 10, 4909–4929, https://doi.org/10.5194/acp-10-4909-2010, 2010.

Schnell, R., Oltmans, S., Neely, R., Endres, M., Molenar, J., and White, A.: Rapid photochemical production of ozone at high concentrations in a rural site during winter, Nature Geoscience, 2, 120–122, https://doi.org/10.1038/ngeo415, 2009.

23

Seinfeld, J. H.: Urban Air Pollution: State of the Science, Science, 243, 745–752, http://www.jstor.org/stable/1703048, 1989.

Shen, X., Yao, Z., Huo, H., He, K., Zhang, Y., Liu, H., and Ye, Y.: PM2.5 emissions from light-duty gasoline vehicles in Beijing, China, Science of The Total Environment, 487, 521 – 527, https://doi.org/10.1016/j.scitotenv.2014.04.059, 2014.

Shon, Z.-H., Kim, K.-H., and Song, S.-K.: Long-term trend in NO2 and NOx levels and their emission ratio in relation to road traffic activities in East Asia, Atmospheric Environment, 45, 3120 – 3131, https://doi.org/10.1016/j.atmosenv.2011.03.009, 2011.

Simmons, W. and Seakins, P.: Estimations of primary nitrogen dioxide exhaust emissions from chemiluminescence NOx measurements in a UK road tunnel, Science of The Total Environment, 438, 248 – 259, https://doi.org/10.1016/j.scitotenv.2012.08.050, 2012.

Sinharay, R., Gong, J., Barratt, B., Ohman-Strickland, P., Ernst, S., Kelly, F., Zhang, J. J., Collins, P., Cullinan, P., and Chung, K. F.: Respiratory and cardiovascular responses to walking down a traffic-polluted road compared with walking in a traffic-free area in participants aged 60 years and older with chronic lung or heart disease and age-matched healthy controls: a randomised, crossover study, The Lancet, https://doi.org/10.1016/S0140-6736(17)32643-0, 2017.

Soltic, P. and Weilenmann, M.: NO2/NO emissions of gasoline passenger cars and light-duty trucks with Euro-2 emission standard, Atmospheric Environment, 37, 5207 – 5216, https://doi.org/10.1016/j.atmosenv.2003.05.003, 11th International Symposium, Transport and Air Pollution, 2003.

Song, C., Li, R., He, J., Wu, L., and Mao, H.: Analysis of pollution characteristics of NO, NO2 and O3 at urban area of Langfang, Hebei, Zhongguo Huanjing Kexue/China Environmental Science, 36, 2903–2912, http://manu36.magtech.com.cn/Jweb_zghjkx/CN/abstract/article_14809.shtml, in Chinese, 2016.

Song, C., He, J., Wu, L., Jin, T., Chen, X., Li, R., Ren, P., Zhang, L., and Mao, H.: Health burden attributable to ambient PM2.5 in China, Environmental Pollution, 223, 575 – 586, https://doi.org/10.1016/j.envpol.2017.01.060, 2017a.

Song, C., Wu, L., Xie, Y., He, J., Chen, X., Wang, T., Lin, Y., Jin, T., Wang, A., Liu, Y., Dai, Q., Liu, B., Wang, Y., and Mao, H.: Air pollution in China: Status and spatiotemporal variations, Environmental Pollution, 227, 334 – 347, https://doi.org/10.1016/j.envpol.2017.04.075, 2017b.

Song, C., Ma, C., Zhang, Y., Wang, T., Wu, L., Wang, P., Liu, Y., Li, Q., Zhang, J., Dai, Q., Zou, C., Sun, L., and Mao, H.: Heavy-duty diesel vehicles dominate vehicle emissions in a tunnel study in northern China, Science of The Total Environment, 637-638, 431 – 442, https://doi.org/10.1016/j.scitotenv.2018.04.387, 2018.

Steinbacher, M., Dommen, J., Ordonez, C., Reimann, S., GrÜebler, F. C., Staehelin, J., and Prevot, A. S. H.: Volatile Organic Compounds in the Po Basin. Part A: Anthropogenic VOCs, Journal of Atmospheric Chemistry, 51, 271–291, https://doi.org/10.1007/s10874-005-3576-1, 2005.

Sun, S., Jiang, W., and Gao, W.: Vehicle emission trends and spatial distribution in Shandong province, China, from 2000 to 2014, Atmospheric Environment, 147, 190 – 199, https://doi.org/10.1016/j.atmosenv.2016.09.065, 2016.

Tan, Z., Wang, Y., Ye, C., Zhu, Y., Li, Y., Liang, P., Wang, Q., Han, Y., Fang, Y., Wang, J., Meng, L., Wang, Y., and Zhu, T.: Evaluating Vehicle Emission Control Policies using on-Road Mobile Measurements and Continuous Wavelet Transform: a Case Study during the Asia-Pacific

Economic Cooperation Forum, China 2014, Atmospheric Chemistry and Physics Discussions, 2016, 1–39, https://doi.org/10.5194/acp-2016-460, 2016.

Tsai, W. Y., Chan, L. Y., Blake, D. R., and Chu, K. W.: Vehicular fuel composition and atmospheric emissions in South China: Hong Kong, Macau, Guangzhou, and Zhuhai, Atmospheric Chemistry and Physics, 6, 3281–3288, https://doi.org/10.5194/acp-6-3281-2006, 2006.

5 Wang, G., Cheng, S., Wei, W., Zhou, Y., Yao, S., and Zhang, H.: Characteristics and source apportionment of VOCs in the suburban area of Beijing, China, Atmospheric Pollution Research, 7, 711 – 724, https://doi.org/10.1016/j.apr.2016.03.006, 2016.

Wang, H., Wang, Q., Chen, J., Chen, C., Huang, C., Qiao, L., Lou, S., and Lu, J.: Do vehicular emissions dominate the source of C6–C8 aromatics in the megacity Shanghai of eastern China?, Journal of Environmental Sciences, 27, 290 – 297, https://doi.org/10.1016/j.jes.2014.05.033, 2015a.

10 Wang, P., Schade, G., Estes, M., and Ying, Q.: Improved MEGAN predictions of biogenic isoprene in the contiguous United States, Atmospheric Environment, 148, 337 – 351, https://doi.org/10.1016/j.atmosenv.2016.11.006, 2017.

Wang, Z., Li, Y., Chen, T., Zhang, D., Sun, F., Wei, Q., Dong, X., Sun, R., Huan, N., and Pan, L.: Ground-level ozone in urban Beijing over a 1-year period: Temporal variations and relationship to atmospheric oxidation, Atmospheric Research, 164-165, 110 – 117, https://doi.org/10.1016/j.atmosres.2015.05.005, 2015b.

15 Wild, R. J., Dubé, W. P., Aikin, K. C., Eilerman, S. J., Neuman, J. A., Peischl, J., Ryerson, T. B., and Brown, S. S.: On-road measurements of vehicle NO_2/NO_x emission ratios in Denver, Colorado, USA, Atmospheric Environment, 148, 182 – 189, https://doi.org/10.1016/j.atmosenv.2016.10.039, 2017.

Williams, M. L. and Carslaw, D. C.: New Directions: Science and policy – Out of step on NO_x and NO_2?, Atmospheric Environment, 45, 3911 – 3912, https://doi.org/10.1016/j.atmosenv.2011.04.067, 2011.

20 Wu, F., Yu, Y., Sun, J., Zhang, J., Wang, J., Tang, G., and Wang, Y.: Characteristics, source apportionment and reactivity of ambient volatile organic compounds at Dinghu Mountain in Guangdong Province, China, Science of The Total Environment, 548-549, 347 – 359, https://doi.org/10.1016/j.scitotenv.2015.11.069, 2016.

Wu, Y., Zhang, S., Hao, J., Liu, H., Wu, X., Hu, J., Walsh, M. P., Wallington, T. J., Zhang, K. M., and Stevanovic, S.: On-road vehicle emissions and their control in China: A review and outlook, Science of The Total Environment, 574, 332 – 349, 25 https://doi.org/10.1016/j.scitotenv.2016.09.040, 2017.

Xue, L. K., Wang, T., Gao, J., Ding, A. J., Zhou, X. H., Blake, D. R., Wang, X. F., Saunders, S. M., Fan, S. J., Zuo, H. C., Zhang, Q. Z., and Wang, W. X.: Ground-level ozone in four Chinese cities: precursors, regional transport and heterogeneous processes, Atmospheric Chemistry and Physics, 14, 13 175–13 188, https://doi.org/10.5194/acp-14-13175-2014, 2014.

Yao, X., Lau, N. T., Chan, C. K., and Fang, M.: The use of tunnel concentration profile data to determine the ratio of NO_2/NO_x directly 30 emitted from vehicles, Atmospheric Chemistry and Physics Discussions, 5, 12 723–12 740, https://doi.org/10.5194/acpd-5-12723-2005, 2005.

Yue, T., Yue, X., Chai, F., Hu, J., Lai, Y., He, L., and Zhu, R.: Characteristics of volatile organic compounds (VOCs) from the evaporative emissions of modern passenger cars, Atmospheric Environment, 151, 62 – 69, https://doi.org/10.1016/j.atmosenv.2016.12.008, 2017.

Zhang, L., Zhao, T., Gong, S., Kong, S., Tang, L., Liu, D., Wang, Y., Jin, L., Shan, Y., Tan, C., Zhang, Y., and Guo, X.: Updated emission inventories of power plants in simulating air quality during haze periods over East China, Atmospheric Chemistry and Physics, 18, 2065–2079, https://doi.org/10.5194/acp-18-2065-2018, 2018a.

Zhang, Q., Wu, L., Liu, M., Fang, X., Zhang, J., Mao, H., Shao, M., and Lu, S.: Pollution characteristics and health risk assessment of VOCs from vehicle exhaust in Nanjing, China, Zhongguo Huanjing Kexue/China Environmental Science, 36, 3118–3125, http://manu36.magtech.com.cn/Jweb_zghjkx/CN/abstract/article_14837.shtml, in Chinese, 2016a.

Zhang, Q., Wu, L., Yang, Z., Zou, C., Liu, X., Zhang, K., and Mao, H.: Characteristics of gaseous and particulate pollutants exhaust from logistics transportation vehicle on real-world conditions, Transportation Research Part D: Transport and Environment, 43, 40 – 48, https://doi.org/10.1016/j.trd.2015.09.005, 2016b.

Zhang, Q., Wu, L., Fang, X., Liu, M., Zhang, J., Shao, M., Lu, S., and Mao, H.: Emission factors of volatile organic compounds (VOCs) based on the detailed vehicle classification in a tunnel study, Science of The Total Environment, 624, 878 – 886, https://doi.org/10.1016/j.scitotenv.2017.12.171, 2018b.

Zhang, Y., Wang, X., Zhang, Z., Lü, S., Shao, M., Lee, F. S., and Yu, J.: Species profiles and normalized reactivity of volatile organic compounds from gasoline evaporation in China, Atmospheric Environment, 79, 110 – 118, https://doi.org/10.1016/j.atmosenv.2013.06.029, 2013.

Zhang, Y., Wang, X., Li, G., Yang, W., Huang, Z., Zhang, Z., Huang, X., Deng, W., Liu, T., Huang, Z., and Zhang, Z.: Emission factors of fine particles, carbonaceous aerosols and traces gases from road vehicles: Recent tests in an urban tunnel in the Pearl River Delta, China, Atmospheric Environment, 122, 876 – 884, https://doi.org/10.1016/j.atmosenv.2015.08.024, 2015.

Zhang, Y., Yang, W., Simpson, I., Huang, X., Yu, J., Huang, Z., Wang, Z., Zhang, Z., Liu, D., Huang, Z., Wang, Y., Pei, C., Shao, M., Blake, D. R., Zheng, J., Huang, Z., and Wang, X.: Decadal changes in emissions of volatile organic compounds (VOCs) from on-road vehicles with intensified automobile pollution control: Case study in a busy urban tunnel in south China, Environmental Pollution, 233, 806 – 819, https://doi.org/10.1016/j.envpol.2017.10.133, 2018c.

Zheng, H., Kong, S., Xing, X., Mao, Y., Hu, T., Ding, Y., Li, G., Liu, D., Li, S., and Qi, S.: Monitoring of volatile organic compounds (VOCs) from an oil and gas station in northwest China for 1 year, Atmospheric Chemistry and Physics, 18, 4567–4595, https://doi.org/10.5194/acp-18-4567-2018, 2018.

Zou, Y., Deng, X. J., Zhu, D., Gong, D. C., Wang, H., Li, F., Tan, H. B., Deng, T., Mai, B. R., Liu, X. T., and Wang, B. G.: Characteristics of 1 year of observational data of VOCs, NO_x and O_3 at a suburban site in Guangzhou, China, Atmospheric Chemistry and Physics, 15, 6625–6636, https://doi.org/10.5194/acp-15-6625-2015, 2015.
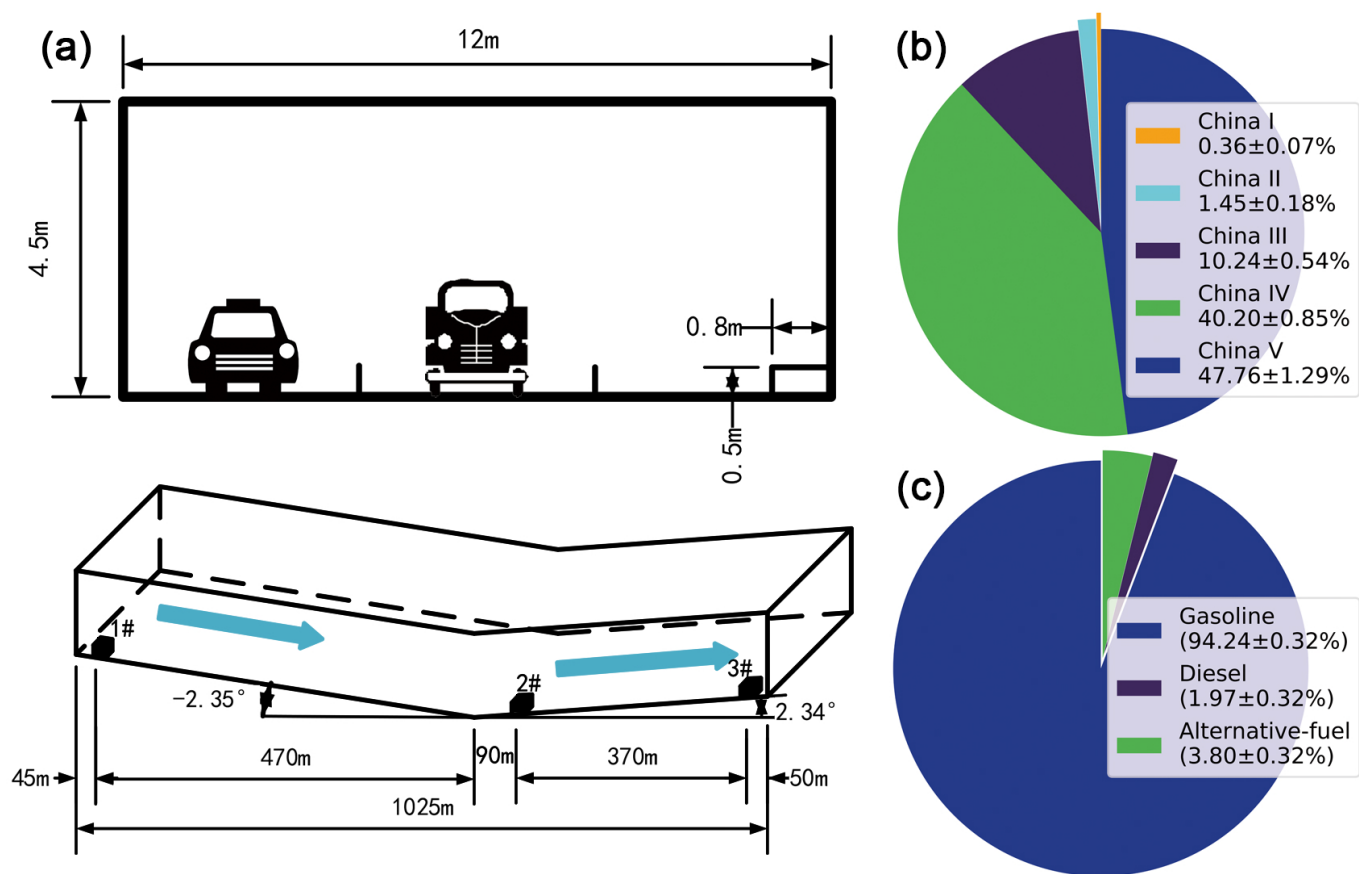
Figure 1. The description of (a) WJL tunnel, and the fleet compostion in (b) vehicle types and (c) in-use fuel types during the measurement campaign .
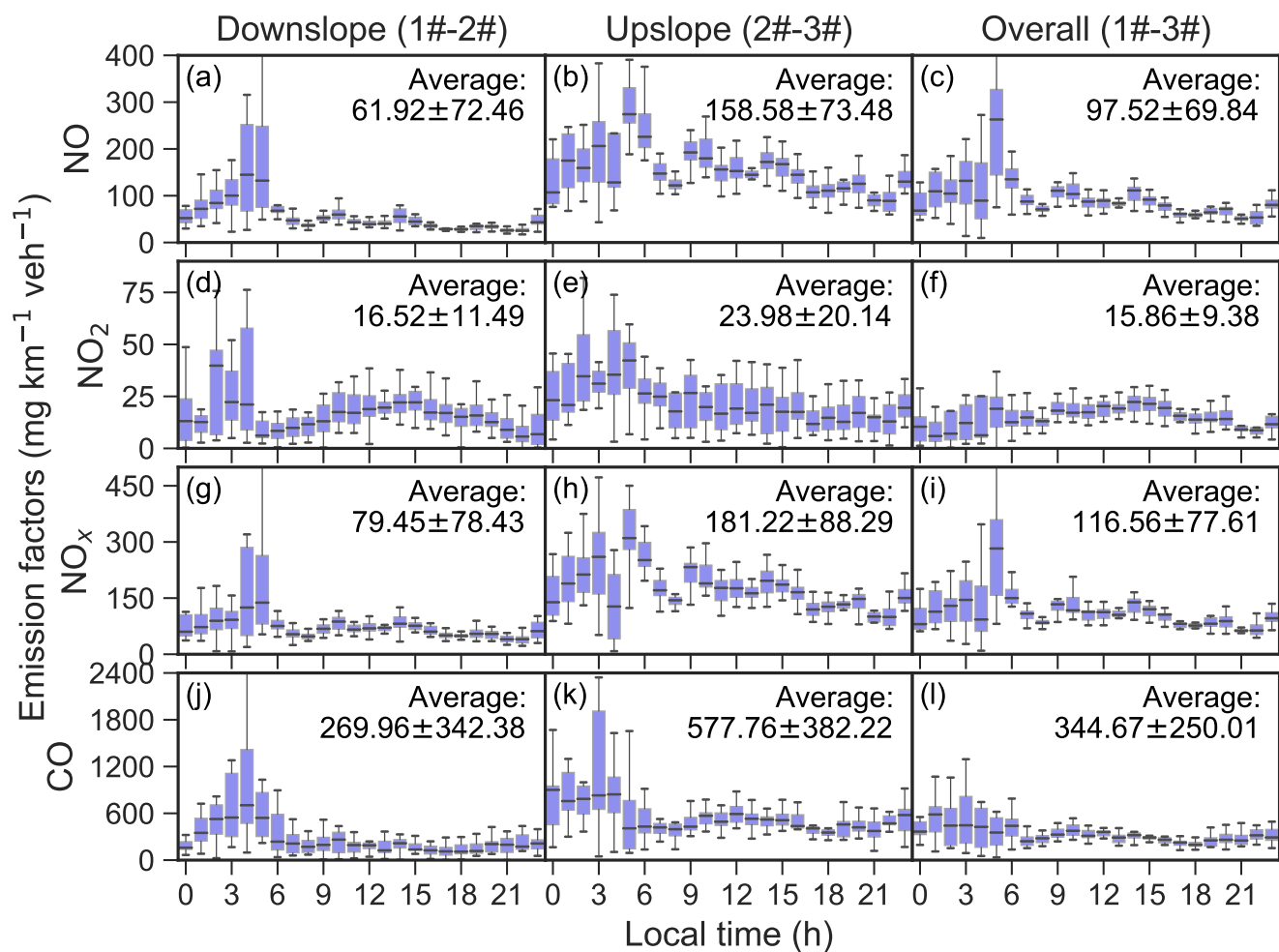
Figure 2. The diurnal variations (represented by boxplots) of emission factors of (a-c) NO, (d-f) NO$_2$, (g-i) NO$_x$, and (j-l) CO for on-road vehicles under downslope (1#-2#, left panel), upslope (2#-3#, middle panel) and overall (1#-3#, right panel) road conditions. The average emission factors (mean±standard deviation) were given on the upper right corner of each subfigure.
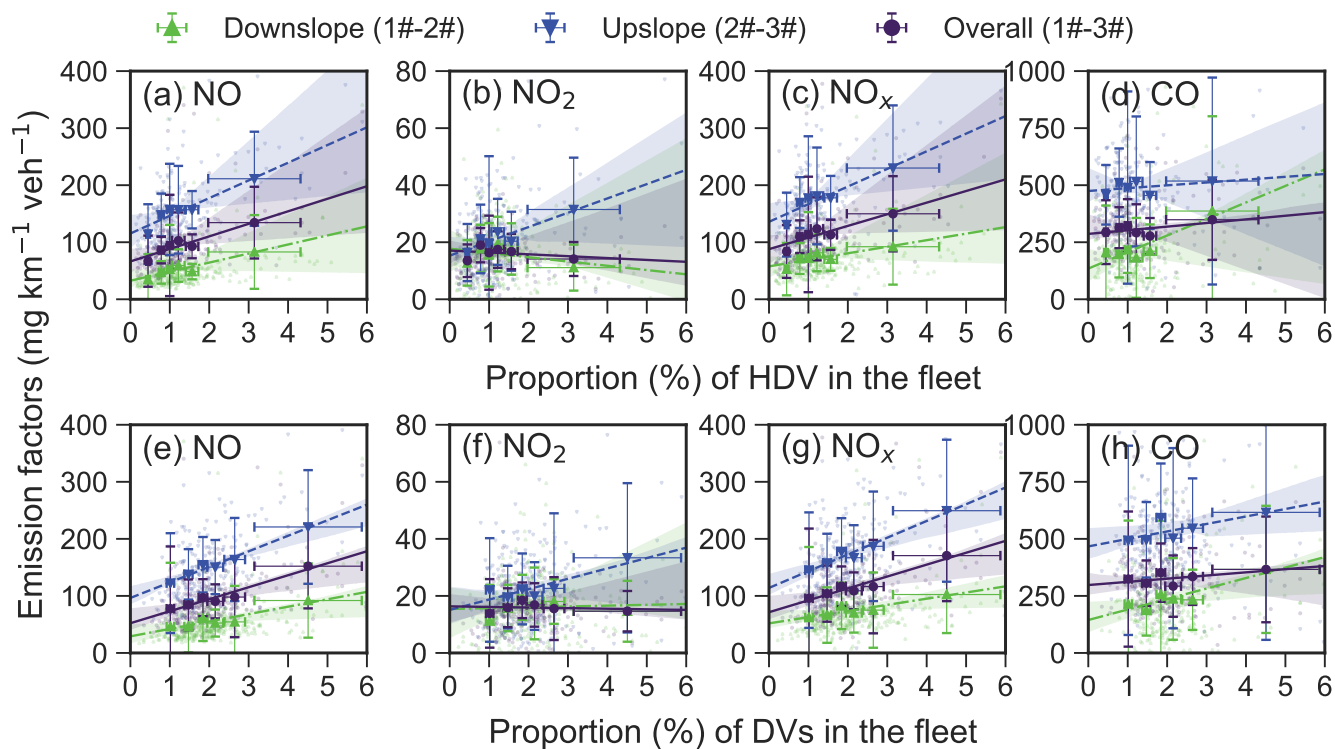
Figure 3. The linear regressions (dash-dot regression lines for the downslope, dash-dash regression lines for the upslope, and solid regression lines for the overall condition) between fleet-average emission factors and proportion of heavy-duty vehicles (HDV, a: NO; b: NO_2; c: NO_x; d: CO) and diesel vehicles (DVs, e: NO; f: NO_2; g: NO_x; h: CO). The parameters of the linear regressions were listed in Table A2.
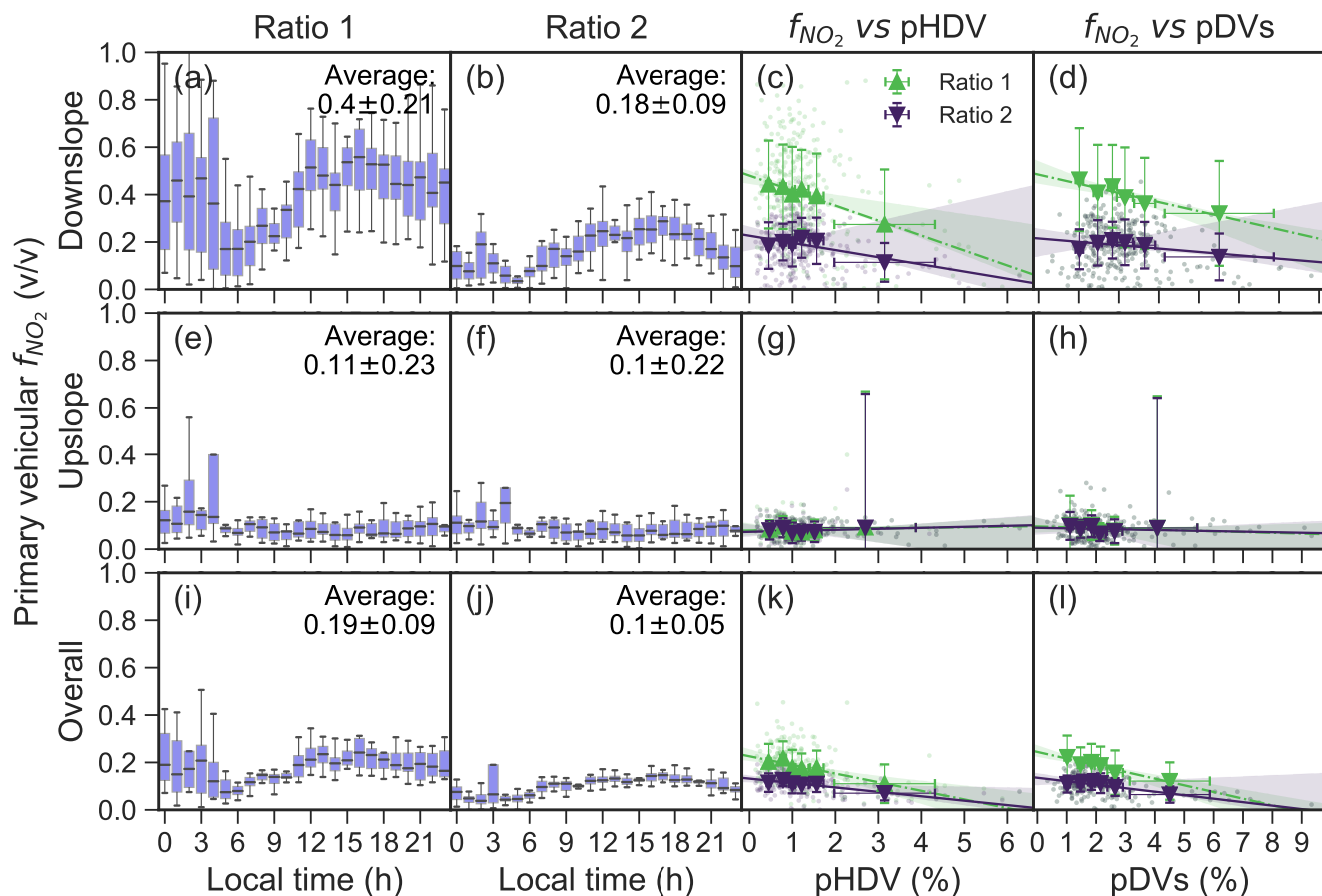
Figure 4. The diurnal variations (represented by boxplots) of primary vehicular f_{NO_2} (Ratio 1: a-e-i, Ratio 2: b-f-j), and the relationships between f_{NO_2} and the proportion of heavy-duty vehicles (pHDV: c-g-k) and diesel vehicles (pDVs: d-h-l). The parameters of the linear regressions (dash-dot regression lines for Ratio 1, solid regression lines for Ratio 2) were listed in Table A2. f_{NO_2} are the fractions (v/v) of NO_2 in NO_x from vehicular emissions. Ratio 1 is the ratio of the primary emitted and transformed NO_2 to primary emitted NO_x by volume. Ratio 2 is the ratio of the primary emitted NO_2 excluding the O_3 titration (Reaction R1) to primary emitted NO_x by volume.
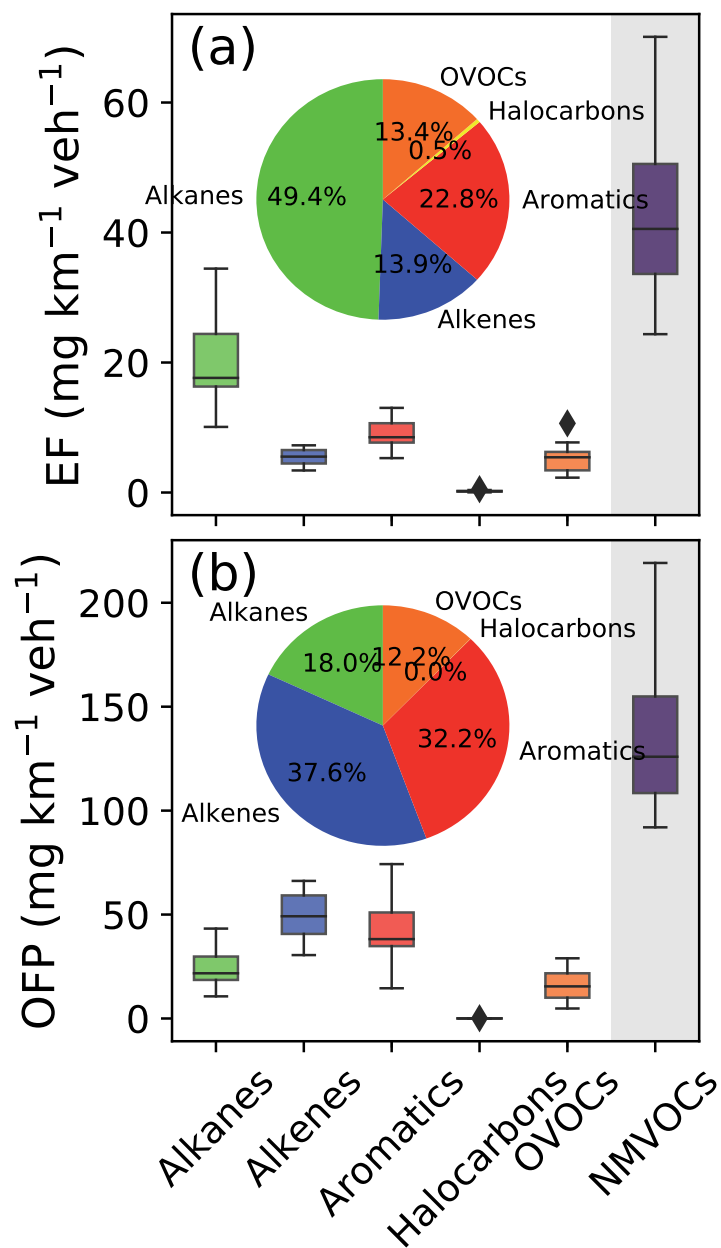
Figure 5. (a) The boxplots of fleet-average emission factors (EFs) for the VOC groups (including Alkanes, Alkenes, Aromatics, Halocarbons, and OVOCs) , and (b) the EFs of the ozone formation potential (OFP) for the VOC groups. The EF and OFP of total NMVOCs (the sum of Alkanes, Alkenes, Aromatics, Halocarbons, and OVOCs) from vehicular emissions were shown in the grey areas.
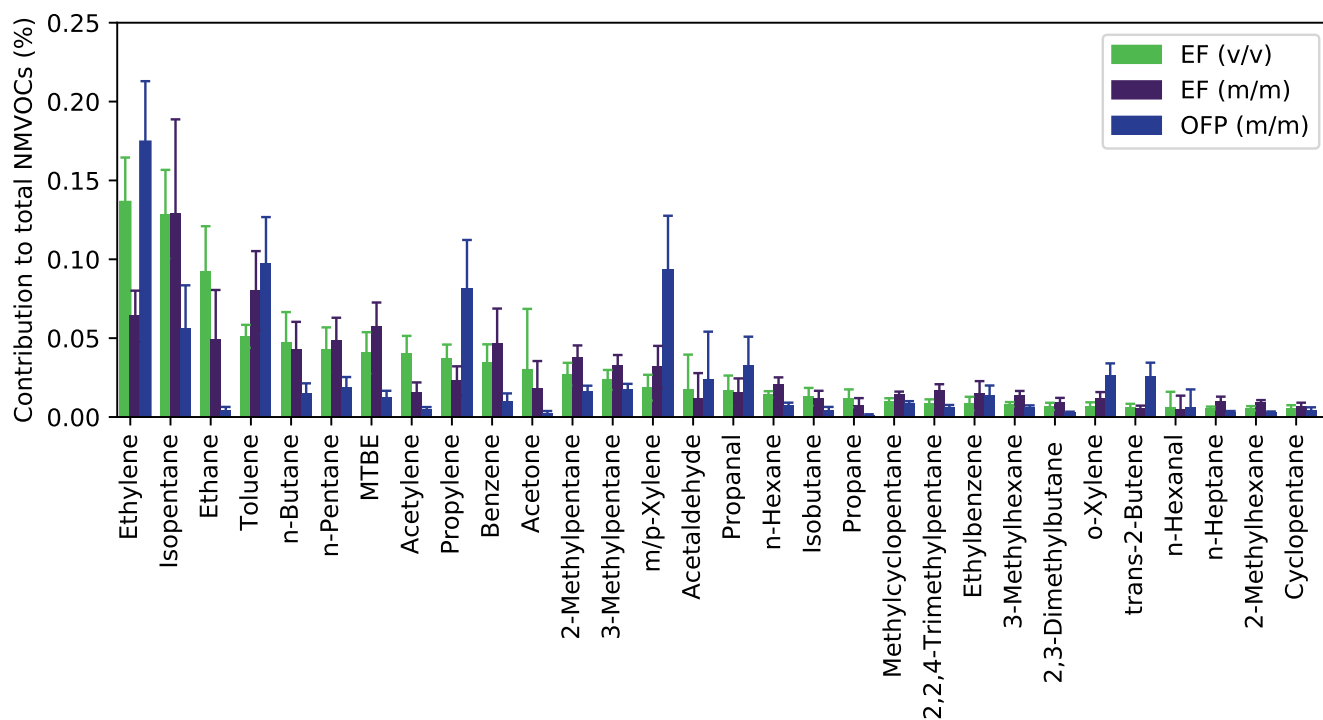
Figure 6. The fleet-average ~~OFP (m/m)~~ EF (v/v) , EF (m/m), and ~~EF (v/v)~~ OFP (m/m) of top 30 NMVOC species from vehicular emissions (sorted by ~~OFP~~ volume).
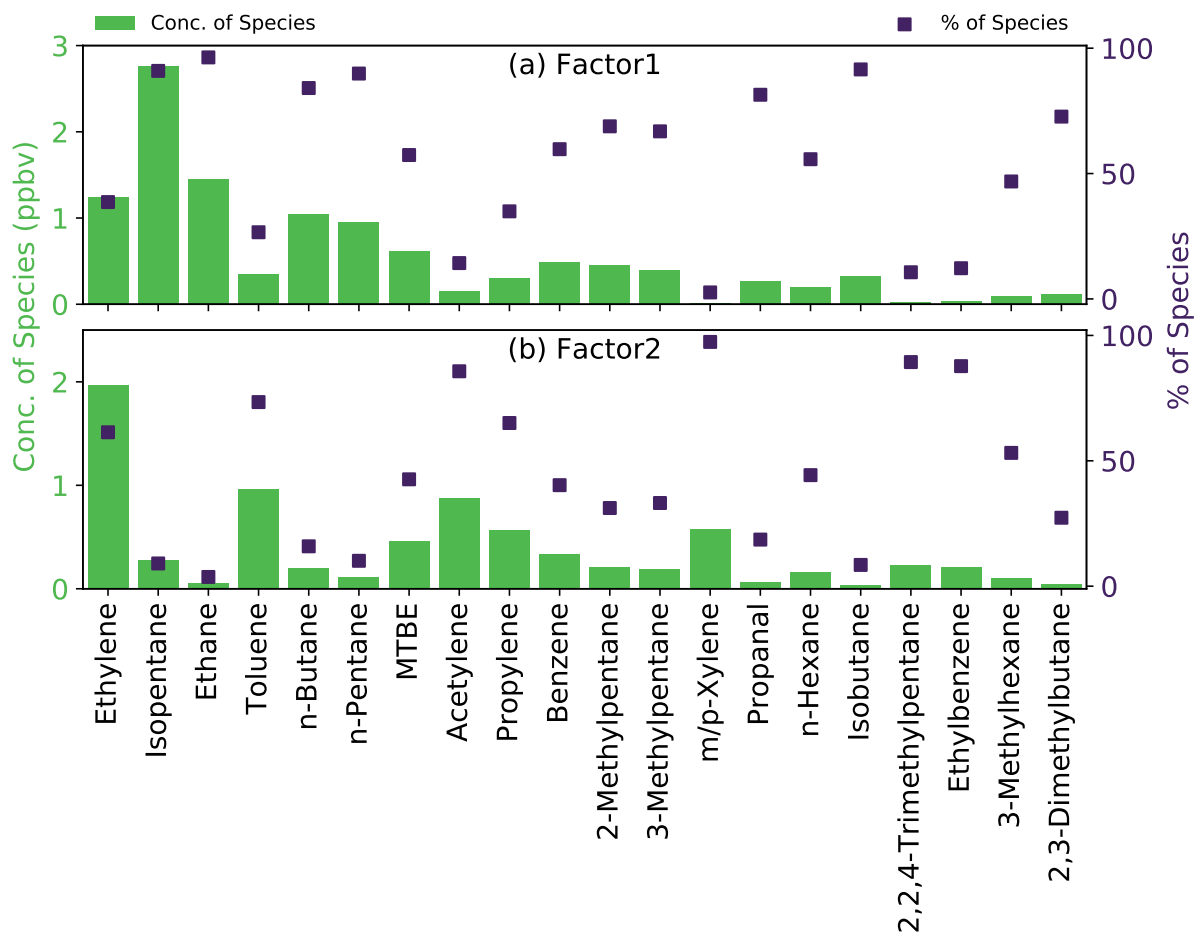
Figure 7. ~~(a) The relative factor contributions to individual VOC species; (b) the source profiles of VOCs by volume; (c) the source profiles of VOCs by volume percentage.~~ The source profiles (% of species, represented by scatters) and contributions (Conc. of Species, represented by bars) of 2-factor (a: Factor1, b: Factor2) solution by the PMF model. Factor1 and Factor2 was identified as evaporative and tailpipe emissions, respectively.
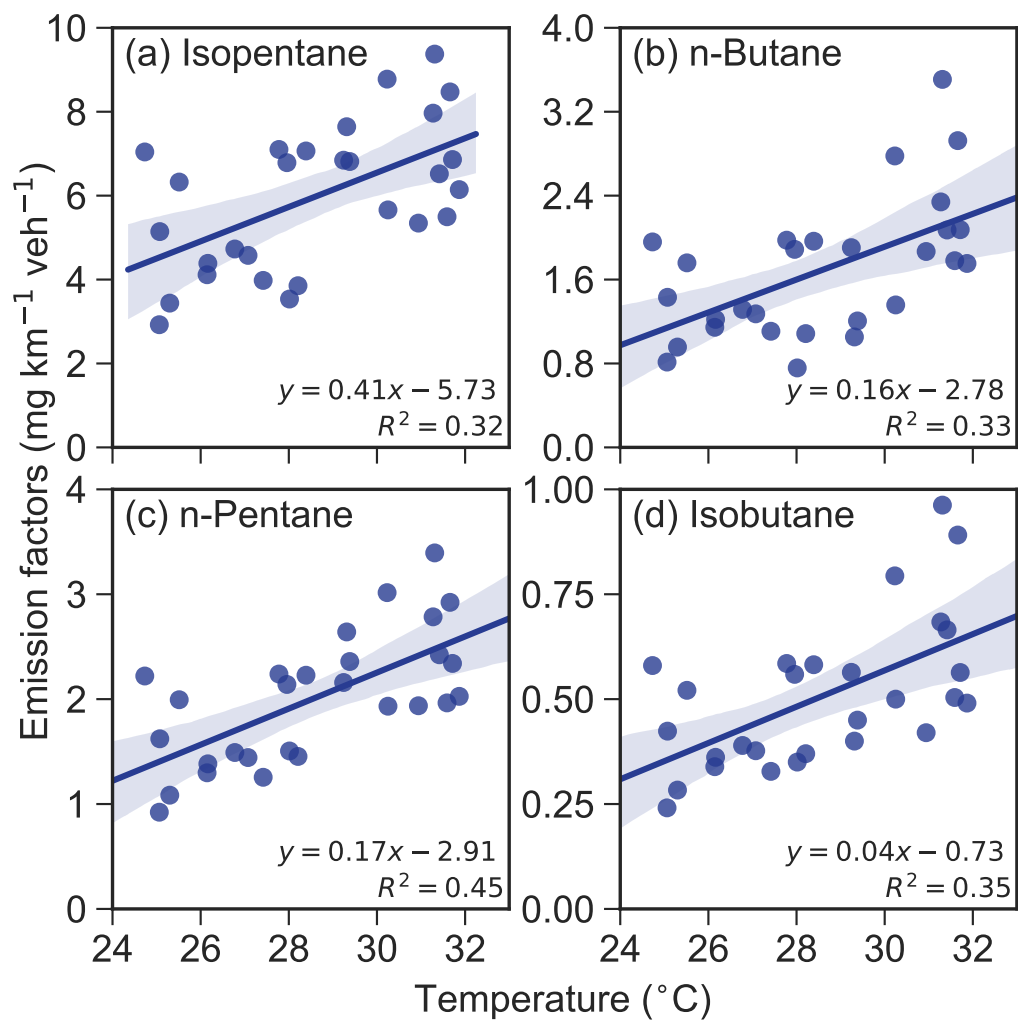
Figure 8. The linear regressions (filled with 95% regression confidence intervals) between emission factors of (a) Isopentane, ~~(b) Toluene~~ (b) n-Butane , (c) n-Pentane, and ~~(d) n-Butane~~ (d) Isobutane against ambient temperature data .
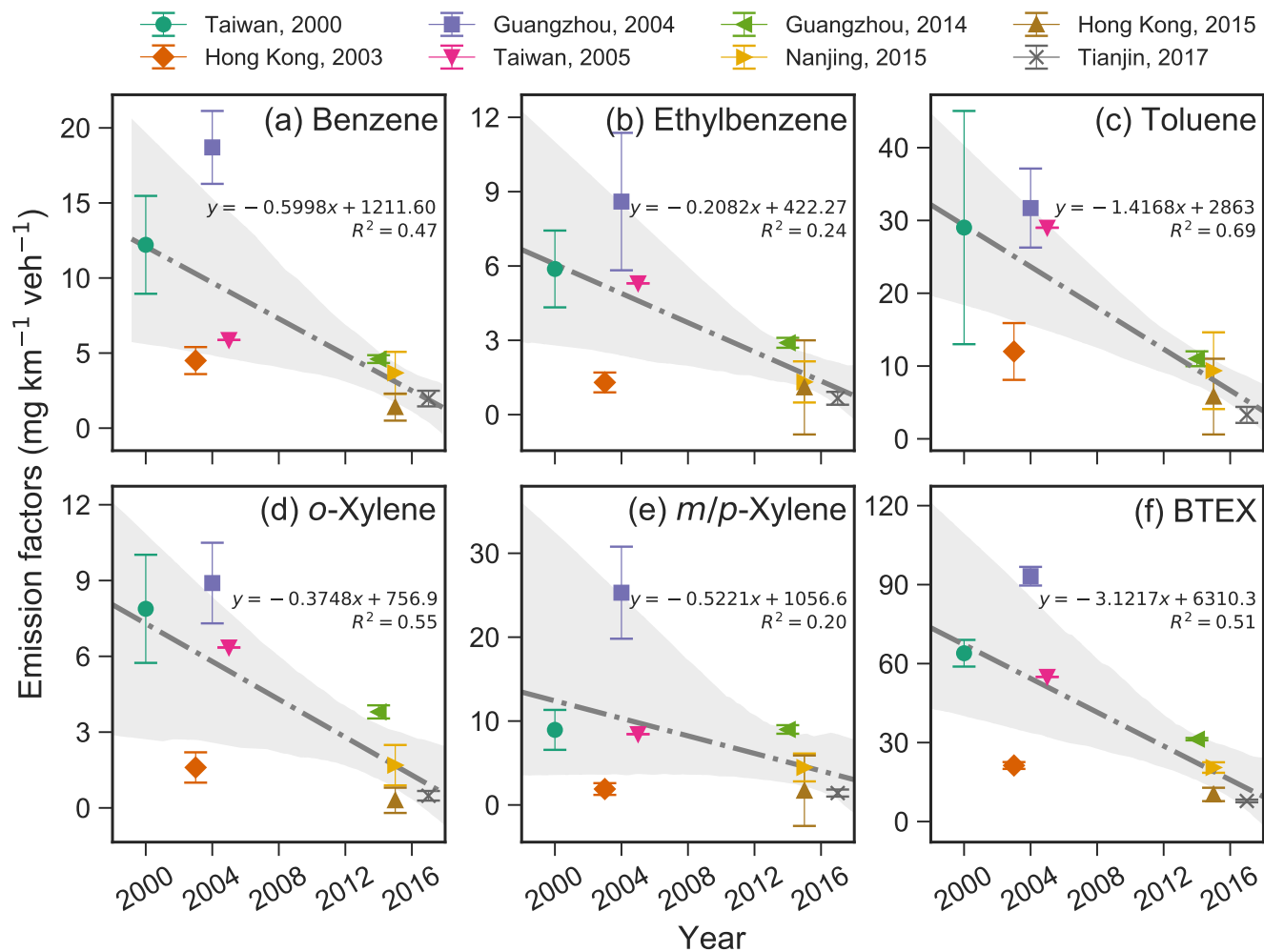
Figure 9. The BTEX (Benzene, Ethylbenzene, Toluene, *o*-Xylene, and *m/p*-Xylene) levels (mean±standard deviation) observed in different tunnel studies (Taiwan in 2000 (Hwa et al., 2002); Hong Kong in 2003 (Ho et al., 2009); Guangzhou in 2004 (Zhang et al., 2018c); Taiwan in 2005 (Hung-Lung et al., 2007); Guangzhou in 2014 (Zhang et al., 2018c); Nanjing in 2015 (Zhang et al., 2018b); Hong Kong in 2015 (Cui et al., 2018)), and the linear regressions (dash-dot lines filled with 95% regression confidence intervals) between the emission factors of BTEX and the test years.
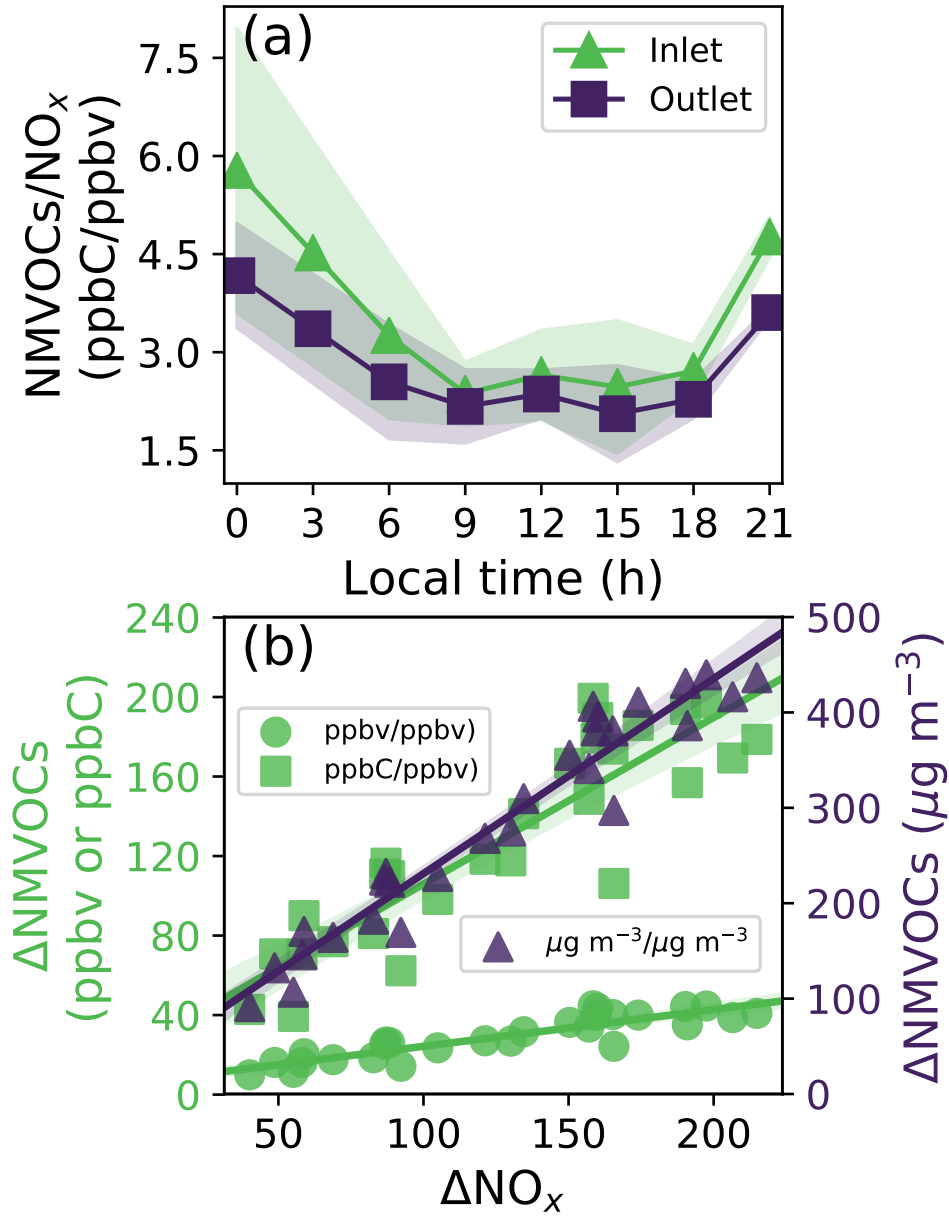
Figure 10. (a)The diurnal variations (filled with one standard deviation) of the NMVOCs/NO$_x$ in the inlet and outlet of the tunnel, and (b) the linear regression (filled with 95% confidence intervals) between ΔNMVOCs (i.e., $C_{Outlet} - C_{Inlet}$) and ΔNO$_x$ (i.e., $C_{Outlet} - C_{Inlet}$), ΔNMVOCs (ppbv)=0.18×ΔNO$_x$ (ppbv)+5.80, ΔNMVOCs (ppbC)=0.84×ΔNO$_x$ (ppbv)+22.16, ΔNMVOCs (μg m^{-3})=2.04×ΔNO$_x$ (μg m^{-3})+26.59.
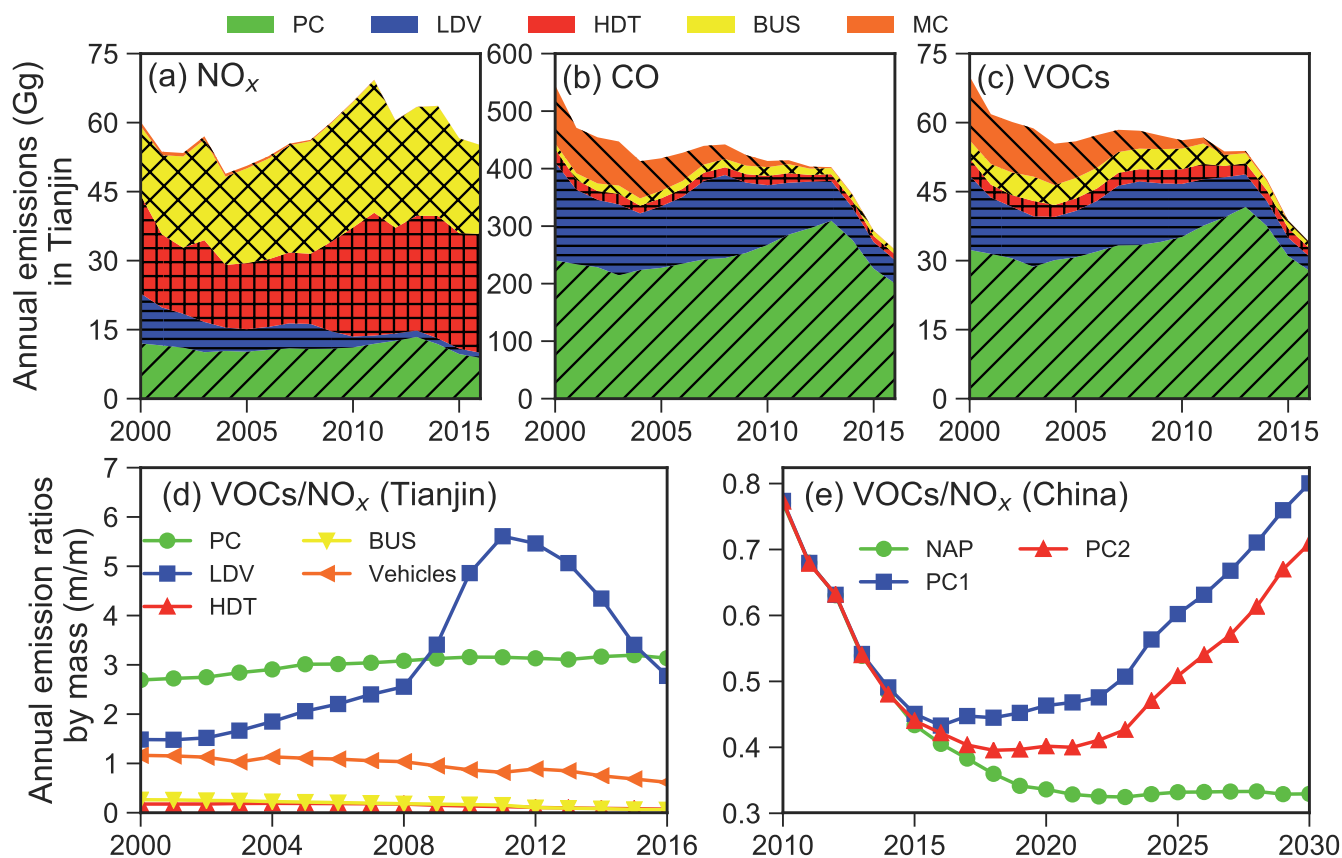
Figure 11. Estimated annual vehicular emissions of (a) NO_X, (b) CO, and (c) VOCs in Tianjin during 2000-2016. The vehicular emission ratios (m/m) of VOCs to NO_x in (d) Tianjin and (e) China. (PC: passenger cars; LDV: light-duty vehicles; HDT: heavy-duty trucks; BUS: buses; MC: motocycles. NAP: Standards are assumed at the same level of 2013 during the future years (e.g., China IV for light-duty gasoline vehicles and China III for heavy-duty diesel vehicls); PC1: Increasingly stringent emission standards and improved fuel quality are implemented according to a probably timetable; PC2: For internal combustion engine vehicles, the implementation of future emission standards is consistent with that under the PC1 scenario. The vehicle emissions of (a) NO_x, (b) CO, and (c) VOCs in Tianjin during 2000-2016 were estimated by the COPERT IV model. The estimated total vehicular emission ratios of VOCs to NO_x in China for NAP, PC1, and PC2 scenarios from 2010 to 2030 were based on Wu et al. (2017)'s study.)

37

Table 1. Average emission factors of Wujinglu tunnel in this study and their comparisons with other tunnel studies.

City	Tunnel	Gradient	Test year	Vehicle type	Emission factors (mg veh^{-1} km^{-1})			
					NO	NO$_2$	NO$_x$	CO
Hong Kong[a]	ShingMun tunnel	1%	2004	50% DVs	N.A.	N.A.	878±308	1845±434
Taiwan[b]	Hsuehshan tunnel	-1.3%	2006	LDV	N.A.	N.A.	145±67	910±470
		1.3%	2006	LDV	N.A.	N.A.	331±166	1470±630
Shanghai[c]	East Yan'an Road tunnel	-3%	2012	94.5% GVs	N.A.	N.A.	N.A.	1266±889
		3%	2012	94.5% GVs	N.A.	N.A.	N.A.	3353±2155
Changsha[d]	Yingpan Road tunnel	-6%	2013	96.3%-98.4% GVs	N.A.	N.A.	121±22	754±561
		6%	2013	96.3%-98.4% GVs	N.A.	N.A.	818±755	6050±5940
Guangzhou[e]	Zhujiang tunnel	N.A.	2013	88.2% GVs	N.A	N.A	560±50	N.A.
		N.A.	2014	61%LDV; 27% LPG; 12% HDV	N.A.	N.A.	1286±204	3096±680
Shanghai[f]	East Yan'an Road tunnel	N.A.	2016	94.1% GVs	N.A	N.A	400±250	1840±900
Tianjin[g]	Wujinglu tunnel	-4%	2017	94.2% GVs	62±72	17±11	79±78	270±342
		4%	2017	94.2% GVs	159±73	24±20	181±88	578±382
		Overall	2017	94.2% GVs	98±70	16±9	117±78	345±250

[a] Hong Kong (Cheng et al., 2006); [b] Taiwan (Chang et al., 2008); [c] Shanghai (Deng et al., 2015); [d] Changsha (Deng et al., 2015); [e] Guangzhou (Liu et al., 2014; Zhang et al., 2015); [f] Shanghai (Huang et al., 2017); [g] This study.

N.A. – not available.

Table 2. Typical ratios (v/v) related to vehicle emissions compared to previous tunnel studies.

	Taiwan[a]	Hong Kong[b]	Guangzhou[c]	Taiwan[d]	Average[e]	Guangzhou[f]	Nanjing[g]	Hong Kong[h]	Tianjin[i]	Average[j]
	2000	2003	2004	2005	2000-2005	2014	2015	2015	2017	2014-2017
T/B	2.01	2.26	1.44	4.19	2.48±1.19	2.03	2.16	3.51	~~1.42~~ 1.38±0.34	2.28±0.88
~~i-P/B~~	~~1.11~~	~~1.35~~	~~2.40~~	~~7.39~~	~~3.06±2.94~~	~~4.00~~	~~5.24~~	~~1.93~~	~~3.74~~	~~3.73±1.36~~
~~i-P/T~~	~~0.55~~	~~0.60~~	~~1.67~~	~~1.76~~	~~1.15±0.66~~	~~1.97~~	~~2.43~~	~~0.55~~	~~2.64~~	~~1.9±0.94~~
~~i-B/n-B~~	~~0.70~~	~~0.63~~	~~0.50~~	~~NA~~	~~0.61±0.1~~	~~0.58~~	~~0.94~~	~~0.72~~	~~0.28~~	~~0.63±0.28~~
~~i-P/n-P~~	~~1.31~~	~~3.29~~	~~2.94~~	~~2.08~~	~~2.41±0.89~~	~~2.43~~	~~3.64~~	~~1.92~~	~~3.18~~	~~2.79±0.77~~
m,p-X/B	0.54	0.31	1.00	1.06	0.73±0.36	1.44	0.89	0.89	0.57±0.23	0.94±0.37
E/m,p-X	0.66	0.68	0.34	0.63	0.58±0.16	0.32	0.30	0.65	0.49±0.19	0.43±0.16
B/i-P	0.90	0.74	0.42	0.14	0.55±0.34	0.25	0.19	0.52	0.29±0.07	0.31±0.14
T/i-P	1.82	1.68	0.60	0.57	1.17±0.68	0.51	0.41	1.82	0.42±0.19	0.78±0.69
m,p-X/i-P	0.49	0.23	0.41	0.14	0.32±0.16	0.36	0.17	0.46	0.17±0.08	0.28±0.15
o-X/i-P	0.43	0.19	0.15	0.11	0.22±0.14	0.15	0.06	0.08	0.06±0.03	0.09±0.05
Styrene/i-P	0.27	N.A.	0.03	0.05	0.11±0.13	0.04	0.02	0.28	0.01±0.00	0.09±0.13
E/i-P	0.32	0.16	0.14	0.09	0.18±0.10	0.12	0.05	0.30	0.08±0.06	0.13±0.11
i-B/n-B	0.70	0.63	0.50	NA	0.61±0.1	0.58	0.94	0.72	~~0.28~~ 0.27±0.04	0.63±0.28
i-P/n-P	1.31	3.29	2.94	2.08	2.41±0.89	2.43	3.64	1.92	~~3.18~~ 2.80±0.18	2.79±0.77
MTBE/B	N.A.	N.A.	N.A.	N.A.	N.A.	N.A.	0.38	N.A.	~~1.12~~ 1.08±0.37	0.75±0.52
MTBE/T	N.A.	N.A.	N.A.	N.A.	N.A.	N.A.	0.18	N.A.	~~0.79~~ 0.82±0.32	0.48±0.43
B/2,2-DimB	10.21	24.82	18.76	2.87	14.16±9.63	6.34	11.28	15.45	~~12.79~~ 16.32±16.80	11.46±3.82
T/2,2-DimB	20.56	56.12	26.95	12.00	28.91±19.15	12.86	24.32	54.25	~~18.10~~ 21.26±19.51	27.38±18.51
E/2,2-DimB	3.62	5.28	6.35	1.90	4.29±1.95	2.94	2.98	8.93	~~3.15~~ 3.58±2.33	4.50±2.95
~~m,p-X/2,3-DimB~~	~~5.40~~	~~5.14~~	~~5.13~~	~~0.54~~	~~4.05±2.35~~	~~4.87~~	~~0.64~~	~~4.60~~	~~2.96~~	~~3.27±1.94~~
m,p-X/2,2-DimB	5.50	7.71	N.A.	9.13	7.45±1.83	10.08	N.A.	6.78	6.96±1.82	7.88±1.90
o-X/2,2-DimB	4.85	6.49	6.57	2.28	5.05±2.01	3.86	3.81	2.44	~~2.29~~ 2.33±0.82	3.10±0.85
B/E	2.82	4.71	2.96	1.51	3±1.31	2.16	3.79	1.73	~~4.06~~ 4.46±1.58	2.93±1.16
T/E	5.69	10.64	4.25	6.30	6.72±2.75	4.37	8.17	6.08	~~5.74~~ 6.10±1.68	6.09±1.57
m,p-X/E	1.51	1.46	2.94	1.59	1.88±0.71	3.10	3.39	1.55	~~2.15~~ 2.29±0.74	2.55±0.85

T: Toluene; B: Benzene; E: Ethylbenzene; m,p-X: m,p-Xylenes; o-X: o-xylene; i-P: i-Pentane; n-P: n-Pentane; i-B: i-Butane; n-B: n-Butane; MTBE: methyl tert-butyl ether; 2,2-DimB: 2,2-Dimethylbutane; ~~2,3-DimB: 2,3-Dimethylbutane;~~

[a] Taiwan (Hwa et al., 2002); [b] Hong Kong (Ho et al., 2009); [c] Guangzhou (Zhang et al., 2018c); [d] Taiwan (Hung-Lung et al., 2007); [e] Averaged values from tunnel studies in Taiwan in 2000, Hong Kong in 2003, Guangzhou in 2004, and Taiwan in 2005. [f] Guangzhou (Zhang et al., 2018c); [g] Nanjing (Zhang et al., 2018b); [h] Hong Kong in 2015 (Cui et al., 2018); [i] This study; [j] Averaged values from tunnel studies in Guangzhou in 2014, Nanjing in 2015, Hong Kong in 2015, and Tianjin in 2017. N.A. – not available.
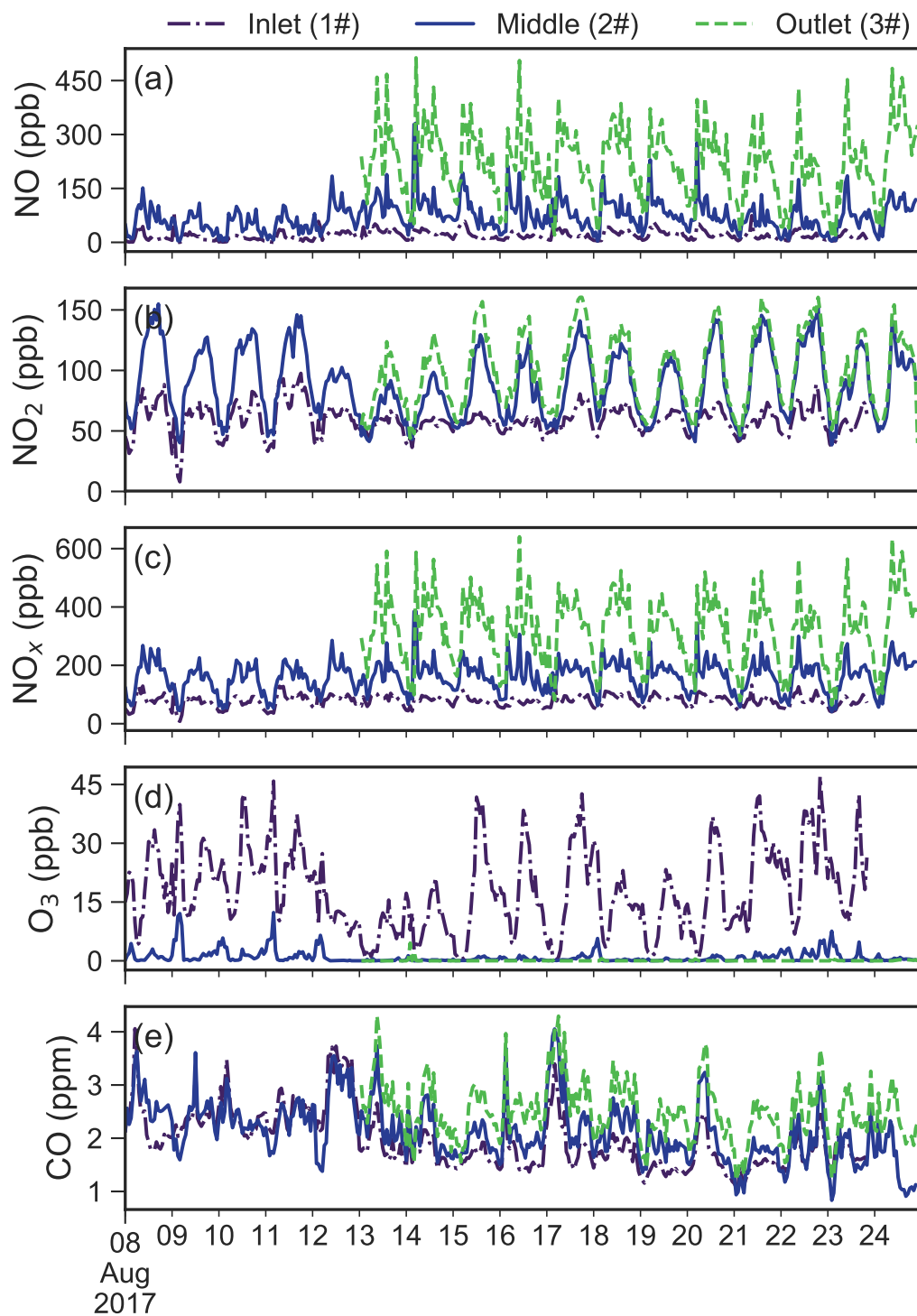
Figure A1. The time series of (a) NO, (b) NO$_2$, (c) NO$_x$, (d) CO and (e) wind speed (WS, measured by Flowsick).

1
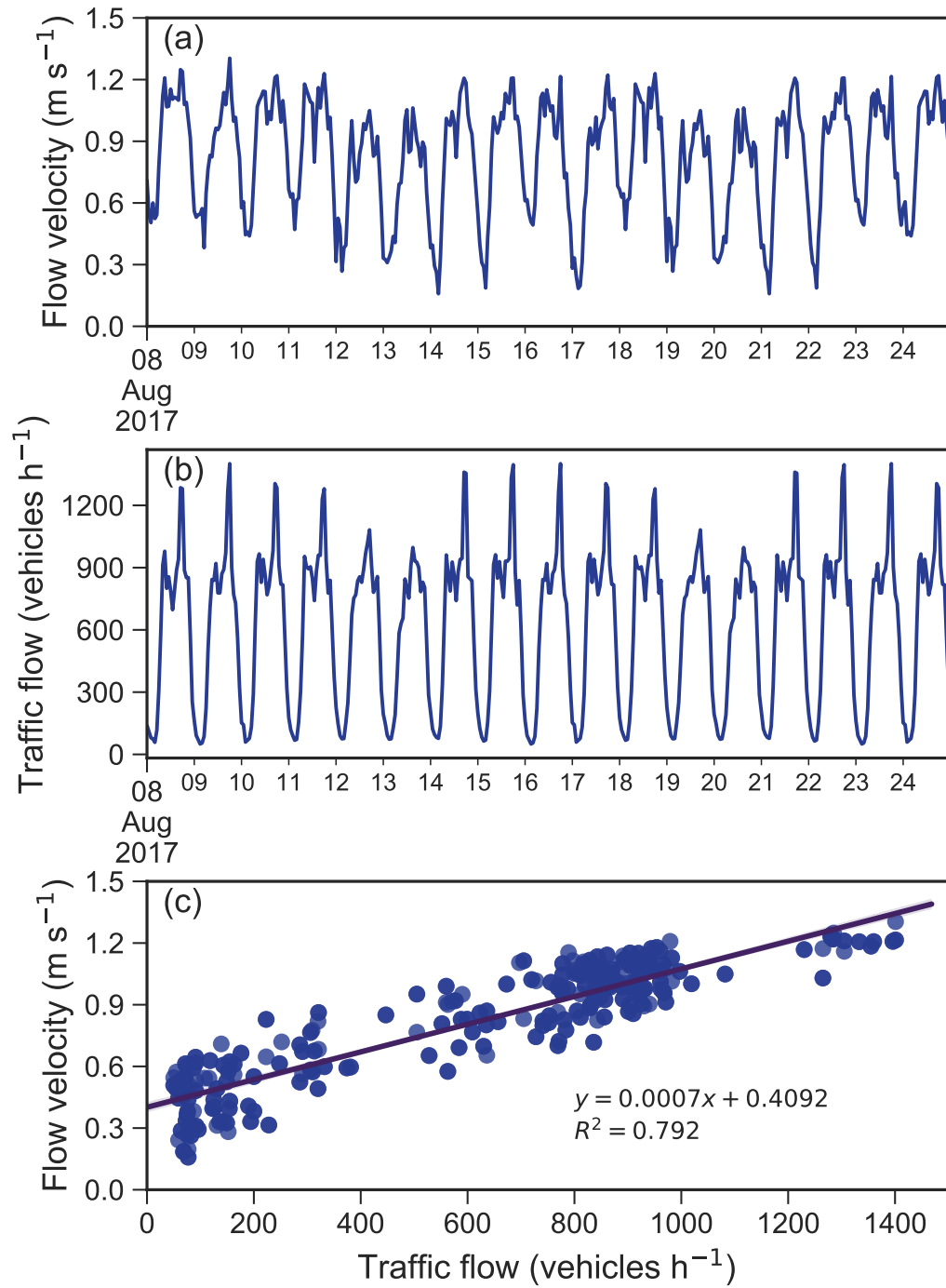
Figure A2. The time series of (a) traffic flow and (b) velocity flow, and (c) their relationships.

In panel (c):

$$y = 0.0007x + 0.4092$$
$$R^2 = 0.792$$
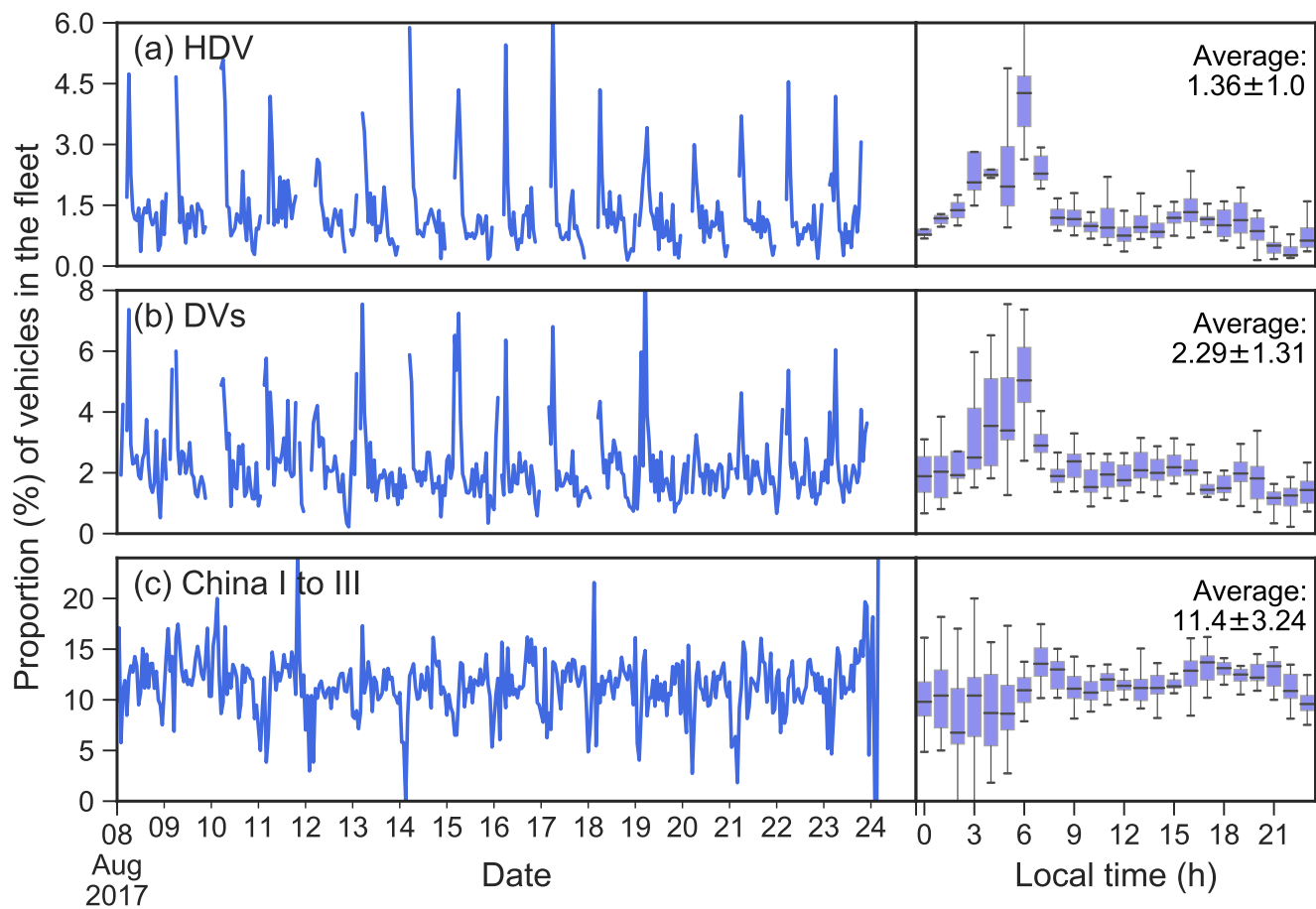
Figure A3. The proportions of (a) heavy-duty vehicles (HDV), (b) diesel vehicles (DVs), and (c) emission standards from China I to China III in the fleet.
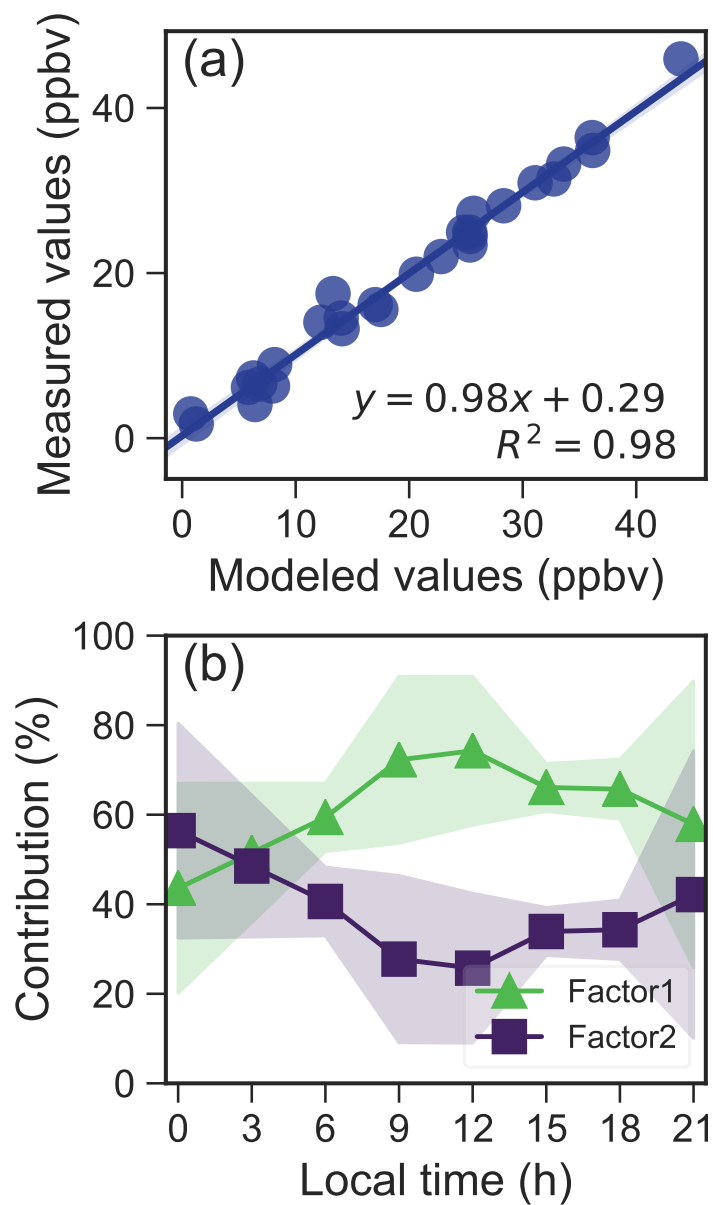
Figure A4. (a) The relationships between the measured and modeled concentrations of NMVOCs for PMF; (b) the diurnal variations (filled with one standard deviation) of the factor contributions to total variance.

Table A1. The meteorological factors and concentrations of air pollutants in the ambient air, and the inlet and outlet of the tunnel.

	Ambient	Inlet (1#)	Middle (2#)	Outlet (3#)
Meteorological factors				
Wind speed (m s^{-1})	1.51±0.65	1.56±0.48	0.88±0.26	N.A.
Pressure (hPa)	1004.57±3.54	1001.12±9.31	1003.86±30.55	N.A.
Temperature (°C)	27.13±2.32	28.52±2.68	29.28±1.50	N.A.
Relative humidity (%)	71.44±10.44	64.92±11.06	62.68±7.68	N.A.
Air pollutants				
NO (ppb)	2.76±3.09	19.42±13.59	72.65±44.84	220.43±99.73
NO_2 (ppb)	14.73±6.90	59.12±12.33	89.06±28.57	99.48±30.48
NO_x (ppb)	17.49±8.85	78.54±20.38	161.71±54.80	319.91±118.35
O_3	45.44±25.86	18.05±10.65	0.96±1.63	0.05±0.32
CO (ppm)	0.97±0.40	1.96±0.55	2.13±0.57	2.50±0.55
O_x (ppb)	60.17±22.38	77.17±17.21	90.03±28.42	99.53±30.42
NO_2/NO_x	0.85±0.08	0.77±0.11	0.58±0.15	0.34±0.11
NMVOCs (ppb)	N.A.	73.46±26.70	104.31±23.06	N.A.
NMVOCs/NO_x (ppbC/ppb)	N.A.	3.43±1.50	2.74±0.90	N.A.

N.A. – not available.

Table A2: The statistical description of the linear regression between fleet-average emission factors (and f_{NO_2}) and the proportions of vehicle types (HDV: heavy-duty vehicles, LDV: light-duty vehicles, DVs: diesel vehicles, GVs: gasoline vehicles).

Vehicle type	Road condition	Target	Intercept	Slope	Pearson's r	Adj. R-Square	Prob>F
DVs	Downslope	NO	29.15±6.57	1298.33±2.59	0.93	0.83	0.01
		NO$_2$	15.41±3.01	29.37±1.19	0.12	-0.23	0.82*
		NO$_x$	51.88±6.15	1081.15±2.43	0.91	0.79	0.01
		CO	144.38±26.55	4598.72±10.47	0.91	0.79	0.01
		f$_{NO_2}$ Ratio1	0.48±0.02	-3.85±0.01	-0.93	0.83	0.01
		f$_{NO_2}$ Ratio2	0.21±0.02	-1.42±0.01	-0.67	0.32	0.14*
	Upslope	NO	96.42±4.95	2724.6±1.95	0.99	0.97	0
		NO$_2$	15.08±2.47	363.77±0.97	0.88	0.72	0.02
		NO$_x$	114.02±7.08	2933.45±2.8	0.98	0.96	0
		CO	466.9±35.73	3279.35±14.1	0.76	0.47	0.08*
		f$_{NO_2}$ Ratio1	0.10±0.01	-0.33±0.53	-0.30	0.14	0.56*
		f$_{NO_2}$ Ratio2	0.09±0.01	-0.23±0.59	-0.19	0.20	0.71*
	Overall	NO	52.13±6.94	2102.17±2.74	0.97	0.92	0
		NO$_2$	16.34±1.65	-20.76±0.65	-0.16	-0.22	0.77*
		NO$_x$	71.42±7.31	2084.32±2.88	0.96	0.91	0
		CO	297.65±22.42	1389.61±8.85	0.62	0.23	0.19*
		f$_{NO_2}$ Ratio1	0.06±0.03	2.46±0.01	0.76	0.47	0.08*
		f$_{NO_2}$ Ratio2	0.04±0.02	2.57±0.01	0.8	0.55	0.06*
HDV	Downslope	NO	32.55±5.06	1586.99±3.14	0.93	0.83	0.01
		NO$_2$	17.73±2.42	-149.63±1.5	-0.45	0	0.37*
		NO$_x$	57.71±6.13	1146.53±3.8	0.83	0.62	0.04
		CO	134.52±27.44	7245.15±17	0.91	0.77	0.01
		f$_{NO_2}$ Ratio1	0.48±0.01	-6.32±0.01	-0.98	0.94	0
		f$_{NO_2}$ Ratio2	0.23±0.02	-3.02±0.01	-0.79	0.52	0.06*
	Upslope	NO	115.34±8.34	3101.09±5.17	0.95	0.88	0
		NO$_2$	15.3±1.62	501.46±1.01	0.93	0.83	0.01
		NO$_x$	135.81±9.77	3090.29±6.05	0.93	0.83	0.01

(Continued on next page)

Vehicle type	Road condition	Target	Intercept	Slope	Pearson's r	Adj. R-Square	Prob>F
		CO	474.6±22.28	1240.84±13.81	0.41	-0.04	0.42*
		f_{NO_2} Ratio1	0.08±0.01	0.27±0.61	0.22	-0.19	0.68*
		f_{NO_2} Ratio2	0.07±0.01	0.42±0.59	0.34	-0.11	0.51*
	Overall	NO	66.33±6.43	2196.89±3.98	0.94	0.85	0.01
		NO_2	17.09±1.66	-65.88±1.03	-0.3	-0.13	0.56*
		NO_x	87.87±7.61	2038.12±4.72	0.91	0.78	0.01
		CO	286.53±17.51	1590.86±10.85	0.59	0.19	0.22*
		f_{NO_2} Ratio1	-0.24±0.52	0.33±0.53	0.3	-0.14	0.56*
		f_{NO_2} Ratio2	-0.14±0.57	0.23±0.59	0.19	0.20	0.71*
GVs	Downslope	NO	1327.48±253.37	-1298.33±2.59	-0.93	0.83	0.01
		NO_2	44.77±115.98	-29.37±1.19	-0.12	-0.23	0.82*
		NO_x	1133.02±237.18	-1081.15±2.43	-0.91	0.79	0.01
		CO	4743.1±1023.68	-4598.72±10.47	-0.91	0.79	0.01
		f_{NO_2} Ratio1	-3.37±0.76	3.85±0.01	0.93	0.83	0.01
		f_{NO_2} Ratio2	-1.21±0.76	1.42±0.01	0.67	0.32	0.14*
	Upslope	NO	282.02±190.93	-2724.6±1.95	-0.99	0.97	0
		NO_2	378.85±95.2	-363.77±0.97	-0.88	0.72	0.02
		NO_x	3047.47±273.2	-2933.45±2.8	-0.98	0.96	0
		CO	3746.25±1377.98	-3279.35±14.1	-0.76	0.47	0.08*
		f_{NO_2} Ratio1	-0.24±0.52	0.33±0.53	0.30	0.14	0.56*
		f_{NO_2} Ratio2	-0.14±0.57	0.23±0.59	0.19	-0.20	0.71*
	Overall	NO	2154.3±267.47	-2102.17±2.74	-0.97	0.92	0
		NO_2	-4.42±63.81	20.76±0.65	0.16	-0.22	0.77*
		NO_x	2155.74±281.88	-2084.32±2.88	-0.96	0.91	0
		CO	1687.25±864.58	-1389.61±8.85	-0.62	0.23	0.19*
		f_{NO_2} Ratio1	2.51±1.02	-2.46±0.01	-0.76	0.47	0.08*
		f_{NO_2} Ratio2	2.61±0.94	-2.57±0.01	-0.8	0.55	0.06*
LDV	Downslope	NO	1619.53±309.53	-1586.99±3.14	-0.93	0.83	0.01
		NO_2	-131.9±147.96	149.63±1.5	0.45	0	0.37*

(Continued on next page)

7

Table A2 : *(Continued)*

Vehicle type	Road condition	Target	Intercept	Slope	Pearson's r	Adj. R-Square	Prob>F
		NO_x	1204.24±374.63	-1146.53±3.8	-0.83	0.62	0.04
		CO	7379.67±1677.3	-7245.15±17	-0.91	0.77	0.01
		f_{NO_2} Ratio1	-5.84±0.7	6.32±0.01	0.98	0.94	0
		f_{NO_2} Ratio2	-2.8±1.18	3.02±0.01	0.79	0.52	0.06*
	Upslope	NO	3216.43±509.5	-3101.09±5.17	-0.95	0.88	0
		NO_2	516.76±99.21	-501.46±1.01	-0.93	0.83	0.01
		NO_x	3226.1±597.22	-3090.29±6.05	-0.93	0.83	0.01
		CO	1715.45±1361.86	-1240.84±13.81	-0.41	-0.04	0.42*
		f_{NO_2} Ratio1	-0.35±0.61	-0.27±0.61	-0.22	0.19	0.68*
		f_{NO_2} Ratio2	-0.49±0.58	-0.42±0.59	-0.34	-0.11	0.51*
	Overall	NO	2263.22±392.93	-2196.89±3.98	-0.94	0.85	0.01
		NO_2	-48.79±101.52	65.88±1.03	0.3	-0.13	0.56*
		NO_x	2126±465.35	-2038.12±4.72	-0.91	0.78	0.01
		CO	1877.39±1070.2	-1590.86±10.85	-0.59	0.19	0.22*
		f_{NO_2} Ratio1	4.4±1.07	-4.35±0.01	-0.9	0.75	0.02
		f_{NO_2} Ratio2	4.22±1.02	-4.18±0.01	-0.9	0.76	0.02

* – The linear regression is not significant at the 0.05 level ($p>0.05$).

8

Table A3. The average (±standard deviation) emission factors (mg km^{-1} veh^{-1}) measured in the WJL tunnel in Tianjin in 2017.

Vehicle type		Road condition	NO	NO$_2$	NO$_x$	CO
Fleet		Downslope	61.92±72.46	16.52±11.49	79.45±78.43	269.96±342.38
		Upslope	158.58±73.48	23.98±20.14	181.22±88.29	577.76±382.22
		Overall	97.52±69.84	15.86±9.38	116.56±77.61	344.67±250.01
GVs/DVs	GVs	Downslope	29.15±6.57	N.A.	51.88±6.15	144.38±26.55
		Upslope	96.42±4.95	15.08±2.47	114.02±7.08	N.A.
		Overall	52.13±6.94	N.A.	71.42±7.31	N.A.
	DVs	Downslope	1133.02±237.18	N.A.	1327.48±253.37	4743.1±1023.68
		Upslope	2802.02±190.93	378.85±95.2	3047.47±273.2	N.A.
		Overall	2154.3±267.47	N.A.	2155.74±281.88	N.A.
LDV/HDV	LDV	Downslope	32.55±5.06	N.A.	57.71±6.13	134.52±27.44
		Upslope	115.34±8.34	15.3±1.62	135.81±9.77	N.A.
		Overall	66.33±6.43	N.A.	87.87±7.61	N.A.
	HDV	Downslope	1204.24±374.63	N.A.	1619.53±309.53	7379.67±1677.3
		Upslope	3216.43±509.5	516.76±99.21	3726.1±597.22	N.A.
		Overall	2126±465.35	N.A.	2263.22±392.93	N.A.

N.A. – The linear regression is not significant at the 0.05 level ($p>0.05$).

Table A4: Average emission factors (mg km^{-1} veh^{-1}) for individual VOC from different tunnel studies.

Compound	CAS No.	Taiwan[a]	Hong Kong[b]	Guangzhou[c]	Taiwan[d]	Guangzhou[e]	Nanjing[f]	Hong Kong[g]	Tianjin[h]
		2000	2003	2004	2005	2014	2015	2015	2017
Alkanes									
Ethane	74-84-0	4.27±0.96	1.7±0.6	4.9±0.72	N.A.	9± 0.51	52.47±6.72	1 ± 0.8	1.91±0.84
Propane	74-98-6	2.4±0.77	5.7±2.5	15.2±16.85	0.2	184±10.71	11.8±3.48	4.8 ± 2.4	0.36±0.21
Isobutane	75-28-5	4.57±0.94	5.5±2.2	5.1±2.37	N.A.	31± 1.53	4.09±1.64	7.3 ± 4.5	0.56±0.27
n-Butane	106-97-8	6.56±1.96	8.7±3.1	10.3±4.98	5.12	53± 3.06	4.34±0.13	10.2 ± 5.9	2.03±0.89
2,2-Dimethylbutane	75-83-2	1.32±0.25	0.2±0.2	1.1±0.32	2.26	0.8± 0.05	0.36±0.23	0.1 ± 0.1	0.17±0.06
2,3-Dimethylbutane	565-59-3	1.33±0.69	0.3±0.2	4±0.64	12.7	1.5± 0.1	5.63±2.71	0.3 ± 0.5	0.39±0.15
n-Pentane	109-66-0	9.52±3.05	1.7±0.6	14.1±2.15	19.28	7± 0.51	4.89±3.59	1.3 ± 1.8	2.14±0.99
Isopentane	78-78-4	12.5±4.09	5.6±2.1	41.5±6.94	40.07	17± 1.53	17.82±11.97	2.5 ± 1.7	6.80±2.35
2-Methylpentane	107-83-5	5.27±1.72	1.8±0.7	20.5±3.36	12.56	5.7± 0.41	4.60±2.69	0.6 ± 0.4	1.59±0.59
3-Methylpentane	96-14-0	6.39±1.53	1.2±0.5	13.2±2.37	5.62	3.6± 0.26	2.03±1.10	0.3 ± 0.2	1.38±0.54
2,3-Dimethylpentane	565-59-3	1.33±0.69	0.1±0.1	1.9±0.4	0.72	0.9±0.05	0.86±0.55	0.1 ± 0.1	0.20±0.04
2,4-Dimethylpentane	108-08-7	0.44±0.07	0.2±0.1	1.4±0.32	0.9	3±0.15	0.23±0.10	0.1 ± 0.1	0.14±0.03
2,2,4-Trimethylpentane	540-84-1	0.29±0.18	1±0.7	N.A.	0.77	1.6± 0.1	0.33±0.17	0.6 ± 0.4	0.66±0.10
2,3,4-Trimethylpentane	565-75-3	N.A.	0.2±0.2	N.A.	0.05	0.6± 0.05	0.16±0.08	0.2 ± 0.2	0.38±0.10
n-Hexane	110-54-3	4.18±1.56	1.3±0.5	8.1±1.52	5.7	2.3± 0.26	1.70±1.35	1.2 ± 1.5	0.85±0.27
2-Methylhexane	591-76-4	N.A.	0.7±0.3	7.3±1.15	2.53	0.6± 0.05	1.2±0.56	0.2 ± 0.1	0.37±0.13
3-Methylhexane	589-34-4	2.94±0.43	0.8±0.3	7.4±1.05	2.75	2.5± 0.15	0.33±0.17	0.3 ± 0.2	0.55±0.15
n-Heptane	142-82-5	1.46±0.24	0.9±0.4	4.7±0.72	1.63	1.9± 0.1	0.85±0.42	0.2 ± 0.2	0.39±0.09
2-Methylheptane	592-27-8	1.05±0.29	0.3±0.1	3.5±0.75	0.79	0.9± 0.05	0.79±0.32	0.1 ± 0.1	0.20±0.05
3-Methylheptane	589-81-1	1.02±0.33	0.2±0.1	4.3±0.83	2.01	0.9± 0.05	0.38±0.18	0.1 ± 0.1	0.17±0.05
Octane	111-65-9	1.31±0.29	0.5±0.2	3.2±0.86	0.78	0.8± 0.05	0.59±0.29	0.1 ± 0.2	0.18±0.05
n-Nonane	111-84-2	0.54±0.13	0.7±0.4	2.7±0.28	0.31	0.6± 0.05	0.10±0.07	0.6 ± 0.7	0.06±0.01
n-Decane	124-18-5	N.A.	0.8±0.6	2.1±0.69	0.07	0.8± 0.05	0.05±0.04	1 ± 1.4	0.07±0.02
Udecane	1120-21-4	N.A.	N.A.	2.2±0.59	1.39	1.8±0.15	N.A.	N.A.	0.04±0.02
Dodecane	112-40-3	N.A.	N.A.	3.1±0.96	N.A.	1.9± 6.06	N.A.	N.A.	0.13±0.09
Cyclopentane	287-92-3	0.89±0.21	1±0.4	4.2±1.42	2	0.8± 5.97	0.33±0.14	0.2 ± 0.9	0.26±0.10
Methylcyclopentane	96-37-7	2.64±0.93	0.7±0.2	N.A.	2.19	0.6± 0.05	1.18±0.60	0.2 ± 0.2	0.58±0.18
Methylcyclohexane	108-87-2	0.94±0.18	0.4±0.2	7±0.57	0.73	1.1± 0.05	0.45±0.25	0.2 ± 0.2	0.26±0.09
Cyclohexane	110-82-7	0.98±0.13	0.3±0.1	1.1±0.13	0.4	2.4± 5.88	0.07±0.05	0.2 ± 0.2	0.24±0.15
Alkenes									
Ethylene	74-85-1	26.23±4.89	13.0±4.0	52.9±7.44	N.A.	16± 9.15	10.17±1.05	4.2 ± 2	2.56±0.47
Acetylene	74-86-2	11.56±3.02	4.0±1.3	N.A.	N.A.	7± 0.51	5.06±1.51	1.5±1	0.69±0.19
Propylene	115-07-1	N.A.	5.3±1.5	22.6±3.21	10.36	9.7± 0.46	6.79±1.55	1.9 ± 0.9	1.02±0.22
cis-2-Butene	590-18-1	1.84±0.46	0.5±0.1	4.6±0.92	1.56	1.3± 0.1	0.49±0.14	0.1 ± 0.1	0.17±0.07
trans-2-Butene	624-64-6	1.61±0.38	0.6±0.2	4.9±1.01	0.81	1.9± 0.15	0.90±0.36	0.2 ± 0.1	0.23±0.11
1-Butene	106-98-9	8.27±1.55	1.6±0.6	17.7±6.26	10.67	2.8± 0.15	0.79±0.13	1.2 ± 1.1	0.19±0.07
1,3-Butadiene	590-19-2	2.56±0.38	0.3±0.6	7.8±1.72	3.83	0.7± 0.2	0.11±0.08	0.2 ± 0.3	0.17±0.06
cis-2-Pentene	627-20-3	1.59±0.43	N.A.	4.6±1.21	1.57	0.8± 0.05	0.39±0.20	0.1 ± 0.1	0.09±0.03
trans-2-Pentene	646-04-8	2.76±0.77	0.6±0.2	8.5±2	4.08	1.5± 0.15	0.9±0.36	0.2 ± 0.1	0.25±0.10

(Continued on next page)

10

Table A4 : *(Continued)*

Compound	CAS No.	Taiwan[a]	Hong Kong[b]	Guangzhou[c]	Taiwan[d]	Guangzhou[e]	Nanjing[f]	Hong Kong[g]	Tianjin[h]
		2000	2003	2004	2005	2014	2015	2015	2017
1-Pentene	109-67-1	1.61±0.38	1.9±2.1	4.6±0.73	0.97	0.8± 0.05	0.23±0.01	0.2 ± 0.1	0.09±0.03
1-Hexene	592-41-6	N.A.	0.4±0.3	4.5±1.02	12.04	0.5± 0.05	0.30±0.14	0.1 ± 0.1	0.08±0.02
Isoprene	78-79-5	N.A.	0±0	N.A.	15.25	N.A.	N.A.	0.2 ± 0.2	0.08±0.03
Aromatics									
Benzene	71-43-2	12.21±3.26	4.5±0.9	18.7±21.13	5.87	4.6± 0.26	3.68±1.40	1.4 ± 0.9	1.97±0.52
Ethylbenzene	100-41-4	5.88±1.55	1.3±0.4	8.6±11.37	5.3	2.9± 0.2	1.32±0.83	1.1 ± 1.9	0.66±0.26
1,4-Diethylbenzene	105-05-5	N.A.	0.6±0.4	N.A.	2.41	2.6±0.15	0.33±0.01	0.1±0.1	0.09±0.04
1,3-Diethylbenzene	141-93-5	N.A.	0.2±0.2	N.A.	0.63	0.9±0.05	0.05±0.01	0±0.1	0.03±0.01
1,2,3-Trimethylbenzene	526-73-8	N.A.	1.4±1.1	2.7±5.13	1.95	4.3± 0.26	0.55±0.18	0.2 ± 0.2	0.12±0.04
1,2,4-Trimethylbenzene	95-63-6	14.28±2.94	3±2.4	11.2±15.08	11.8	7.7± 0.46	2.42±0.93	0.9 ± 1	0.48±0.19
1,3,5-Trimethylbenzene	108-67-8	2.31±0.38	0.8±0.4	3.1±3.67	3.72	3.6± 0.20	0.35±0.10	0.2 ± 0.2	0.13±0.04
n-Propylbenzene	103-65-1	1.68±0.6	0.5±0.2	1.8±2.2	1.7	1.6± 0.1	0.33±0.11	0.2 ± 0.2	0.10±0.04
Isopropylbenzene	98-82-8	N.A.	0.1±0.1	0.5±0.64	1.21	0.4± 0.05	0.12±0.07	0.2 ± 0.4	0.04±0.01
Toluene	108-88-3	29.02±16.02	12±3.9	31.7±37.13	29	11± 1.02	9.36±5.27	5.8 ± 5.2	3.29±1.10
2-Ethyltoluene	611-14-3	1.09±0.44	1.0±0.7	N.A.	3.91	2.5±0.15	0.54±0.19	0.2±0.2	0.12±0.04
3-Ethyltoluene	620-14-4	N.A.	1.4±0.9	N.A.	5.3	3.9±0.46	1.41±0.55	0.5±0.7	0.30±0.11
4-Ethyltoluene	622-96-8	N.A.	0.7±0.8	N.A.	2.79	3.1±0.2	0.56±0.20	0.3±0.5	0.14±0.06
o-Xylene	95-47-6	7.88±2.14	1.6±0.6	8.9±10.5	6.35	3.8± 0.26	1.69±0.80	0.3 ± 0.5	0.48±0.19
m/p-Xylene	108-38-3/ 106-42-3	8.95±2.38	1.9±0.7	25.3±30.79	8.44	9± 0.51	4.47±1.66	1.7±4.2	1.42±0.42
Styrene	100-42-5	4.81±1.33	N.A.	1.8±2.4	2.75	1.1± 0.2	0.44±0.19	1 ± 2.3	0.08±0.04
Halocarbons									
Chloromethane	74-87-3	N.A.	0±0	N.A.	N.A.	N.A.	0.39±0.29	N.A.	0.02±0.01
Dichloromethane	75-09-2	N.A.	0.1±0.1	N.A.	N.A.	N.A.	3.76±2.96	N.A.	0.12±0.06
Bromomethane	74-83-9	N.A.	0.1±0.5	N.A.	N.A.	N.A.	N.A.	N.A.	0±0
Bromodichloromethane	75-27-4	N.A.	N.A.	N.A.	N.A.	N.A.	N.A.	N.A.	0±0
Chloroethane	75-00-3	N.A.	N.A.	N.A.	N.A.	N.A.	N.A.	N.A.	0±0
1,2-Dibromoethane	106-93-4	N.A.	N.A.	N.A.	N.A.	N.A.	N.A.	N.A.	0±0
1,1-Dichloroethane	75-34-3	N.A.	N.A.	N.A.	N.A.	N.A.	N.A.	N.A.	0±0
1,2-Dichloroethane	107-06-2	N.A.	N.A.	N.A.	N.A.	N.A.	N.A.	N.A.	0.02±0.01
1,1,1-Trichloroethane	71-55-6	N.A.	N.A.	N.A.	N.A.	N.A.	N.A.	N.A.	0±0
1,1,2-Trichloroethane	79-00-5	N.A.	N.A.	N.A.	N.A.	N.A.	0.19±0.11	N.A.	0±0
1,2-Dichloropropane	78-87-5	N.A.	N.A.	N.A.	N.A.	N.A.	N.A.	N.A.	0.12±0.11
Vinylchloride	75-35-4	N.A.	N.A.	N.A.	N.A.	N.A.	N.A.	N.A.	0±0
Trichloroethylene	79-01-6	N.A.	0±0	N.A.	N.A.	N.A.	N.A.	N.A.	0±0
Tetrachloroethylene	127-18-4	N.A.	0±0	N.A.	N.A.	N.A.	N.A.	N.A.	0±0
1,1-Dichloroethylene	75-35-4	N.A.	N.A.	N.A.	N.A.	N.A.	N.A.	N.A.	0±0
cis-1,2-Dichloroethylene	156-59-2	N.A.	0±0	N.A.	N.A.	N.A.	N.A.	N.A.	0±0
cis-1,3-Dichloropropene	10061-01-5	N.A.	N.A.	N.A.	N.A.	N.A.	N.A.	N.A.	0±0
trans-1,3-Dichloropropene	10061-02-6	N.A.	N.A.	N.A.	N.A.	N.A.	N.A.	N.A.	0±0
Chlorobenzene	108-90-7	N.A.	N.A.	N.A.	N.A.	N.A.	N.A.	N.A.	0±0

Table A4 : *(Continued)*

Compound	CAS No.	Taiwan[a]	Hong Kong[b]	Guangzhou[c]	Taiwan[d]	Guangzhou[e]	Nanjing[f]	Hong Kong[g]	Tianjin[h]
		2000	2003	2004	2005	2014	2015	2015	2017
1,2-Dichlorobenzene	95-50-1	N.A.	N.A.	N.A.	N.A.	N.A.	N.A.	N.A.	0±0
1,3-Dichlorobenzene	541-73-1	N.A.	N.A.	N.A.	N.A.	N.A.	N.A.	N.A.	0±0
1,4-Dichlorobenzene	106-46-7	N.A.	N.A.	N.A.	N.A.	N.A.	N.A.	N.A.	0.01±0
Benzylchloride	100-44-7	N.A.	N.A.	N.A.	N.A.	N.A.	N.A.	N.A.	0±0
Carbontetrachloroide	56-23-5	N.A.	0±0	N.A.	N.A.	N.A.	0.24±0.19	N.A.	0±0
Chloroform	67-66-3	N.A.	N.A.	N.A.	N.A.	N.A.	0.39±0.29	N.A.	0.01±0.01
Freon11(CFCl3)	75-69-4	N.A.	N.A.	N.A.	N.A.	N.A.	1.22±0.90	N.A.	0±0
Freon113(C2F3Cl3)	76-13-1	N.A.	N.A.	N.A.	N.A.	N.A.	N.A.	N.A.	0±0
Freon114(C2F4Cl2)	76-14-2	N.A.	N.A.	N.A.	N.A.	N.A.	N.A.	N.A.	0±0
OVOCs									
Acetone	67-64-1	N.A.	N.A.	N.A.	12.6	N.A.	N.A.	N.A.	1.20±0.62
Methylethyl ketone	78-94-4	N.A.	N.A.	N.A.	2.85	N.A.	N.A.	N.A.	0.31±0.24
Methylvinylketone	78-94-4	N.A.	N.A.	N.A.	N.A.	N.A.	0.14±0.14	N.A.	0.14±0.07
Acetaldehyde	75-07-0	N.A.	N.A.	N.A.	N.A.	N.A.	N.A.	N.A.	0.73±0.57
acrolein	107-02-8	N.A.	N.A.	N.A.	N.A.	N.A.	N.A.	N.A.	0.10±0.03
Propanal	123-38-6	N.A.	N.A.	N.A.	N.A.	N.A.	N.A.	N.A.	0.64±0.35
Methacrolein	78-85-3	N.A.	N.A.	N.A.	N.A.	N.A.	N.A.	N.A.	0.08±0.15
n-Butanal	123-72-8	N.A.	N.A.	N.A.	N.A.	N.A.	0.05±0.04	N.A.	0.23±0.13
2-Pentanone	107-87-9	N.A.	N.A.	N.A.	N.A.	N.A.	N.A.	N.A.	0.02±0.01
3-Pentanone	96-22-0	N.A.	N.A.	N.A.	N.A.	N.A.	N.A.	N.A.	0.01±0
n-Pentanal	110-62-3	N.A.	N.A.	N.A.	N.A.	N.A.	N.A.	N.A.	0±0
n-Hexanal	66-25-1	N.A.	N.A.	N.A.	N.A.	N.A.	N.A.	N.A.	0.44±0.40
MTBE	1634-04-4	N.A.	N.A.	N.A.	N.A.	N.A.	1.58±0.28	N.A.	2.48±1.21
Acetonitrile	75-05-8	N.A.	N.A.	N.A.	N.A.	N.A.	0.11±0.11	N.A.	0.04±0.03
Alkanes		74.14	23±66	194.1	123.53	338.6±16.84	117.63	34	19.59±6.84
Alkenes		58.03	35±9.4	132.7	61.14	42±3	26.13	10.1	5.52±1.31
Aromatics		88.11	33±11	114.3	93.13	63±7	27.62	14.1	9.02±2.25
Halocarbons		N.A.	0.5±0.5	N.A.	N.A.	N.A.	6.19	N.A.	0.20±0.14
OVOCs		N.A.	N.A.	N.A.	N.A.	N.A.	1.88	N.A.	5.29±2.22
NMVOCs		400±60	115±26	493±120	277.8	449±20	179.45 ±65.94	58.8±50.7	40.56±12.18

[a] Taiwan (Hwa et al., 2002); [b] Hong Kong (Ho et al., 2009); [c] Guangzhou (Zhang et al., 2018c); [d] Taiwan (Hung-Lung et al., 2007); [e] Guangzhou (Zhang et al., 2018c); [f] Nanjing (Zhang et al., 2018b); [g] Hong Kong in 2015 (Cui et al., 2018); [h] This study. N.A. – not available.

Table A5: The slope and R^2 from the linear regression between the measured and modeled VOCs concentrations for 2-factor solution, and the estimated EFs (mg km^{-1} veh^{-1}) of VOCs from evaportative and tailpipe emissions.

Compound	Slope	R^2	EFs (mg km^{-1} veh^{-1})	
			Evaporative	Tailpipe
Ethylene	1.02	0.83	0.99±0.18	1.57±0.28
Isopentane	0.98	0.83	6.19±2.14	0.62±0.2
Ethane	0.84	0.76	1.85±0.82	0.07±0.03
Toluene	0.91	0.72	0.88±0.3	2.42±0.79
n-Butane	0.99	0.87	1.71±0.75	0.3±0.16
n-Pentane	0.99	0.95	1.93±0.9	0.22±0.1
MTBE	0.79	0.86	1.43±0.7	1.06±0.5
Acetylene	0.76	0.45	0.1±0.03	0.59±0.16
Propylene	0.92	0.70	0.36±0.08	0.67±0.14
Benzene	0.99	0.87	1.16±0.31	0.78±0.2
2-Methylpentane	0.97	0.95	1.1±0.41	0.5±0.18
3-Methylpentane	0.90	0.94	0.93±0.37	0.46±0.17
m/p-Xylene	0.79	0.67	0.04±0.01	1.39±0.4
Propanal	0.50	0.44	0.52±0.29	0.12±0.06
n-Hexane	0.82	0.93	0.48±0.15	0.38±0.12
Isobutane	0.89	0.65	0.51±0.25	0.05±0.02
2,2,4-Trimethylpentane	1.00	0.92	0.07±0.01	0.6±0.09
Ethylbenzene	0.70	0.58	0.08±0.03	0.58±0.22
3-Methylhexane	0.92	0.97	0.26±0.07	0.29±0.08
2,3-Dimethylbutane	0.91	0.94	0.29±0.11	0.11±0.04
NMVOCs	0.98	0.98	24.89±7.52	15.67±3.32